ERASMUS UNIVERSITY ROTTERDAM

Erasmus School of Economics

Master Thesis in Econometrics and Management Science:
Quantitative Finance

Modeling Systemic Risk in Banking Using a Graphical Extremal Model

Author:
R. Smitshoek

Student number:
511299

Supervisor:
Prof. Dr. C. Zhou

Second assessor:
Dr. P. Wan

March 11, 2021

Abstract

In this paper we model systemic risk in European banking using a graphical extremal model, based on conditional (in)dependence and the Hüsler-Reiss distribution, using data from 55 European banks. We analyse the position of banks in estimated graphical structures in relation to bank size, systemic importance, as designated by the Financial Stability Board, and region. Furthermore we use several model-implied systemic importance measures to identify the designated systemically important banks. Finally we compare model-implied tail dependence to empirical tail dependence. We find that the estimated graphs show strong signs of regional and inter-country clustering, but weaker evidence of any relation between systemic importance of banks and node importance in the estimated graphs. Graph-induced centrality measures do not correspond to designated systemic importance. Simulated systemic impact measures are somewhat more in line, but the size of banks is most closely aligned to systemic importance. Model-implied tail dependence is accurate for directly connected pairs of banks, but far less accurate for directly unconnected pairs of banks, when compared to empirical tail dependence.

Contents

1 Introduction

The global financial crisis in 2007-2008 brought new attention to the concept systemic risk. The massive global distress gave a prime example of systemic risk and its effects. The events that started with turmoil in the American housing market evolved through the American financial sector to a overwhelming global financial and economical crisis, which showed the interconnectedness of the global financial market and the potential of localized shocks to spread to the entire financial system. To better manage systemic risk and prevent new systemic crisis the Basel III regulatory framework was erected (Basel Committee on Banking Supervision (2010)). These new regulatory agreements in particular impacted (Global) Systemically Important Financial Institutions; (G-)SIFIs, and (Global) Systemically Important Banks; (G-)SIBs. More extensive regulations were applied to these large and highly connected institutions, as failure of these particular institutions could possibly generate system-wide economical effects.

The ability to model, analyze and visualize systemic risk in banking and its network structure is of great importance. Clearly from a regulator's perspective the interconnections between banks is of great importance when assessing potential risks to a entire financial system. To manage stability of a financial system one needs to go beyond risk management on an individual basis. Traditionally the size of a financial institution has been the most important factor in assessing its impact on the financial system during crisis. However, network connections also matter. A simulation study in Krause and Giasante (2012) shows that, while system-wide crisis are likely to be triggered by failure of a large bank, it is the network structure that determines the spread and severity of the crisis. This implies that, regarding the stability of a financial system, not only the size of a bank is important (too big to fail), but also the connections it has within the system (too interconnected to fail).

In this paper we model systemic risk and its network structure in banking. Using a graphical extremal model based on conditional (in)dependence, proposed in Engelke and

Hitz (2020), we aim to identify systemically important banks and the network structure of systemic risk in the European banking sector. As a data set we use daily log-returns of 55 European banks in the period 2008-2019 and as an assessment of systemic importance we use the classification of G-SIBs by the Financial Stability Board (FSB) in 2011-2019. After altering this data to remove temporal dependence, we assume that the threshold exceedances of the altered residuals follow a Hüsler-Reiss distribution, proposed in Hüsler and Reiss (1989). We then estimate the optimal underlying graph structure, using numerical methods, a decomposition of likelihood functions and a greedy algorithm. To determine whether the graphical extremal model is successful in identifying systemically important banks and the network structure of systemic risk, we analyse the estimated graphical structures in three ways. Firstly, we compare estimated graphs for different periods and explore whether G-SIBs and large banks take on important positions within the graphical structures. We also investigate whether regional or inter-country clusters can be observed. Secondly, we compare the model-implied systemic importance of G-SIBs, using graph-induced centrality measures and simulated systemic impact measures, to systemic importance as determined by the FSB. Finally, we compare bivariate tail dependencies implied by the estimated graphical structures to empirical tail dependencies.

Estimating the underlying network of systemic risk in European banking is essentially modeling an extremal dependence structure for high-dimensional data. For low-dimensional random variables copulas are a common instrument to analyze extremal dependence of random variables (see for example Chapter 5 of McNeil, Frey, and Embrechts (2015)). Extending this approach to a high number of dimensions, in our case 55, is near impossible without enforcing some form of sparsity. The graphical extremal model we use in this paper has the potential to be applied to high-dimensional data. Not only does its graphical structure provide sparsity, factorization of the likelihood function makes parameter estimation using numerical methods feasible. Furthermore the graphical structure gives interpretability by showing the interconnections in high-dimensional data. It may be fruitful to also give some alternative methods that are potentially also useful in this

sense, and compare these to the graphical extremal model. A similar model is proposed in Gissibl and Klüppelberg (2018), where a recursive max-linear model is defined on graphs. This model differs in that graphs are directed and this model does not use continuous densities, as is in the case of the graphical extremal model. Vine copulas, proposed in Bedford and Cooke (2002), can be used to connect multiple bivariate copulas through a graph structure and applications of vine copulas in finance can be found for example in Low, Alcock, Faff, and Brailsford (2013) and Low (2018), where it is used in the context of portfolio (risk) management. Furthermore factor copulas can be used to reduce dimension (see for example Krupskii and Joe (2013) and Oh and Patton (2017)) and are therefore applicable to data of high dimension. No network structure is obtained however, such that interpretability in terms of network structure may be limited compared to graph-based methods.

In this paper we find that the estimated graphs show strong signs of regional and inter-country clustering, but weaker evidence of a relation between the designated systemic importance, or size, of banks and node importance within the graphical structure. We also find that graph-induced centrality measures do not correspond to systemic importance of banks as determined by the FSB. The simulated systemic impact measures, in particular average affected proportion of capital, are more in line with the G-SIBs designation, but all model-implied measures are outperformed by using the size of banks to identify G-SIBs. Model-implied tail dependence corresponds closely to empirical tail dependence for connected pairs of banks, however for unconnected pairs of banks model-implied tail dependence is significantly lower than empirical tail dependence.

The structure of this paper is as follows. Section 2 describes the data of daily log-returns and market capitalizations used in the paper. Section 3 introduces the methodology. In particular we determine the model assumptions for the log-losses, define the graphical extremal model, describe the estimation procedures and describe the methods of analysis for the estimated graphs. In Section 4 we present and analyse our results, including the estimated graphical structures, model-implied systemic importance measures

and model-implied bivariate tail dependencies. In Section 5 we summarize and discuss the findings of this paper. Appendix A contains some additional sections including additional figures, tables and background studies. Appendix B contains the Matlab programming code, used to obtain the results in this paper.

2 Data

In this paper we use daily log-returns and (previous day) market capitalizations from a selection of European banks over the complete period covering 2008-2019. All banks were a constituent of the STOXX Europe 600 Banks index at some point during the period 2008-2019. The sample of banks consists of 55 banks from 17 European countries. The data consist of 3080 daily log-returns and market capitalizations. All data are obtained through Bloomberg. The list of banks, and the indices used to refer to all banks in this paper, can be found in Tables 7a and 7b in the Appendix A.1. Figure 1 shows the log-returns of the portfolio consisting of the entire sample of banks, weighed according to the market capitalization and rebalanced daily.

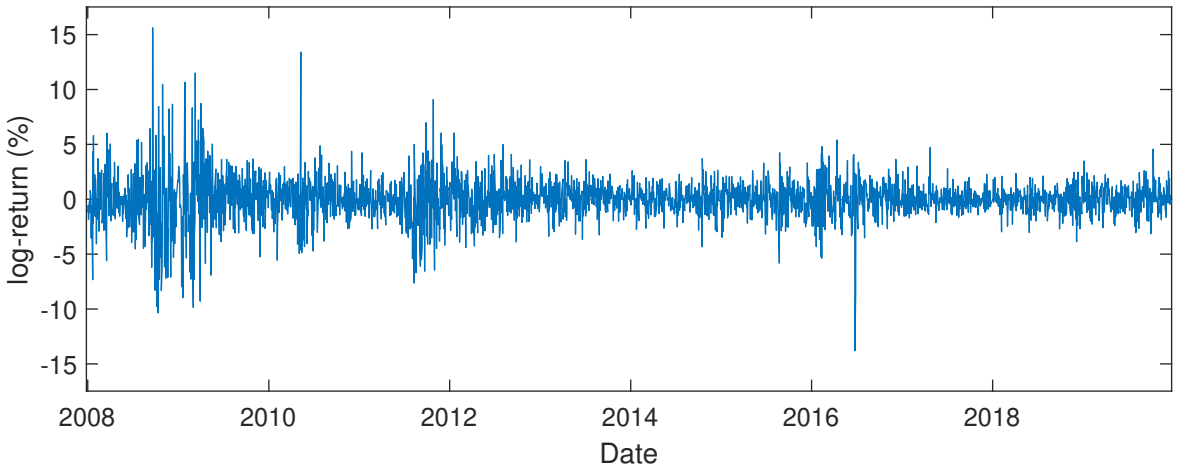

Figure 1: log-returns (in %) of portfolio of all 55 banks weighed by market capitalization and rebalanced daily in the period 2008-2019

Figure 1 gives a good representation of the movement of the European banking sector as a whole and shows strong signs of volatility clustering. In particular we note a period of high volatility in 2008-2009, corresponding to the global financial crisis. The figure also shows periods of increased volatility in 2010-2013, corresponding to effects of the Eurozone crisis, and 2015-2016, which included events as the Chinese stock market crash and the Brexit referendum.

3 Methodology

In this section we lay out the methodology. In Section 3.1 we describe the model assumptions needed to obtain normalized, i.i.d. multivariate extremal data from the daily log-losses. In Section 3.2, using graph theory and a definition of conditional independence, we define the graphical extremal model, and in particular define the Hüsler-Reiss distribution. In Section 3.3 we cover the estimation procedures and algorithms to determine the optimal parameters and underlying graph for data following a Hüsler-Reiss distribution. In Section 3.4 we lay out our methods to analyse the estimated graphical structures, define the model-implied systemic importance measures, and describe the model-implied tail dependencies.

3.1 Model for log-losses of banks

The graphical extremal model requires i.i.d. multivariate extremal data. In this section we show how to obtain these data from the log-losses of banks. In Section 3.1.1 we first use an autoregressive model with GARCH-errors to obtain i.i.d. residuals from the log-losses for each of the banks, which we transform to i.i.d. standard Pareto distributed data. Then, in Section 3.1.2, we use the transformed data of all banks to obtain an i.i.d. sample of multivariate Pareto variables, using multivariate extreme value theory and threshold exceedances. Throughout this paper we adopt the following conventions for notation. Subscripts of variables refer to indices of the banks, shown in tables 7a and 7b in Appendix A.1. Superscripts are used to denote indices of time and are shown between brackets to distinguish them from exponents.

3.1.1 Data filtering

The volatility clustering, shown in Figure 1, motivates the choice for an autoregressive model with GARCH errors (see Chapter 4 of McNeil et al. (2015)). We therefore model the log-losses according to an AR(1) model with GARCH(1,1) errors as follows. Let

$i \in \{1, \ldots, d\}$ denote a bank, and $L_i^{(1)}, \ldots, L_i^{(T)}$ be the daily log-losses over a sequential period of days $1, \ldots, T$. We assume the log-losses are modeled according to

$$\begin{aligned} L_i^{(t)} &= \mu_i + \phi_i L_i^{(t-1)} + \sigma_i^{(t)} Z_i^{(t)} \\ \left(\sigma_i^{(t)}\right)^2 &= \gamma_i + \alpha_i \left(\sigma_i^{(t-1)} Z_i^{(t-1)}\right)^2 + \beta_i \left(\sigma_i^{(t-1)}\right)^2 \\ Z_i &\sim WN(0,1). \end{aligned}$$

We assume that the white noise processes $Z_i^{(1)}, \ldots, Z_i^{(T)}$ follow i.i.d. standardized students t-distribution with degrees of freedom ν_i; with zero location parameter and scale parameter $\sqrt{\frac{\nu_i - 2}{\nu_i}}$. Estimation of parameters is performed using numerical ML methods. After the filtering through the described model we perform Ljung-Box test for serial dependence on the obtained residuals $Z_i^{(1)}, \ldots, Z_i^{(T)}$.

To perform the cross-sectional analysis between the different banks we normalise the white noise processes to standard Pareto processes. To do this we use the transformation given by

$$X_i^{(t)} := \frac{1}{1 - F_{\hat{\nu}_i}\left(Z_i^{(t)}\right)},$$

where $F_{\hat{\nu}_i}$ is the cumulative distribution function of the standardised students t-distribution with degrees of freedom $\hat{\nu}_i$. We regard the normalised white noise terms $X_i^{(1)}, \ldots, X_i^{(T)}$ as an i.i.d. sample of standard Pareto distributed random variables, with its upper tails corresponding to the upper tails of the original white noise terms.

3.1.2 Multivariate extreme value theory

Similar to univariate extreme value theory, we can describe tail behaviour of the multivariate distribution $\mathbf{X} = (X_1, \ldots, X_d)$. As in the univariate case, two related approaches exists; using block maxima and using threshold exceedances. In this paper we use the approach utilizing threshold exceedances. For the normalised residual process $\mathbf{X}$, with standard Pareto marginals we assume that there exists a limiting vector of random vari-

ables $\mathbf{Y}$ such that

$$\mathrm{P}\left(\mathbf{Y} \leq \mathbf{z}\right) = \lim_{u \to \infty} \mathrm{P}\left(\frac{\mathbf{X}}{u} \leq \mathbf{z} \;\middle|\; \max\{X_1, \ldots, X_d\} > u\right).$$

The distribution of $\mathbf{Y} \in \{\mathbf{y} \in [0, \infty)^d \backslash \{\mathbf{0}\} \mid \max\{y_1, \ldots, y_d\} > 1\}$ is called a multivariate Pareto distribution. Its probability density function, given some general assumptions (see Engelke and Hitz (2020)), is

$$f(\mathbf{y}) = \frac{\lambda(\mathbf{y})}{\Lambda},$$

where λ is its exponent measure density and Λ is a normalizing constant obtained from the exponent measure. The importance of the exponent measure density will become clear in Section 3.2.2, where it is necessary for the definition of conditional independence. More theoretical background on multivariate extreme value theory and the exponent measure can be found in Chapter 8 of Beirlant et al. (2004).

For our data we use a high threshold value to approximate a multivariate Pareto distribution. To do this we limit our data to only the days where the normalised residual of at least one bank exceeds a high threshold u, and divide all remaining normalised residuals by this threshold. In other words we obtain $\mathbf{Y}^{(1)}, \ldots \mathbf{Y}^{(N)}$, $N < T$, defined by

$$\mathbf{Y}^{(n)} = \frac{\mathbf{X}^{(t_n)}}{u}, \text{ where } \{t_1, \ldots, t_N\} = \left\{1 \leq t \leq T \;\middle|\; \max\{X_1^{(t)}, \ldots, X_d^{(t)}\} > u\right\}. \quad (1)$$

We then assume that $\mathbf{Y}^{(1)}, \ldots, \mathbf{Y}^{(N)}$ are an i.i.d. sample of multivariate Pareto random variables. The threshold is set to $u = 10$, determined by a threshold selection procedure using parameter stability described in Kiriliouk, Rootzén, Segers, and Wadsworth (2018). The threshold selection procedure in our case can be found in Appendix A.3. A robustness study on the threshold choice, using a random subset of 25 banks, is given in Appendix A.4.

3.2 Graphical extremal model

In this section we describe the theoretical background of the graphical extremal model, which models the network of systemic risk given the extremal data obtained in the previous section. First, in Section 3.2.1, we describe basic concepts in graph theory, where graphs are the mathematical representations of the networks of systemic risks. In Section 3.2.2 we define conditional independence and markov properties for multivariate Pareto distributed variables. These definitions connect the structure of extremal dependence, in our case between banks, to a graphical structure. Finally, in Section 3.2.3, we describe the Hüsler-Reiss distribution; the specific multivariate Pareto distribution we use in this paper, and show how this distribution and its parameters relate to the underlying graphical structure.

3.2.1 Graph theory

We give some notions of graph theory, based on Lauritzen (1996). We define a graph $\mathcal{G} = (V, E)$ to be a pair consisting of a set of vertices V and a set of edges $E \subset \{(i, j) \in V \times V \mid i \neq j\}$. Graphs used in this paper are assumed to be undirected, that is it holds that $(i, j) \in E \iff (j, i) \in E$. For this reason, in any case we assume that the set of edges E contains only 1 edge (i, j) for all undirected edges, and that in this case $i < j$. For any subset of vertices $W \subset V$ we define subgraph $\mathcal{G}_W := (W, E_W)$, where $E_W := \{(i, j) \in E \mid i, j \in W\}$. In our model the vertices in a graph represent the different banks, that is $V = \{1, \ldots, d\}$. The structure of connecting edges represent a type of extremal dependence structure of the network of banks, which is defined in Section 3.2.2.

Two vertices in a graph are connected if there exists a path of edges between them or if they are the same vertex. A graph is said to be connected if every vertex is connected to any vertex in the graph. All graphs discussed in this paper will be connected, as we assume that between any two banks there is at least some form of extremal dependence, albeit possibly through other banks. A set of vertices $W \subset V$ in a graph is called complete if every vertex $i \in W$ is directly connected by a single edge to any other vertex $j \in W$,

that is $(i, j) \in E_W$ if $i, j \in W$. A clique C is a complete set that is maximal in the sense that there are no larger complete sets containing C. The minimal clique size is 2, as each vertex is connected to at least 1 other vertex, together forming a complete set

The triple (A, B, C), where $\{A, B, C\}$ form a partition of the set of vertices V, is a decomposition of the graph $\mathcal{G}$ if

1. B separates A and C; that is any path from a vertex in A to a vertex in C goes through B.

2. B is complete.

A graph is called decomposable if its set of vertices is complete or there exists decomposition into non-empty sets such that the subgraphs $\mathcal{G}_{A\cup B}$ and $\mathcal{G}_{B\cup C}$ are decomposable. This is a recursive definition intuitively meaning that decomposable graphs can be formed by joining cliques together by complete sets. The set of all cliques in a decomposable graph is called the clique set, and denoted by $\mathcal{C}$. The multiset $\mathcal{D}$ of all non-empty intersections between distinct pairs of cliques is called the separator set, where the term multiset implies that it can contain multiples of the same element if it separates more than 2 cliques.

A final important definition is a block graph, which is a decomposable graph where all sets separating sets are singletons. Hence block graphs can be formed by joining cliques together by single vertices. A tree is an example of a block graph, where all cliques are of size 2. In this paper we only use block graphs, due to the useful properties it yields.

3.2.2 Conditional independence and Markov properties

Estimating the multivariate Pareto distribution using the extremal data is near impossible without forcing some sort of sparsity to reduce the number of parameters. A first step is to use a definition of conditional independence stated in Engelke and Hitz (2020), using undirected graphs. We assume $\mathbf{Y} = (Y_1, \ldots, Y_d)$ follows a multivariate Pareto distribution with standard Pareto marginals. For any subset $I \subset \{1, \ldots, d\}$ we denote $\mathbf{Y}_I$ the subvector of variables $(Y_i)_{i\in I}$. This subvector of variables does not follow a multivariate

distribution, as $\max\{Y_i \mid i \in I\}$ may be smaller than 1. However the conditional marginal

$$\mathbf{Y}_I^* := \mathbf{Y}_I \,\Big|\, \max\{y_i \mid i \in I\} > 1$$

does follow a multivariate Pareto distribution (see Rootzén and Tajvidi (2006)). We define λ_I to be the exponent measure density of this conditional marginal and Λ_I its normalization constant. For singletons $I = \{i\}$ we have $\lambda_i(y_i) = \frac{1}{y_i^2}$, which is equal to probability density function of a standard Pareto random variable. This also implies $\Lambda_i = 1$.

Now let $A, B, C \neq \emptyset$ be a partition of $\{1, \ldots, d\}$. We say that $\mathbf{Y}_A$ is conditionally independent of $\mathbf{Y}_C$ given $\mathbf{Y}_B$, denoted by $\mathbf{Y}_A \perp_e \mathbf{Y}_C \mid \mathbf{Y}_B$, if the exponent measure density can be factorized as follows

$$\lambda(\mathbf{y}) = \frac{\lambda_{A\cup B}(\mathbf{y}_{A\cup B})\lambda_{B\cup C}(\mathbf{y}_{B\cup C})}{\lambda_B(\mathbf{y}_B)}.$$

Note that this does not imply a factorization of the probability density function, since the normalization constant Λ in general does not factorize in the same manner. With this definition we can relate graphs to multivariate Pareto distributions. We say that $\mathbf{Y}$ satisfies the global Markov property with respect to graph $\mathcal{G} = (V, E)$ if for each partition $\{A, B, C\}$ of vertex set V, where B separates A and C, we have $\mathbf{Y}_A \perp_e \mathbf{Y}_C \mid \mathbf{Y}_B$. This is equivalent to the, perhaps more intuitively clear, pairwise Markov property. This property means that for any vertices $i, j \in V$ that are not directly connected through a single edge, that is $(i, j) \notin E$, we have: $Y_i \perp_e Y_j \mid \mathbf{Y}_{V\setminus\{i,j\}}$. In relation to our application this means that pairs of banks not directly connected in the graph only have extremal dependence through other banks.

The Markov properties give a partial decomposition of the probability density in terms of cliques and separators of a graph. If $\mathcal{C}$ is the clique set of a graph, and $\mathcal{D}$ the separator set, then we have

$$f(\mathbf{y}) = \frac{1}{\Lambda} \frac{\prod_{C \in \mathcal{C}} \lambda_C(\mathbf{y}_C)}{\prod_{D \in \mathcal{D}} \lambda_D(\mathbf{y}_D)}.$$

In case of block graphs, where the separator sets are singleton sets, this decomposition becomes even more manageable, as the univariate marginal exponent measure densities do not depend on any parameters, giving

$$f(\mathbf{y}) = \frac{1}{\Lambda} \frac{\prod_{C \in \mathcal{C}} \lambda_C(\mathbf{y}_C)}{\prod_{\{i\} \in \mathcal{D}} y_i^{-2}} = \frac{1}{\Lambda} \prod_{C \in \mathcal{C}} \frac{\lambda_C(\mathbf{y}_C)}{\prod_{j \in C} y_j^{-2}} \prod_{1 \leq k \leq d} y_k^{-2}. \tag{2}$$

3.2.3 Hüsler-Reiss distribution

We now define a specific multivariate Pareto distribution for $\mathbf{Y}$; the Hüsler-Reiss Pareto distribution (see Engelke, Malinowski, Kabluchko, and Schlather (2015)). This distribution was first described in Hüsler and Reiss (1989), and occurs as extremal limiting distributions of multivariate normal distributions. Central to this distribution is the variogram matrix Γ, a $d \times d$ matrix with the following properties

1. Zero diagonal: $\text{diag}(\Gamma) = (\Gamma_{11}, \ldots, \Gamma_{dd}) = \mathbf{0}$.
2. Symmetric: $\Gamma = \Gamma'$.
3. Non-negative: $\Gamma_{ij} \geq 0$ for all $1 \leq i, j \leq d$.
4. Strictly conditionally negative definite: $x^T \Gamma x < 0$ for all $x \in \mathbb{R}^d \backslash \{0\}$ with $\sum_{i=1}^d x_i = 0$.

The variogram entries Γ_{ij} determine the extremal dependence of the variables i and j, where $\Gamma_{ij} = 0$ implies a complete extremal dependence, while $\Gamma_{ij} \to \infty$ implies an extremal independence (see Section 3.4.4).

To describe the probability density function of the Hüsler-Reiss distribution, with variogram Γ, we first define for any $k \in \{1, \ldots, d\}$ the $(d-1) \times (d-1)$-matrix $\Sigma^{\backslash k} := \frac{1}{2}(\Gamma_{ik} + \Gamma_{jk} - \Gamma_{ij})_{i,j \neq k}$ and the vector $\tilde{\mathbf{y}}^{\backslash k} := \left(\log\left(\frac{y_i}{y_k}\right) + \frac{\Gamma_{ik}}{2}\right)_{i \neq k}$. The exponent measure

density is the given by

$$\lambda(\mathbf{y}) = \frac{\phi\left(\tilde{\mathbf{y}}^{\setminus k} \mid \mathbf{0}, \Sigma^{\setminus k}\right)}{y_k^2 \prod_{i \neq k} y_i}, \tag{3}$$

where $\phi(\cdot \mid \mu, \Sigma)$ is the probability density function of the $(d-1)$-variate normal distribution with mean μ and covariance matrix Σ. This representation of exponent measure density is independent of the choice for k. The normalizing constant Λ is given by

$$\Lambda = \sum_{j=1}^{d} \Phi\left(\left(\frac{\Gamma_{ji}}{2}\right)_{i \neq j} \,\middle|\, \mathbf{0}, \Sigma^{\setminus j}\right), \tag{4}$$

where Φ is the $(d-1)$-variate normal cumulative distribution function.

We give some additional properties of the Hüsler-Reiss distribution. Any conditional marginal $\mathbf{Y}_I^*$ also follows a Hüsler-Reiss distribution and its variogram is the restricted variogram: $\Gamma_I = (\Gamma_{ij})_{i,j \in I}$. This means that the marginal exponent measure density λ_I and normalizing constant Λ_I can be described in similar manner through equations (3) and (4), assuming $|I| > 1$. Furthermore any Hüsler-Reiss variable satisfies the global Markov property, as defined in section 3.2.2. The underlying graph $\mathcal{G} = (V, E)$ and variogram Γ are directly related and any of the two implies the other through the following relation. Let $\Sigma^{\setminus k} := \frac{1}{2}(\Gamma_{ik} + \Gamma_{jk} - \Gamma_{ij})_{i,j \neq k}$ and $\Theta^{\setminus k} := \left(\Sigma^{\setminus k}\right)^{-1}$ be $(d-1) \times (d-1)$ matrices. If we denote the elements of the matrix $\Theta^{\setminus k}$ with indices running in $\{1, \ldots, d\} \setminus \{k\}$ instead of $\{1, \ldots, d-1\}$ we have:

$$(i,j) \in E \iff \begin{cases} \Theta_{ij}^{\setminus k} \neq 0 & \text{if } i, j \neq k \\ \sum_{l \neq k} \Theta_{lj}^{\setminus k} \neq 0 & \text{if } i = k, j \neq k \\ \sum_{l \neq k} \Theta_{il}^{\setminus k} \neq 0 & \text{if } i \neq k, j = k. \end{cases} \tag{5}$$

This relation is independent of the choice for k. With this relation and an assumed underlying graph we obtain the precise restrictions for the parameters in variogram. In particular if we have for all edges $(i,j) \in E$ the variogram elements Γ_{ij}, then there is an unique Γ, restricting to Γ_{ij} on the edges, such that the relation (5) is satisfied (see

Engelke and Hitz (2020)). In the case of block graphs this gives an manageable algorithm to obtain Γ from the parameters Γ_{ij} on the edges. This algorithm for block graphs is given in Appendix A.2. The relation also implies that essentially the number of parameters in a Hüsler-Reiss distribution is equal to the number of edges in the underlying graph. The graphical structure, therefore, provides some form of sparsity in case of the Hüsler-Reiss distribution.

3.3 Estimation of the graphical extremal model

In this section we describe the methods to estimate the variogram parameters of the Hüsler-Reiss distribution and select the optimal underlying graphical structure. For any underlying block graph we use a likelihood decomposition, discussed in Section 3.3.1, such that numerical estimation of the variogram parameters is feasible for the large dimension of our data. The optimal graph structure itself is selected using a greedy algorithm described in Section 3.3.2.

3.3.1 Hüsler-Reiss likelihood decomposition using block graphs

In a general case, estimating the variogram Γ for a Hüsler-Reiss distribution requires estimation of $\frac{1}{2}(d-1)d$ parameters, due to the symmetry and zero diagonal. This corresponds to a fully connected underlying graph. Any graphical structure that is not fully connected reduces this number to the number of edges on the underlying graph as shown in Section 3.2.3. In case of a block graph, with clique set $\mathcal{C}$, this number reduces to $\sum_{C\in\mathcal{C}} \frac{1}{2}\left(|C|-1\right)|C|$. This number can be significantly less than the original number, but is still larger then $d-1$.

With the large number of parameters, numerical optimization would only be feasible if the likelihood function could be factorized and smaller sets parameters sets could be estimated separately. The issue is, however, that even though block graphs give a manageable decomposition of the exponent measure density this does not translate in a decomposition of the likelihood function. This is because the normalization constant Λ

does not factorize over the cliques, while still being dependent on the parameters in the variogram Γ, that is

$$f(\mathbf{y} \mid \Gamma) = \frac{1}{\Lambda(\Gamma)} \frac{\prod_{C \in \mathcal{C}} \lambda_C(\mathbf{y}_C \mid \Gamma_C)}{\prod_{\{i\} \in \mathcal{D}} y_i^{-2}} \propto \frac{1}{\Lambda(\Gamma)} \prod_{C \in \mathcal{C}} \lambda_C(\mathbf{y}_C \mid \Gamma_C).$$

However, a simulation study in Engelke and Hitz (2020) shows that the estimated Γ obtained by separate optimization over the cliques does not differ significantly from joint optimization. Hence we can estimate Γ by first numerically maximizing the log-likelihood functions ℓ_C over the cliques $C \in \mathcal{C}$ to obtain

$$\widehat{\Gamma_C} := \arg\max_{\Gamma_C} \ell_C \left(\mathbf{y}_C^{(1)}, ..., \mathbf{y}_C^{(N)} \;\middle|\; \Gamma_C \right) = \arg\max_{\Gamma_C} \sum_{n=1}^{N} \left(\log \lambda_C \left(\mathbf{y}_C^{(n)} \mid \Gamma_C \right) - \log \Lambda_C \left(\Gamma_C \right) \right),$$

where λ_C and Λ_C are described as in equations (3) and (4). Note that λ_C requires a choice of $k \in C$, as shown in equation (3). Theoretically this choice is not relevant. In our estimation method we always choose the smallest index, where the indices of all banks can be found in Tables 7a and 7b in the Appendix. After this we join together the ML estimates $\widehat{\Gamma_C}$ to the unique matrix $\hat{\Gamma}$ that restricts to $\hat{\Gamma}_C = \widehat{\Gamma_C}$ and corresponds to the underlying graph using the relation between variogram and graph of Equation (5) (see Appendix A.2).

Data realizations restricted to cliques may not have any threshold exceedances. We remove these data realization in our estimation procedure for these cliques specifically. Furthermore, we follow Engelke and Hitz (2020) and use data censoring. This means that for any data point that does not exceed the threshold, we adjust its contribution to the likelihood function, such that only the failure to exceed the threshold is used, not the precise value. For any subset of indices $W \subset \{1, \ldots, d\}$ and $J := \{j \in W \mid y_j \leq 1\}$ we use the censored likelihood function:

$$f_W^*(\mathbf{y}_W) := \int_{[0,1]^{|W|}} f_W(\mathbf{y}_W) d\mathbf{y}_W.$$

Censoring data prevents small data realizations affecting the estimation of parameters disproportionately and reduces bias (see Kiriliouk et al. (2018)).

3.3.2 Algorithm for selecting underlying graph

To select an optimal underlying graphical structure we use a procedure identical to the one described in Engelke and Hitz (2020). This procedure includes the restriction of underlying graphs to block graphs with cliques of size at most 3. As mentioned in Section 3.3.1, block graphs allow us to use a decomposition of the likelihood function for estimating the variogram. The limit on the clique size is there to keep computation of the optimal graph feasible, given the large number of banks.

We start by calculating the spanning tree that maximizes the log-likelihood function. To do this we use the decomposition in Equation (2), the approximation of the likelihood discussed in section 3.3.1 and censoring. We approximate the log-likelihood $\ell\left(\mathbf{y}^{(1)}, ..., \mathbf{y}^{(N)} \mid \hat{\Gamma}\right)$ for a tree $\mathcal{T} = (V, E)$ connecting all vertices by

$$\sum_{(i,j)\in E} \left(\ell^*_{\{i,j\}}\left(\mathbf{y}^{(1)}_{\{i,j\}}, ..., \mathbf{y}^{(N)}_{\{i,j\}} \mid \widehat{\Gamma_{\{i,j\}}}\right) + 2 \sum_{n|y_i^{(n)}>1} \log\left(y_i^{(n)}\right) + 2 \sum_{n|y_j^{(n)}>1} \log\left(y_j^{(n)}\right) \right) - 2 \sum_{\substack{1\le k\le d \\ n|y_k^{(n)}>1}} \log\left(y_k^{(n)}\right),$$

where $\ell^*_{\{i,j\}}$ is the censored log-likelihood on the clique. Since the last term in this equation is the same for any tree, we only need to solve

$$\arg\max_{\mathcal{T}} \sum_{(i,j)\in E} \left(\ell^*_{\{i,j\}}\left(\mathbf{y}^{(1)}_{\{i,j\}}, ..., \mathbf{y}^{(N)}_{\{i,j\}} \mid \widehat{\Gamma_{\{i,j\}}}\right) + 2 \sum_{n|y_i^{(n)}>1} \log\left(y_i^{(n)}\right) + 2 \sum_{n|y_j^{(n)}>1} \log\left(y_j^{(n)}\right) \right).$$

We can solve this maximization problem using Kruskal's algorithm (see Kruskal (1956)). We set $\mathcal{G}_0 = \mathcal{T}$ and the determine $\mathcal{G}_1, \dots \mathcal{G}_M$ by sequentially adding cliques of size 3 in greedy algorithm, that is for each step we add a single edge, forming a new clique, such that the log-likelihood is maximized. Once no more cliques can be added we determine the optimal graphical structure by selecting the graph from $\mathcal{G}_1, \dots \mathcal{G}_M$ that has the lowest

Akaike information criterion:

$$\mathrm{AIC}_m = 2p_m - 2\ell^* \left(\mathbf{y}^{(1)}, \ldots, \mathbf{y}^{(N)} \;\middle|\; \hat{\Gamma}_m \right),$$

where we again use censored log-likelihood.

3.4 Graph analysis

We apply the methodology of Sections 3.1 to 3.3 to obtain, observe and compare estimated graphical structures for the full sample of 55 banks for 4-year windows 2016-2019, 2012-2015 and 2008-2011. The size of the windows provides us with just over 1000 observations per graphical estimation. In particular we observe the position of large banks and systemically important banks. We use average market capitalization as a measure of size. For assessment of the systemic importance we use the classification of G-SIBs by the FSB. This classification is published yearly each November since 2011. Table 8 in the Appendix shows the list of banks considered as G-SIBs by the FSB in our sample and also the corresponding years for these designations of systemic importance. We do note that using this particular classification is not the only possible method of assessing systemic importance of banks and it does not guarantee an accurate representation of true systemic importance. However comparison of the graphical model to this classification is still useful. It gives a sense of whether systemic importance implied by the graphical extremal model, based on only the log-losses of the banking sample, is in line with systemic importance as designated by the FSB, based on several indicators as size, interconnectedness and complexity (see Basel Committee on Banking Supervision (2011)). Furthermore we investigate whether some form of regional grouping of banks can be observed in the graphs. In Appendix A.6 we also estimate graphical structures with a smaller subsample of 25 banks and compare these to their larger counterparts in terms of consistency of its connections, as a measure of the robustness of the graphical estimates.

Additionally, we perform some further analysis of the estimated graphical structures,

described in the remainder of this section. Firstly we use several measures of systemic importance implied by the estimated graphs and model parameters and compare these for G-SIBs against normal banks. We use two types of measures; the centrality measures, defined in Section 3.4.1, and the simulated systemic impact measures, defined in Section 3.4.2. Furthermore in Section 3.4.3 we describe the binary logistic regression method we use to investigate if G-SIBs can be identified using the estimated structures and variogram parameters. In Section 3.4.4 we describe the model-implied bivariate tail dependencies, which we compare to empirical bivariate tail dependencies.

3.4.1 Node centrality

The importance of banks implied by the estimated graphical structures can be evaluated using centrality measures. These measures quantify importance of nodes in a graph depending on their position in the graph and connections to other nodes (see Freeman (1978)). We use three measures of centrality. Firstly we use closeness centrality. This is a measure of the centrality of nodes using the average shortest distances of a node to all other nodes. It is defined (for bank i) by

$$C_c(i) = \frac{d-1}{\sum_{j \neq i} l(i,j)},$$

where $l(i,j)$ is the shortest distance (in number of edges) between banks i and j. The term $d-1$ is a normalization term, such that the measure can be used for graphs of different sizes. For banks that are in the centre of the graph structure the average distance is smaller than for banks that are located at the fringes, which implies a larger closeness centrality measure.

Another measure we use is betweenness centrality, which uses the number of times a node is traversed by shortest paths between other nodes. In case of a block graph, where

shortest paths are unique, this is defined by

$$C_b(i) = \sum_{(j,k)\in E, j,k\neq i} \frac{2\delta_{jk}(i)}{(d-1)(d-2)},$$

where $\delta_{jk}(i) = 1$ if and only if node i is traversed by the shortest path between nodes j and k, and zero otherwise. The term $\frac{2}{(d-1)(d-2)}$ is a normalization term in this case.

Finally we use degree centrality, which uses the degree of a node: the number of directly connected nodes. It is defined by

$$C_d(i) = \frac{\deg(i)}{d-1},$$

where $\deg(i)$ denotes the degree of node i and $d-1$ normalizes the measure.

For each of the estimated graphs we report all centrality measures and determine whether these measures are significantly higher for G-SIBs than for normal banks using one-tailed Mann-Whitney U tests.

3.4.2 Simulated systemic impact

Even though the graphical structure, and corresponding centrality measures, give a good idea of the relative implied importance of banks in the banking system, some aspects may not be properly represented by the graph alone. Firstly, while a graph shows the structure of extremal dependence, through the Markov properties of Section 3.2.2, it does not take into account the strength of these connections, which are represented by the variogram parameters. Two banks, closely connected in the graph, may have relatively low tail dependence due to the connections between them being weak. In this way systemic importance implied by the model may be different from node centrality in the graph. To account for this we define two additional measures for systemic importance in the network of bank. Firstly, we define the expected affected number of banks. Given that for a bank i we have $Y_i > 1$, and therefore the GARCH-error exceeds its 90th percentile, we say that

(another) bank j is affected if $Y_j > 1$. The expected affected number of banks for a bank i is then given by

$$A_b(i) := \mathrm{E}\left[\sum_{j=1}^{d} \mathbb{1}(Y_j > 1) \;\middle|\; Y_i > 1\right] \in [1, d].$$

In comparison to the centrality measures defined in Section 3.4.1, the expected affected number of banks does take into account the strength of connections.

A second issue with the graphical structure representing the network of systemic risk is that it does not take into account the size of banks. A bank with high connectivity to multiple small banks may overall be of less systemic importance than a bank with only a few connections to large banks. Therefore we define an second additional measure of systemic importance; the expected affected proportion of capital, given by

$$A_c(i) := \mathrm{E}\left[\sum_{j=1}^{d} \frac{c_j}{c_{\text{tot}}} \mathbb{1}(Y_j > 1) \;\middle|\; Y_i > 1\right] \in \left[\frac{c_i}{c_{\text{tot}}}, 1\right],$$

where c_i is the (average) market capitalization of bank i (in a certain period), and $c_{\text{tot}} = \sum_{i=1}^{d} c_i$. We do note that this particular measure implicitly takes the size of banks into account. Since a bank always affects itself, its size has a significant influence on the actual affected proportion of capital. However, correcting for this would be unreasonable, as the banks itself are part of the system of banks.

Both measures can be estimated using a simulation procedure described in Engelke and Hitz (2020), giving estimates of the measures which we refer to as simulated systemic impact measures. We simulate for each of the three time windows $N = 1,000,000$ Hüsler-Reiss realizations, using the estimated variogram parameters. We then obtain the simulated systemic impact measures, that is the (simulated) average affected number of banks

$$\overline{A}_b(i) := \frac{\sum_{n=1}^{N} \sum_{j=1}^{d} \mathbb{1}\left(Y_i^{(n)} > 1\right) \mathbb{1}\left(Y_j^{(n)} > 1\right)}{\sum_{n=1}^{N} \mathbb{1}\left(Y_i^{(n)} > 1\right)}$$

and the (simulated) average affected proportion of capital

$$\overline{A}_c(i) := \frac{\sum_{n=1}^{N}\sum_{j=1}^{d}\mathbb{1}\left(Y_i^{(n)}>1\right)\frac{c_j}{c_{\text{tot}}}\mathbb{1}\left(Y_j^{(n)}>1\right)}{\sum_{n=1}^{N}\mathbb{1}\left(Y_i^{(n)}>1\right)}.$$

As in the case for the centrality measures discussed in Section 3.4.1 we report the simulated systemic impact measures for all estimated graphical structures and determine whether these measures are significantly higher for G-SIBs than for normal banks using one-tailed Mann-Whitney U tests.

3.4.3 Binary logistic regression

To better investigate whether the estimated graphs are able to identify systemically important banks we perform binary logistic regressions. We focus on data and estimates from the period 2016-2019, though regression results for the other two periods are also given in Appendix A.10. As a binary dependent variable we use a G-SIB indicator, which indicates whether the bank was considered a G-SIB by the FSB at least once during the corresponding time window (see Table 8 in Appendix A.1). We estimate parameters in the model

$$\log\left(\frac{\pi(i)}{1-\pi(i)}\right) = a_0 + a_1x_1(i) + \ldots a_mx_m(i),$$

where $\pi(i)$ is the probability bank i is a G-SIB given predictor variables $x_1(i),\ldots,x_m(i)$. We use, besides no predictors as baseline, various combinations from the log-average market capitalization ($\log(c_i)$) and the model-implied importance measures given in Section 3.4.1 and 3.4.2.

For every regression we have 55 data points, which is a small sample. Therefore the results of the regressions should not taken too strongly in itself, but rather as a supplement to the analysis on the graphical estimates. In particular the regressions provide us with an hit rate (percentage of correctly classified banks in the sample) and a decision boundary to visualize the relation between the predictors and the designation of G-SIBs by the FSB.

3.4.4 Bivariate tail dependencies

To determine whether the estimated graphs retain bivariate tail dependence, given by $\chi_{ij} = \lim_{y\to\infty} \mathrm{P}(Y_i > y \mid Y_j > y)$, between pairs of banks we compare model-implied tail dependencies to empirical tail dependencies for each of the estimated graphical structures. The tail dependence implied by the graphical extremal model is given by

$$\chi_{ij}^{\mathrm{im}} := 2 - \Lambda_{\{i,j\}} = 2 - 2\Phi\left(\frac{\sqrt{\Gamma_{ij}}}{2}\right),$$

where Φ is the standard normal cumulative probability density function (see Engelke and Hitz (2020)). Note that from this equation we obtain that $\Gamma_{ij} = 0$ implies a complete extremal dependence, while a large Γ_{ij} implies a low extremal dependence. We compare the model-implied bivariate tail dependencies χ_{ij}^{im}, using estimated variogram $\hat{\Gamma}$, to empirical tail dependencies given by

$$\chi_{ij}^{\mathrm{em}} := \frac{1}{m}\sum_{n=1}^{N} \mathbb{1}\left(Y_i^{(n)} > \tilde{Y}_i^{(N-m)}, Y_j^{(n)} > \tilde{Y}_j^{(N-m)}\right),$$

where $\tilde{Y}_i$ and $\tilde{Y}_j$ denote the ordered versions of Y_i and Y_j, such that $\tilde{Y}_i^{(n)} < \tilde{Y}_i^{(n+1)}$ and $\tilde{Y}_j^{(n)} < \tilde{Y}_j^{(n+1)}$ for all $1 \leq n < N$. We use $m = 60$, determined using parameter stability plots in Appendix A.5.

4 Results

In this section we present and review our results. In Section 4.1 we show the estimated graphs for all three periods 2016-2019, 2012-2015 and 2008-2011, and analyse the position of banks, first in relation to size and systemic importance (according to the FSB), then in relation to region and country. In Section 4.2 we present and discuss the model-implied importance measures for G-SIBs and attempt to identify G-SIBs using binary logistic regression. In Section 4.3 we compare the model-implied bivariate tail dependencies to empirical bivariate tail dependencies.

4.1 Estimated graphical structures

4.1.1 Systemic importance and size

Figures 2, 3 and 4 show the estimated graphical structures for the full sample of 55 banks for the windows 2016-2019, 2012-2015 and 2008-2011 respectively in relation to size, determined by average market capitalization in the corresponding period, and whether it was considered a G-SIB by the FSB during the corresponding years. The estimation results of the univariate model for the log-losses (see Section 3.1.1) are given in Appendix A.7, while the variogram parameters corresponding to the estimated graphs are given in Appendix A.8.

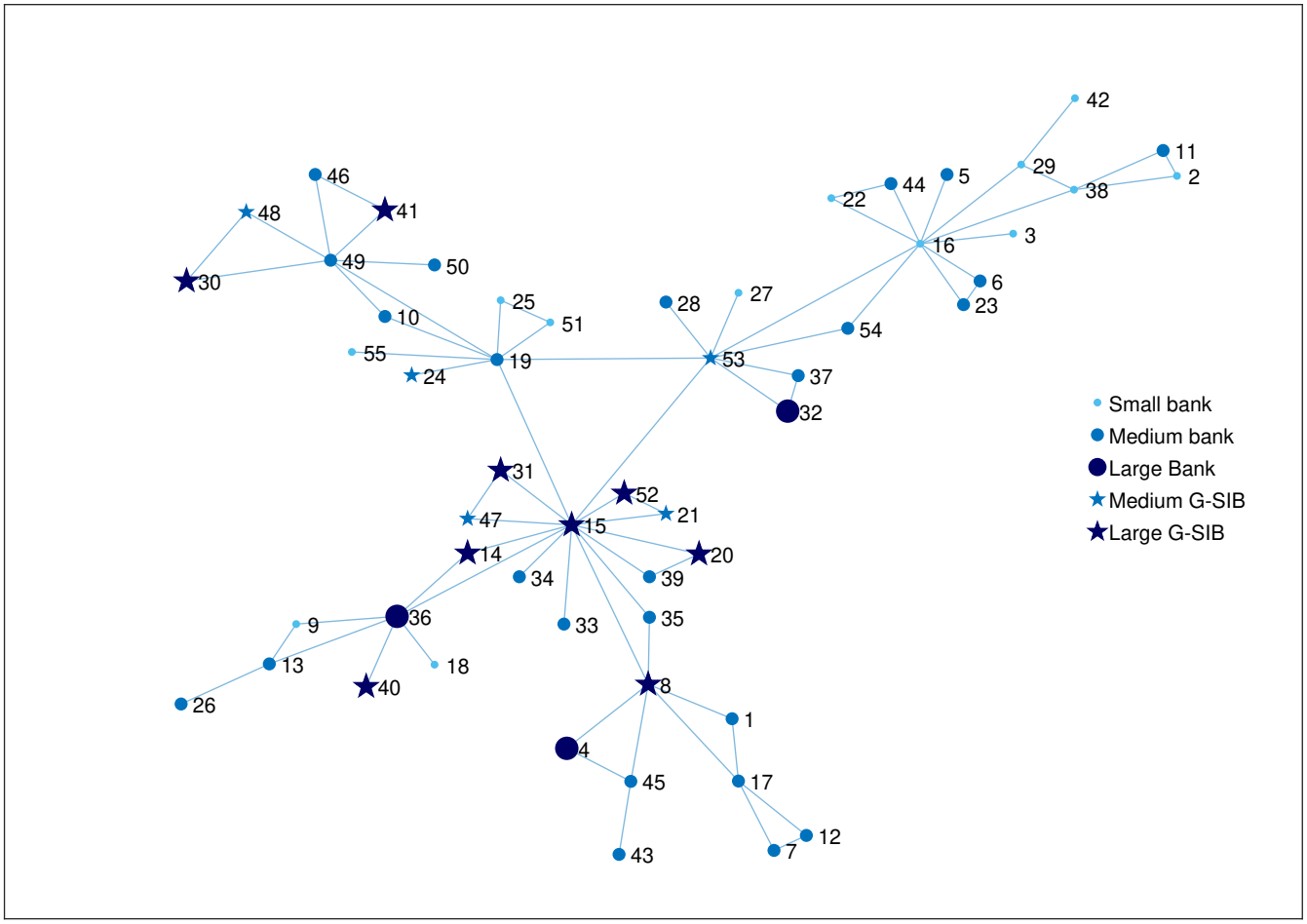

Figure 2: Estimated graph for 2016-2019 in relation to size and a systemic importance. Bank size is determined from average market capitalization in 2016-2019, with an average market capitalization smaller than 3 billion Euros corresponding to a small bank and an average market capitalization larger than 30 billion Euros corresponding to a large bank. The G-SIB indicator indicates if the banks was considered a G-SIB at least once during 2016-2019.

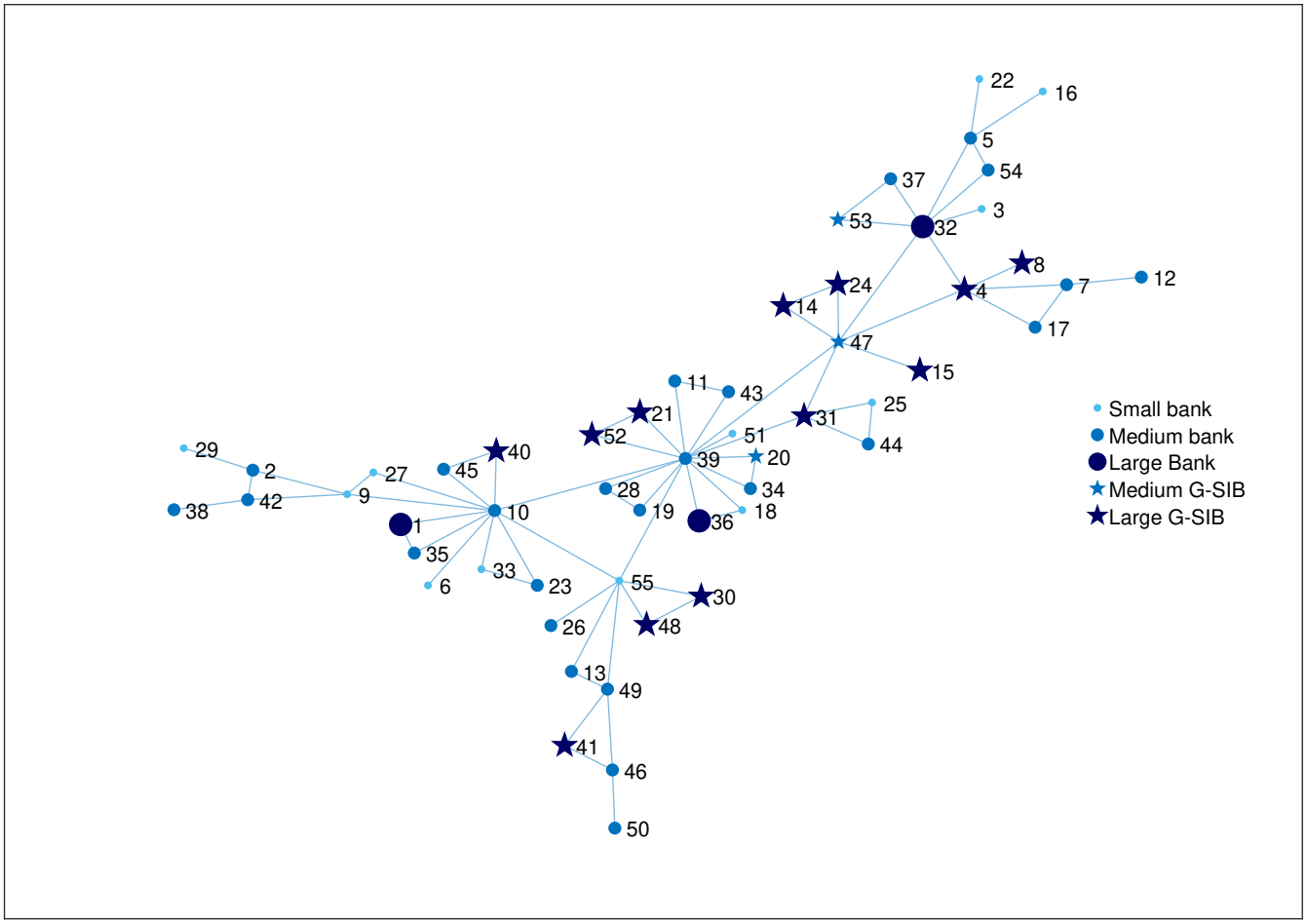

Figure 3: Estimated graph for 2012-2015 in relation to size and a systemic importance. Bank size is determined from average market capitalization in 2012-2015, with an average market capitalization smaller than 3 billion Euros corresponding to a small bank and an average market capitalization larger than 30 billion Euros corresponding to a large bank. The G-SIB indicator indicates if the banks was considered a G-SIB at least once during 2012-2015.

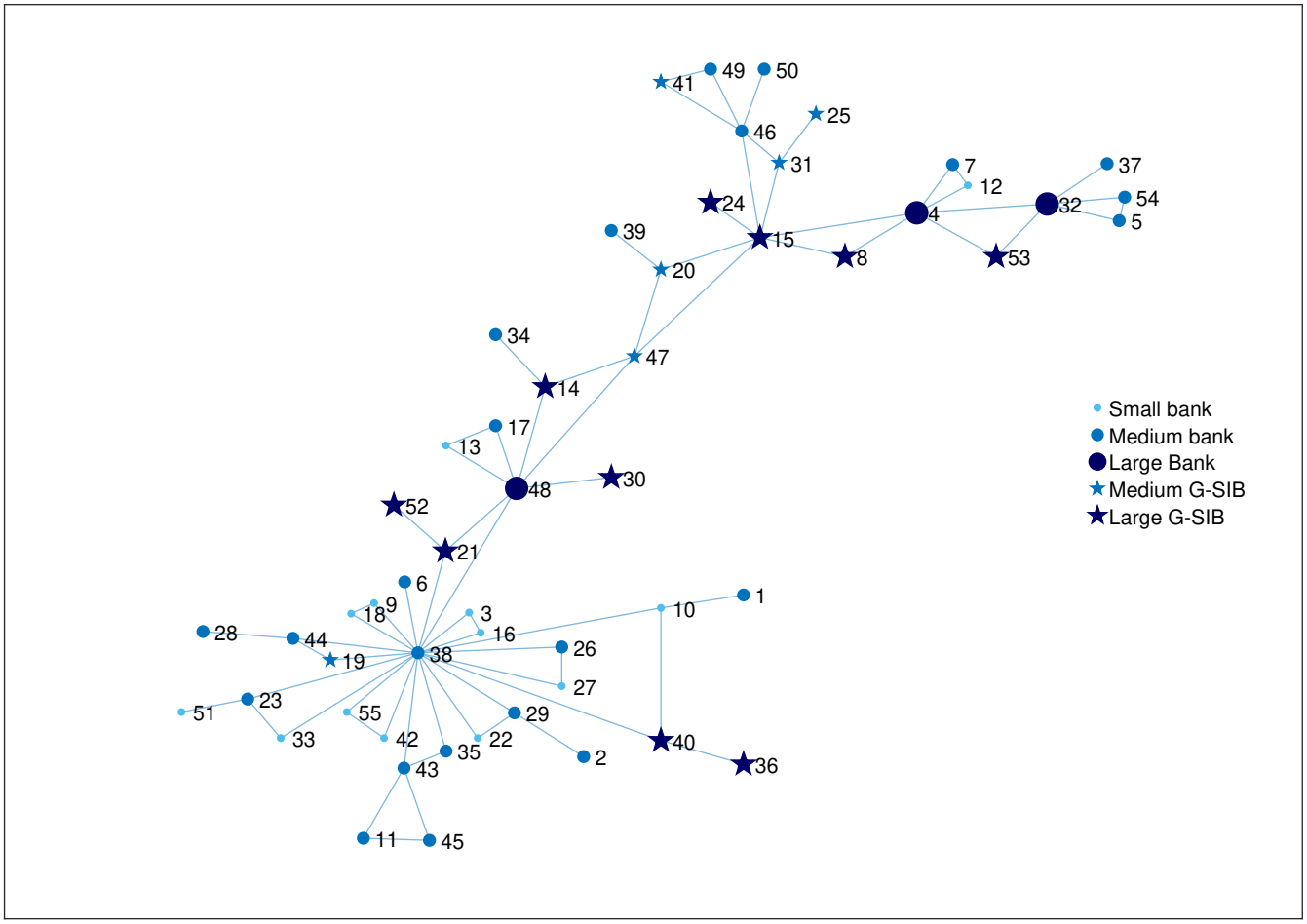

Figure 4: Estimated graph for 2008-2011 in relation to size and a systemic importance. Bank size is determined from average market capitalization in 2008-2011, with an average market capitalization smaller than 3 billion Euros corresponding to a small bank and an average market capitalization larger than 30 billion Euros corresponding to a large bank. The G-SIB indicator indicates if the banks was considered a G-SIB in 2011.

For a proper representation of the network structure of systemic risk we expect that G-SIBs, and to a lesser extend large banks, take on a central position in the graph. The figures show some signs that G-SIBs and larger banks occupy more central positions, while smaller banks are mostly located on the outer regions, but the evidence is thin. For example, in Figure 2 we observe a prominent central cluster of G-SIBs, and large banks, where in particular the G-SIBs Banco Santander (index 8), BNP Paribas (index 15), UniCredit (index 53) and the large bank Lloyds Banking Group (index 36) are centrally positioned and highly connected. Figure 3 shows a similar cluster of G-SIBs, largely consisting of the same banks, with Banco Bilbao Vizcaya Argentaria (index 4), ING

Groep (index 31), Intesa Sanpaolo (index 32) and Societe Generale (index 47) now taking on the central positions. The cluster itself is located at a less central position, however. In Figure 4 a similar cluster is centered around BNP Paribas (index 15).

On the other hand all figures also show G-SIBs that are isolated on the outer regions of the graphs. The most prominent examples are Natwest Group (index 40) and Nordea Bank (index 41), which are located on the boundary in each case. We note that both Natwest Group and Nordea lost their designation as G-SIB in 2018 (see Table 8), however, to take these results from the estimated graphical structures as a precursor for this decline in systemic importance is a step too far. The largest European bank, consistently considered as systemically important, HSBC (index 30) has a low degree in each case, and is located at the edge of the graph for 2016-2019.

There are also cases of systemically unimportant banks, even smaller ones, that occupy important positions in the graphical structures. Notable examples are BPER Banca (index 16) and Commerzbank (index 19) in Figure 2 or Bank of Ireland (index 10), Natixis (index 39) and Valiant Holding (index 55) in Figure 3. Furthermore, in Figure 4 we observe the highly connected National Bank of Greece (index 38) with a degree of 21.

From these graphs we observe no clear relation between designated systemic importance, or size, and its location in the graph. Even though smaller systemically less important banks taking on a central position in the graph are somewhat rarer than centrally located G-SIBs or large banks, the evidence is not conclusive. However, from observing these estimated graphs there is also insufficient evidence to dismiss the graphical extremal model in its entirety, without further exploring the centrality measures.

4.1.2 Regional and inter-country clustering

Figures 5, 6 and 7 show the same estimated graphs as in Section 4.1.1, only now in relation to the region and country of the bank. The regional division of Europe is obtained from EuroVoc, while the two-letter country codes can be found in Tables 7a and 7b.

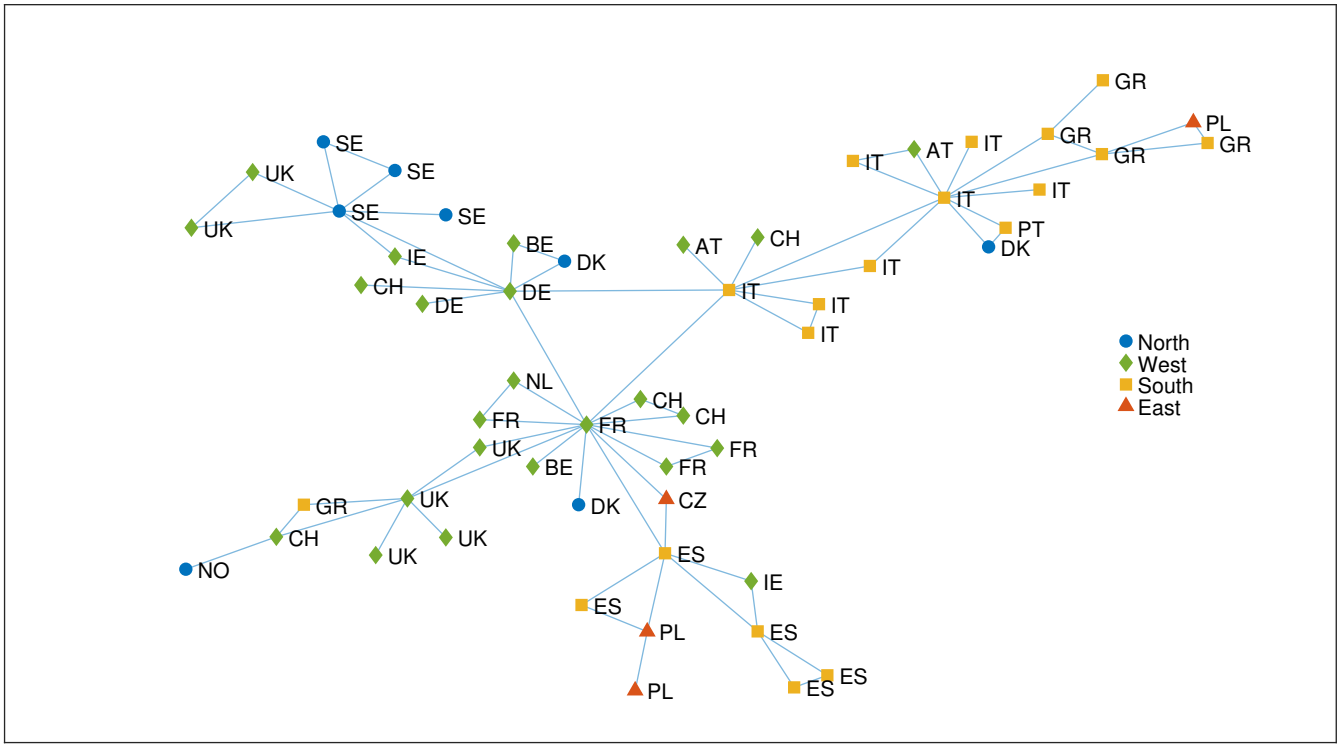

Figure 5: Estimated graphical structure for 2016-2019 for all 55 banks in relation to country and region of the banks.

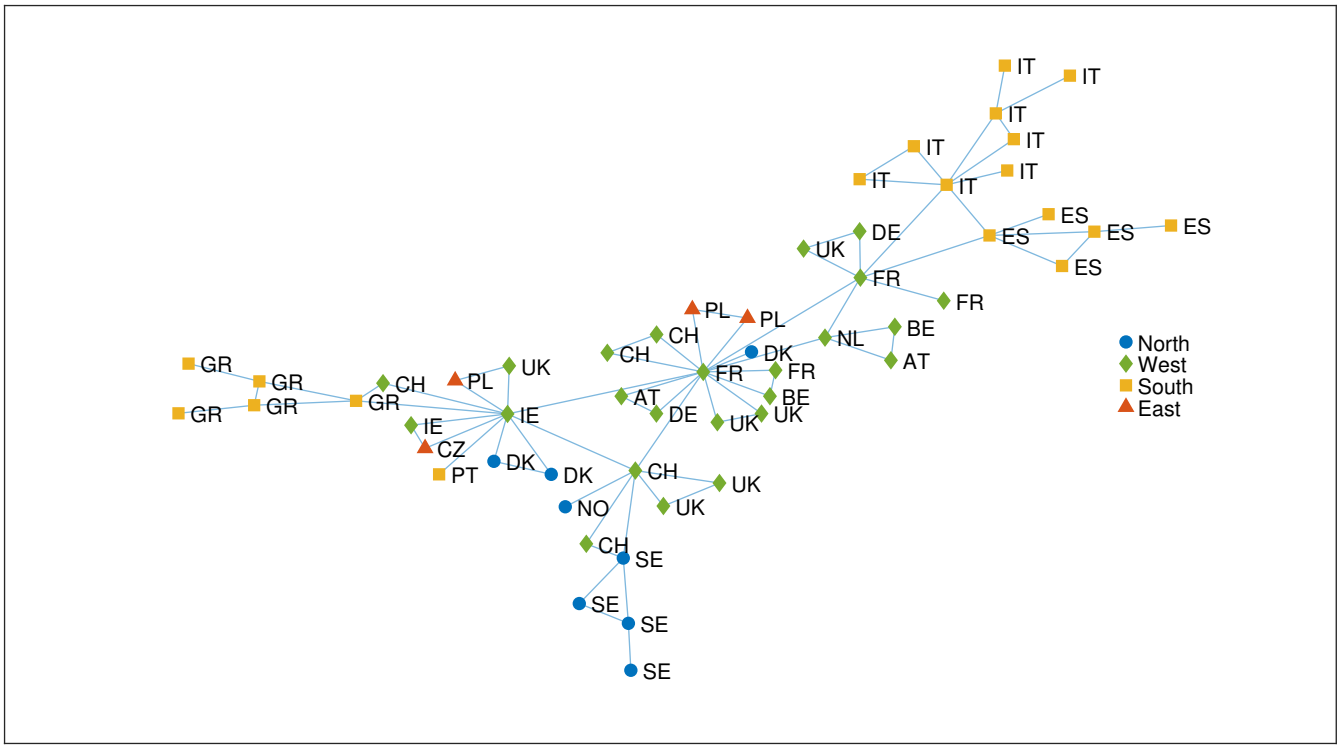

Figure 6: Estimated graphical structure for 2012-2015 in relation to country and region of the banks.

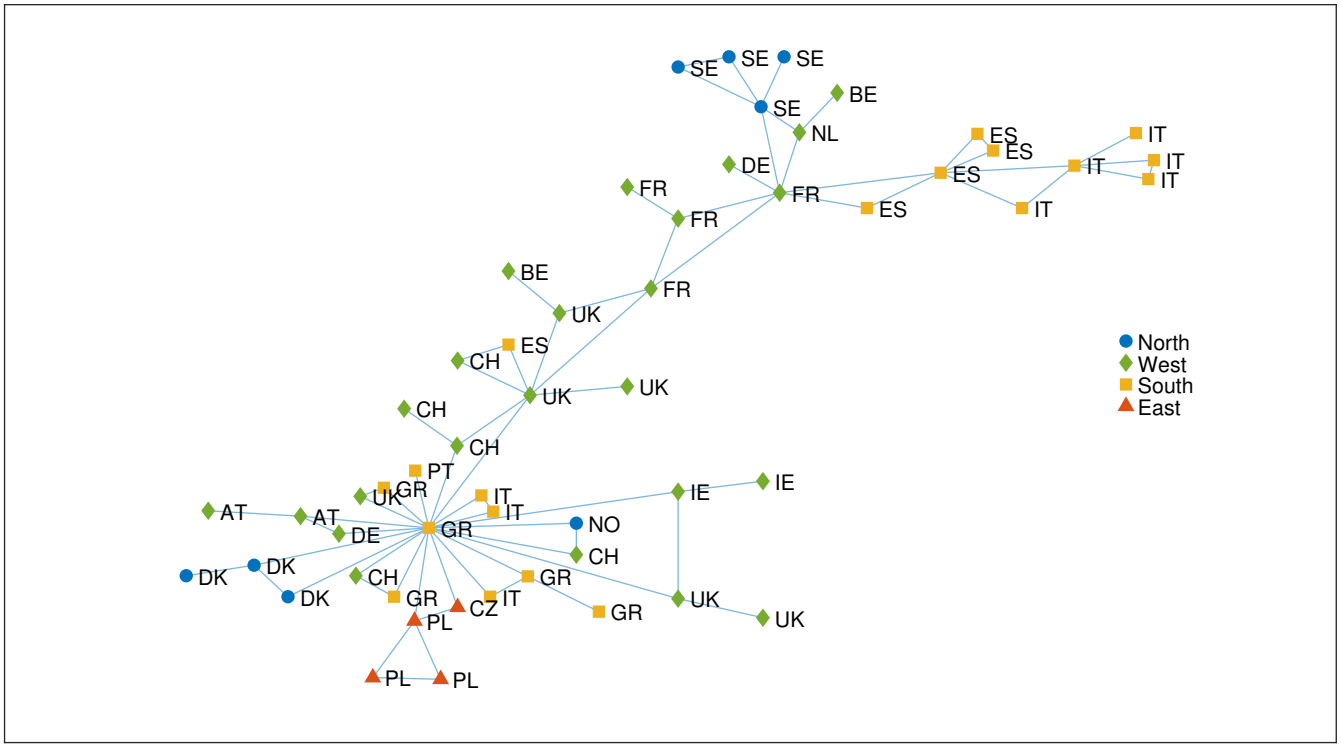

Figure 7: Estimated graphical structure for 2008-2011 in relation to country and region of the banks.

We observe clear signs of regional and inter-county clustering in all figures. For example, Spanish, Italian, Greek and Swedish banks are almost exclusively connected in its own connected cluster in each graph, while connections within other countries are common. Countries within a region, or countries geographically close, are also closely connected in the graphical structures, though the precise connections are not entirely consistent throughout the three time windows. For example the Southern region in each of the graphs is separated in two not directly connected groups. In Figure 5 we observe that Italian and Greek banks, clustered together, are separated from Spanish banks, while in Figure 6 a cluster of Italian and Spanish banks is separated from the Greek banks. In Figure 7 the Italian banks are divided, some connected to a Greek cluster and some connected to a Spanish cluster. Similarly we observe that the 4 eastern European banks are only directly connected in the graph for 2008-2011.

4.2 Importance measures and G-SIB identification

4.2.1 Model-implied systemic importance measures for G-SIBs

Tables 1, 2 and 3 show for all G-SIBs the three centrality measures (closeness, betweenness and degree), described in Section 3.4.1, and the two simulated systemic impact measures (average affected number of banks and average affected proportion of capital), described in Section 3.4.2. The tables also show the rank, averaged in case of ties, and the average measures and ranks for all G-SIBs. Furthermore the tables report the p-value of one-tailed Mann-Whitney U tests, to determine whether G-SIBs have statistically significantly higher measures when compared to other banks. The full tables of measures for all 55 banks can be found in the Appendix A.9. The three centrality measures are obtained from the estimated graphical structures, shown in Section 4.1. The other two measures are obtained from 1,000,000 simulations using the estimated variogram parameters (Appendix A.8).

Table 1: Centrality measures and simulated systemic impact measures and their (averaged) ranks for all G-SIBs for 2016-1019. The average measures and ranks for all G-SIBs and p-values for Mann-Whitney U tests (one-tailed) are also reported.

ID	$C_c(i)$		$C_b(i)$		$C_d(i)$		$\overline{A}_b(i)$		$\overline{A}_c(i)$ (%)	
8	0.348	5	0.238	5	0.111	6½	12.24	4	30.07	2
14	0.329	8	0	34	0.037	27	10.15	13	23.93	9
15	0.462	1	0.654	1	0.259	1	14.33	1	34.38	1
20	0.320	12½	0	34	0.037	27	11.62	5	27.04	4
21	0.320	12½	0	34	0.037	27	9.98	14	23.52	11
24	0.295	26½	0	34	0.019	48½	8.77	20	18.44	22
30	0.241	45½	0	34	0.037	27	5.25	50	21.96	14
31	0.320	12½	0	34	0.037	27	11.50	6	27.65	3
40	0.255	42½	0	34	0.019	48½	8.07	22	18.91	20
41	0.241	45½	0	34	0.037	27	5.71	47	14.42	29
47	0.320	12½	0	34	0.037	27	11.29	8	26.32	5
48	0.241	45½	0	34	0.037	27	4.85	51	14.75	28
52	0.320	12½	0	34	0.037	27	9.69	15	23.86	10
53	0.435	2	0.479	2	0.148	3½	12.83	2	25.30	7
Av.	0.318	20.29	0.098	27.29	0.064	25.07	9.73	18.43	23.61	11.79
p		0.02		0.42		0.21		< 0.01		< 0.01

Table 2: Centrality measures and simulated systemic impact measures and their (averaged) ranks for all G-SIBs for 2012-1015. The average measures and ranks for all G-SIBs and p-values for Mann-Whitney U tests (one-tailed) are also reported.

ID	$C_c(i)$		$C_b(i)$		$C_d(i)$		$\overline{A}_b(i)$		$\overline{A}_c(i)$ (%)	
4	0.314	18	0.142	6	0.093	6	11.56	4	25.62	4
8	0.240	45	0	35	0.019	49½	9.88	11	23.41	7
14	0.289	25½	0	35	0.037	29	8.93	15	20.30	9
15	0.287	30½	0	35	0.019	49½	11.46	5	25.80	2
20	0.320	11	0	35	0.037	29	8.92	16	17.77	16
21	0.320	11	0	35	0.037	29	7.66	25	16.78	22
24	0.289	25½	0	35	0.037	29	10.55	7	23.01	8
30	0.281	33½	0	35	0.037	29	3.96	48	18.42	13
31	0.362	5	0.073	10	0.074	8½	11.41	6	24.23	5
40	0.289	25½	0	35	0.037	29	5.79	36	12.37	32
41	0.228	49	0	35	0.037	29	3.80	50	8.33	40
47	0.400	2½	0.454	2	0.130	4	13.10	1	28.19	1
48	0.281	33½	0	35	0.037	29	3.71	51	12.20	33
52	0.320	11	0	35	0.037	29	8.44	19	19.27	11
53	0.244	40½	0	35	0.037	29	10.07	9	20.06	10
Av.	0.298	24.47	0.045	29.2	0.047	27.17	8.62	20.2	19.72	14.2
p		0.16		0.63		0.40		0.01		< 0.01

Table 3: Centrality measures and simulated systemic impact measures and their (averaged) ranks for all G-SIBs for 2008-2011. The average measures and ranks for all G-SIBs and p-values for Mann-Whitney U tests (one-tailed) are also reported.

ID	$C_c(i)$		$C_b(i)$		$C_d(i)$		$\overline{A}_b(i)$		$\overline{A}_c(i)$ (%)	
8	0.250	32	0	36½	0.037	29½	9.78	4	29.20	2
14	0.318	5	0.037	13	0.056	13	8.11	11	22.43	10
15	0.316	6	0.473	3	0.130	2½	10.49	1	30.26	1
19	0.286	16	0	36½	0.037	29½	5.57	38	7.99	39
20	0.290	7½	0.037	13	0.056	13	9.26	7	25.34	7
21	0.331	4	0.037	13	0.056	13	7.34	18	18.52	16
24	0.241	36	0	36½	0.019	48½	7.92	15	22.21	11
25	0.199	52	0	36½	0.019	48½	6.16	29	14.82	26
30	0.281	29	0	36½	0.019	48½	7.18	19	26.41	5
31	0.248	34	0.037	13	0.056	13	8.30	10	22.06	12
36	0.225	40½	0	36½	0.019	48½	4.71	50	10.18	32
40	0.289	9½	0.037	13	0.056	13	5.80	34	12.03	30
41	0.201	49½	0	36½	0.037	29½	6.57	25	16.05	18
47	0.355	3	0.465	4	0.074	7½	9.64	5	26.74	4
52	0.250	32	0	36½	0.019	48½	5.73	35	15.27	23
53	0.209	46	0	36½	0.037	29½	8.09	12	22.68	9
Av.	0.268	25.13	0.070	25.03	0.045	27.22	7.54	19.56	20.14	15.31
p		0.20		0.19		0.41		< 0.01		< 0.01

The graph-induced centrality measures shown in the table echo some of the observations we noted in Section 4.1.1. Some of the G-SIBs have high centrality measures, in particular closeness centrality, and it is more the case for the time window 2016-2019 than for the other two periods. We clearly note the central cluster of G-SIBs in Table 1, where 9 out of 14 G-SIBs have a relatively high closeness centrality with ranks between 1 and 12½. The difference between G-SIBs and other banks is also statistically significant (at a 5% significance level) in this case. In the other two tables the closeness centrality is lower, still ranking above average, but the difference is not statistically significant according to the Mann-Whitney U tests. This corresponds to the less central positions of the clusters of G-SIBs.

The other two centrality measures are less capable of showing any kind of relation to the designated systemic importance, with most of the G-SIBs having average or even low ranks. The Mann-Whitney U tests show no significant positive differences. We also notice that there are G-SIBs that rank low for all centrality measures, such as HSBC (index 30). Furthermore the centrality measures show a lack of consistency over time. Take for example BNP Paribas (index 15), ranking high for all measures in 2016-2019 and 2008-2011, but clearly below average in 2012-2015. Other examples are Banco Santander (index 8) and UniCredit (index 53). While a change in systemic importance over the years is entirely possible, such radical changes for banks that are considered G-SIBs throughout all these years are not realistic.

The average affected number of banks is more in line with the G-SIB designation of the FSB than the centrality measures. The average rank for all G-SIBs is clearly higher when compared to the centrality measures and, according to the Mann-Whitney tests, the average affected number of banks is significantly higher for G-SIBs at 1% significance level in each of the time windows. Due to taking into account the strength of the connections of the graph, we observe some shifts in rankings when compared to the centrality measures. Clear examples of this occur for BNP Paribas (index 15) in 2012-2015 and Banco Santander (index 8) in 2008-2011. The ranking of the average affected number of banks

(respectively 5 and 4) is much higher than any of the corresponding centrality measures (all below average). This may point to some increased stability of this measure. Where the centrality measures, in particular betweenness and degree, may be very sensitive to small changes in graphical structure, the average affected number of banks is potentially more stable. There are, however, still some banks with vastly changing rankings between the three time windows, as for example HSBC (index 30), which ranks respectively 50, 48 and 19 in the three periods of time. The shift in ranking between the centrality measures and the average affected number of banks also occurs in opposite direction, as can be seen for the Natwest Group (index 40) in Table 3. These results suggest that the variogram parameters for the estimated graphs do provide some additional information that helps to better identify G-SIBs, compared to only using the graphical structure itself.

The average affected proportion of capital shows the greatest potential to identify the designated G-SIBs. The average rank of all G-SIBs is higher when compared to all other measures. Consequently the difference between G-SIBs and other banks is also significant. Most G-SIBs rank better when compared to the average affected number of banks, while the banks that rank worse usually rank only marginally worse. A point to make is that this measure, as opposed to the other 4 measures, is not entirely dependent on the estimated parameters of the graphical extremal model, but also on the market capitalizations of the banks.

4.2.2 G-SIB identification using binary logistic regressions

Table 4 shows the results of the binary logistic regression we described in Section 3.4.3, using the estimated graphical structures of 2016-2019. The same regression results for the other two time windows are givn in Appendix A.10 and in general these results are comparable to the results for 2016-2019. Table 5 shows the results of regressions using closeness centrality, average affected number of banks and average affected proportion of capital combined with log-average market capitalization. Figure 8 shows three scatterplots of these three measures against log-average market capitalizations for all 55 banks and

decision boundaries based on the binary logistic regressions.

Table 4: Parameters estimates (with standard errors), McFadden R^2 and Hit Rates (both for all banks and G-SIBs only) for logistic regression of the G-SIB indicator against, log-capitalization, closeness centrality, all centrality measures (closeness, betweenness and degree respectively), average affected number of banks and average affected proportion of capital. A single asterisk denotes significance of the predictor at 5% significance level, while a double asterisk denotes significance of the predictor at 1% significance level. Data and graphical estimates are from the time window 2016-2019.

Predictor(s)	None	$log\,(c_i)$	$C_c(i)$	$C_c(i); C_b(i); C_d(i)$	$\overline{A}_b(i)$	$\overline{A}_c(i)$
$\hat{a}_0$	-1.07	-35.49	-5.32	-5.48	-4.51	-6.49
	(0.31)	(12.43)	(1.96)	(3.01)	(1.34)	(1.70)
$\hat{a}_1$		3.45**	14.39*	17.40	0.40**	28.71**
		(1.21)	(6.45)	(9.79)	(0.14)	(8.06)
$\hat{a}_2$				4.97		
				(10.05)		
$\hat{a}_3$				-19.4		
				(26.63)		
McFadden R^2	0	0.54	0.09	0.11	0.15	0.37
Hit Rate (All)	0.75	0.89	0.76	0.76	0.80	0.84
Hit Rate (G-SIBs)	0	0.79	0.14	0.14	0.43	0.64

The results in Table 4 show that the centrality measures are not able to distinguish G-SIBs, as classified by the FSB, from normal banks. Closeness centrality, which was most in line with the G-SIB designation of all the centrality measures in Section 4.2.1, has a comparable performance to our baseline model without predictors. Using all centrality measures jointly to identify the G-SIBs provides barely any change, and none of the predictors in this case are significant at 5% significance level. The average affected number of banks and average affected proportion of capital are somewhat better able to identify the G-SIBs, though the former still fails to identify over half of the G-SIBs. On the other hand, the size of banks, through log-average market capitalization, outperforms all other predictors, with a high McFadden R^2 and successfully identifying most of the G-SIBs from normal banks.

Table 5: Parameters estimates (with standard errors), McFadden R^2 and Hit Rates (both for all banks and G-SIBs only) for logistic regression of the G-SIB indicator against jointly log-average market capitalization (predictor 1) and respectively closeness centrality, average affected number of banks and average affected proportion of capital (predictor 2). A single asterisk denotes significance of the predictor at 5% significance level, while a double asterisk denotes significance of the predictor at 1% significance level. Data and graphical estimates are from the time window 2016-2019.

Predictor 2	$C_c(i)$	$\overline{A}_b(i)$	$\overline{A}_c(i)$
$\hat{a}_0$	-36.09	-33.44	-30.70
	(12.39)	(12.12)	(12.26)
$\hat{a}_1$	3.25**	3.13**	2.79*
	(1.20)	(1.23)	(1.27)
$\hat{a}_2$	8.91	0.14	9.74
	(9.30)	(0.20)	(9.85)
McFadden R^2	0.56	0.55	0.56
Hit Rate (All)	0.91	0.91	0.89
Hit Rate (G-SIBs)	0.86	0.86	0.79

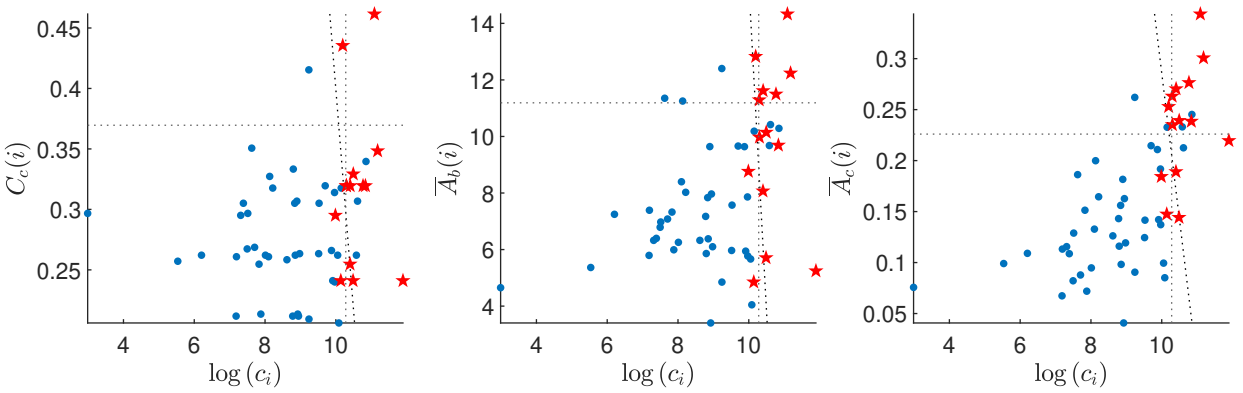

Figure 8: Scatterplots of log-average market capitalization against closeness centrality (left), average affected number of banks (middle) and average affected proportion of capital (right) in 2016-2019. The dotted lines represent the decision boundaries obtained from the binary logistic regressions (using a single predictor and both predictors). G-SIBs are denoted by a red star, while normal banks are denoted by a blue dot.

When combining the predictor of size with one of other predictors we note only minor improvements in McFadden R^2 and Hit Rates. More importantly, while the estimated parameters for size remain significant, those for the additional predictors are not. For closeness centrality and average affected number of banks this is expected, due to the relatively low McFadden R^2 and Hit Rates for these predictors in comparison to the predictor of size. For the average affected proportion of capital this may imply that the

performance of this measure in identifying the G-SIBs is largely due to the high correlation of this measure to size itself. These results are also perceivable in Figure 8, which shows the decision boundaries obtained from the binary logistic regression. It shows the weak relation between closeness centrality, or the average affected number of banks, and the classification of G-SIBs by the FSB. Furthermore Figure 8 shows a correlation of the average affected proportion of capital to the size of the banks itself. It also shows in all three cases that identification based on two predictors is dominated by the predictor of size.

4.3 Bivariate tail dependencies

Figure 9 shows the tail dependencies implied by the three estimated graphs against the empirical tail dependencies for all pairs of banks. The figure also shows a distinction between tail dependencies corresponding to pairs of directly connected banks in the estimated graph structure and pairs of directly unconnected banks. Table 6 shows t-statistics and p-values for two-tailed t-tests, with a null hypothesis of equal model-implied and empirical tail dependence.

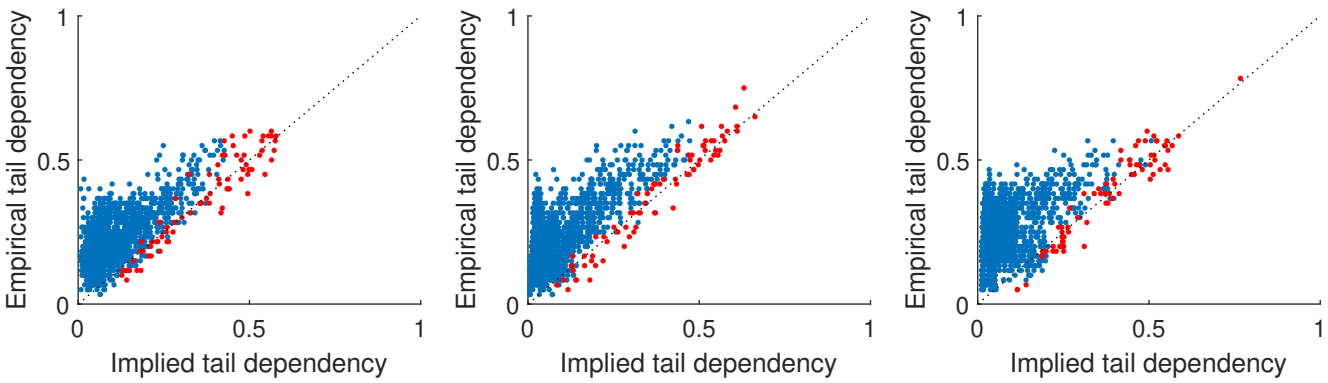

Figure 9: Model implied bivariate tail dependencies against empirical bivariate tail dependencies for all pairs of banks for 2016-2019 (left), 2012-2015 (middle) and 2008-2011 (right). Red points represent pairs of banks that are directly connected in the estimated graphical structures, while blue points represent pairs of banks that are not directly connected.

Table 6: t-statistics and p-values for two-tailed t-tests with null hypothesis $\chi_{ij}^{\text{im}} = \chi_{ij}^{\text{em}}$ for respectively directly connected, directly unconnected and all pairs of banks for all periods.

Period	t (conn.)	p (conn.)	t (unconn.)	p (unconn.)	t (all)	p (all)
2016-2019	-0.06	0.95	65.35	< 0.01	60.04	< 0.01
2012-2015	0.04	0.97	66.52	< 0.01	61.34	< 0.01
2008-2011	-0.02	0.98	74.69	< 0.01	67.85	< 0.01

From Figure 9 we note that generally the estimated graphical structure underestimates the tail dependencies with respect to the empirical tail dependencies. Furthermore there is a clear distinction between pairs banks that are directly connected in the estimated graph structure and pairs that are not. The implied tail dependencies corresponding to directly connected are much closer to the empirical counterparts. Table 6 shows clear statistical evidence for this distinction between directly connected and directly unconnected pairs of banks. We do not reject equal tail dependencies for directly connected pairs of banks at any reasonable significance level, while we reject equal tail dependence for directly unconnected pairs of banks at 1% significance level. Furthermore, since directly unconnected pairs of banks make up the large majority of all pairs, we also clearly reject equal tail dependence for all pairs of banks.

These results can be explained from the procedure for obtaining the graphical structure, as described in Section 3.3. We estimate our variogram parameters on the block graph by optimization on small cliques of size 2 (starting tree) or size 3 (adding edges). It is therefore reasonable to expect that the variogram parameters on the cliques yield accurate tail dependencies, which correspond to pairs of banks directly connected through the graphical structure. Variogram parameters corresponding to pairs of banks that are not directly connected are only indirectly obtained through the relation in Equation (5). Consequently, tail dependencies for these pairs are far less accurate.

The magnitude of the inaccuracy for pairs of unconnected banks, however, is quite large. In particular there are a large number of implied tail dependencies that are very close to zero, when the corresponding empirical tail dependencies are much larger. A potential explanation is that restrictive structure of the graphs severely underestimates

dependency between specific banks, depending on their particular locations in the starting tree and subsequent graphs. When adding an edge to the graph in the algorithm the resulting graphs are restricted to be block graphs with only cliques of 2 and 3. Accordingly there is not much flexibility in increasing the tail dependence between some specific banks, especially when there is a large number of edges between them in the starting tree. This potentially results in very small implied tail dependencies for some banks.

5 Conclusion

In this paper we model systemic risk using a graphical extremal model, based on conditional (in)dependence and the Hüsler-Reiss distribution. Using data from 55 banks we estimate underlying graphical structures for 3 different periods, using a greedy algorithm. We analyse graphical structure, in relation to bank size, systemic importance and region. Furthermore we compare model-implied importance measures and identify systemically important banks, as classified by the FSB, using these model-implied measures and bank size. Finally we compare model-implied tail dependence to empirical tail dependence. From the obtained graphs we observe strong signs of regional and inter-country clustering, but a weak relation between systemic importance, or size, of banks and the centrality of the position in the graph. The centrality measures and average affected number of banks provide a weak identifier for the systemic importance as designated by the FSB. The average affected proportion of capital performs better, but is still outperformed by using the size of banks to identify designated G-SIBs. Model-implied tail dependence is accurate for directly connected pairs of banks, but far less accurate for directly unconnected pairs of banks.

From the results of this paper we conclude that the graphical extremal model, using the specified estimation methods and greedy algorithm, is not able to model systemic risk in European banking effectively. The graphical structures show both large and systemically important banks occupying unimportant positions, and small banks occupying crucial positions. In identifying G-SIBs, as designated by the FSB, the model was outperformed by a simple identifier as size, through the log-average market capitalization, of a bank. These results can potentially be attributed to the significant restrictions applied to graphical structure by the algorithm to determine this structure. These restrictions generate graphical structures that lack flexibility to properly model the complex network of systemic risk, and consequently to identify systemically important banks. The clear distinction between directly connected and directly unconnected pairs of banks in the

accuracy of the model-implied tail dependence compared to empirical tail dependence support this notion. We point out that these limitations are not connected to the underlying theoretical model, but only to the algorithm in determining the optimal graph. If the flexibility of the estimated graphical structures can be increased, allowing for more complex network structures, then the results from this paper can be interpreted as a sign of potential of the model. This potential can be derived from the fact the model-implied systemic importance measures do show some ability to identify G-SIBs based on the significantly higher simulated systemic impact measures of the G-SIBs when compared to other banks. In particular the average number of affected banks is worth mentioning. This measure is significantly (at 1% significance level) higher for G-SIBs than for normal banks in each of the time windows, while the measure is completely dependent on the estimated variogram parameters of the model. Furthermore, the graphical structures show clear signs of regional and inter-country clustering, indicating that graphical structure is certainly not arbitrary.

With an increased complexity of the graphical structure, the model can possibly better model the network of systemic risk in a fully automated manner. The potential improvements of this model therefore should be focused on changing the algorithm to allow for more complex structures. For example, using larger cliques would allow for structures far more complex, though without significant changes in the algorithm this would require a immense increase in computational time. Increasing clique size would increase concurrent parameter estimation, based on numerical methods, while also increasing the complexity in each step of adding an edge. Furthermore replacing block graphs by general decomposable graphs poses similar problems, while replacing decomposable graphs by general graph structures would pose even more significant problems, as the methodology is heavily based on decomposition of graphs.

A Appendix

A.1 Sample of banks

Tables 7a and 7b list the sample of banks used, together with the index number, country, country code (ISO 3166-1 alpha-2), mean market capitalization and rank of mean market capitalization in the period 2008-2019. Table 8 denotes the designation of G-SIBs by the FSB in the years 2011-2019.

Table 7a: Banks used in this paper (1/2). Mean market capitalization is obtained from the entire period 2008-2019.

ID	Bank	Country	Country code	Mean market cap. ($\times 10^9$€)	Rank mean market cap.
1	AIB Group	Ireland	IE	21.176	18
2	Alpha Bank	Greece	GR	3.478	42
3	Banca Popolare di Sondrio	Italy	IT	1.664	50
4	Banco Bilbao Vizcaya Argentaria	Spain	ES	40.941	6
5	Banco BPM	Italy	IT	3.542	41
6	Banco Comercial Portugues	Portugal	PT	3.259	43
7	Banco de Sabadell	Spain	ES	6.779	31
8	Banco Santander	Spain	ES	71.034	2
9	Bank of Greece	Greece	GR	0.446	55
10	Bank of Ireland Group	Ireland	IE	5.760	36
11	Bank Polska Kasa Opieki	Poland	PL	9.520	30
12	Bankinter	Spain	ES	4.499	39
13	Banque Cantonale Vaudoise	Switzerland	CH	3.979	40
14	Barclays	United Kingdom	UK	38.872	8
15	BNP Paribas	France	FR	59.446	3
16	BPER Banca	Italy	IT	2.326	48
17	CaixiaBank	Spain	ES	16.783	23
18	Close Brothers Group	United Kingdom	UK	1.979	49
19	Commerzbank	Germany	DE	10.049	29
20	Credit Agricole	France	FR	26.978	17
21	Credit Suisse Group	Switzerland	CH	32.357	13
22	Credito Valtellinese	Italy	IT	0.754	54
23	Danske Bank	Denmark	DK	17.672	22
24	Deutsche Bank	Germany	DE	28.850	15
25	Dexia	Belgium	BE	2.745	45
26	DNB	Norway	NO	18.446	19
27	EFG International	Switzerland	CH	1.560	52
28	Erste Group Bank	Austria	AT	11.034	27

Table 7b: Banks used in this paper (2/2). Mean market capitalization is obtained from the entire period 2008-2019.

ID	Bank	Country	Country code	Mean market cap. (10^9€)	Rank mean market cap.
29	Eurobank Ergasias	Greece	GR	2.603	47
30	HSBC Holdings	United Kingdom	UK	137.814	1
31	ING Groep	The Netherlands	NL	37.402	9
32	Intesa Sanpaolo	Italy	IT	36.085	10
33	Jyske Bank	Denmark	DK	2.777	44
34	KBC Group	Belgium	BE	17.857	21
35	Komercni banka	Czech Republic	CZ	6.114	34
36	Lloyds Banking Group	United Kingdom	UK	47.344	5
37	Mediobanca Banca	Italy	IT	6.531	32
38	National Bank of Greece	Greece	GR	5.302	37
39	Natixis	France	FR	12.929	26
40	Natwest Group	United Kingdom	UK	39.426	7
41	Nordea Bank	Sweden	SE	33.101	11
42	Piraeus Bank	Greece	GR	2.633	46
43	Powszechna Kasa Oszczednosci Bank	Poland	PL	10.683	28
44	Raiffeisen Bank International	Austria	AT	6.339	33
45	Santander Bank Polska	Poland	PL	5.986	35
46	Skandinaviska Enskilda Banken	Sweden	SE	16.202	25
47	Societe Generale	France	FR	28.755	16
48	Standard Chartered	United Kingdom	UK	32.769	12
49	Svenska Handelsbanken	Sweden	SE	18.089	20
50	Swedbank	Sweden	SE	16.707	24
51	Sydbank	Denmark	DK	1.546	53
52	UBS Group	Switzerland	CH	48.316	4
53	UniCredit	Italy	IT	30.465	14
54	Unione di Banche Italiane	Italy	IT	4.649	38
55	Valiant Holding	Switzerland	CH	1.585	51

Table 8: Banks considered to be G-SIBs by the FSB in the years 2011-2019.

ID	Bank	Years considered a G-SIB
4	Banco Bilbao Vizcaya Argentaria	2012-2014
8	Banco Santander	2011-2019
14	Barclays	2011-2019
15	BNP Paribas	2011-2019
19	Commerzbank	2011
20	Credit Agricole	2011-2019
21	Credit Suisse Group	2011-2019
24	Deutsche Bank	2011-2019
25	Dexia	2011
30	HSBC Holdings	2011-2019
31	ING Groep	2011-2019
36	Lloyds Banking Group	2011
40	Natwest Group	2011-2017
41	Nordea Bank	2011-2017
47	Societe Generale	2011-2019
48	Standard Chartered	2012-2019
52	UBS Group	2011-2019
53	UniCredit	2011-2019

A.2 Algorithm to determine variogram for block graphs

The following algorithm describes how to obtain a full variogram matrix Γ, for which the relation shown in Equation (5) holds from parameters restricted to the edges of a block graph. The proof can be found in Engelke and Hitz (2020). We first order all cliques $C_1, ..., C_M$ of the graph in such a way that $(C_1 \cup \cdots \cup C_m) \cap C_{m+1} \neq \emptyset$ for all $2 \leq m \leq M$. Since $\mathcal{G}$ is a block graph, and therefore all separator sets are singletons, we have that $(C_1 \cup \cdots \cup C_{m-1}) \cap C_m = \{k_m\}$ for some node k_m. We first denote $\Gamma^{(1)}$ to be the symmetric matrix such that the ijth and jith entries correspond to the parameters on the edges of the block graph, and is zero otherwise. We then define $\Gamma^{(m)}$, for $2 \leq m \leq M$, recursively by

$$\Gamma_{ij}^{(m)} = \begin{cases} \Gamma^{(m-1)} & \text{if } i, j \in C_1 \cup \cdots \cup C_{m-1} \\ \Gamma_{ij}^{(1)} & \text{if } i, j \in C_m \\ \Gamma_{ik_m}^{(m-1)} + \Gamma_{jk_m}^{(m-1)} & \text{if } i \in C_1 \cup \cdots \cup C_{m-1} \text{ and } j \in C_m \text{ or visa versa.} \end{cases} \tag{6}$$

We then have that $\Gamma := \Gamma^{(M)}$ is the variogram that restricts to the parameters on the block graph. This construction does not depend on the chosen order of cliques, as long as each cliques intersects at least one of the previous cliques.

A.3 Parameter stability plots for threshold

To determine the threshold choice u in Equation (1) we observe several parameter stability plots. This procedure is based on the notion that for $\mathbf{Y}$ following a multivariate Pareto distribution, with marginals F_i, and a sufficiently large quantile $\tilde{q}$ we have that $\chi^q_{(1,..,d)} := \frac{1}{1-q}\,\mathrm{P}\left(F_1(Y_1) > q, ..., F_d(Y_d) > q\right)$ is constant for $q > \tilde{q}$. Since we assume the marginals X_i follow standard Pareto distributions, we estimate this parameter empirically by:

$$\hat{\chi}^q_{\{1,\dots,d\}} = \frac{1}{T(1-q)} \sum_{t=1}^{T} \mathbb{1}\left(1 - \frac{1}{X_1^{(t)}} > q, \dots, 1 - \frac{1}{X_d^{(t)}} > q\right),$$

where $\mathbb{1}$ is the indicator function. This is procedure is described in Kiriliouk et al. (2018). In our case, if d is large, the empirical estimator will be zero for any reasonable quantile, as there will be no realizations that exceed all quantiles. Hence we estimate the parameter for smaller subsamples of banks of sizes 2, 3 and 4. We first obtain $\mathbf{X}^{(1)}, ..., \mathbf{X}^{(T)}$ by applying the methodology of Section 3.1.1 on the log-losses in the 4-year window 2016-2019. We then choose several random subsamples of banks and plot the nonzero estimated parameters against quantiles $q \in [0.5, 1)$. The resulting parameter stability plots are shown in Figure 10. The 95% confidence intervals are based on bootstrapping.

From the figure a quantile of around 0.9 appears to be a reasonable choice, as most of the estimated parameters stabilize around this quantile. We choose as threshold the 90th percentile of the standard Pareto, hence $u = \frac{1}{1-q} = 10$. In Appendix A.4 we also perform a robustness study on the threshold.

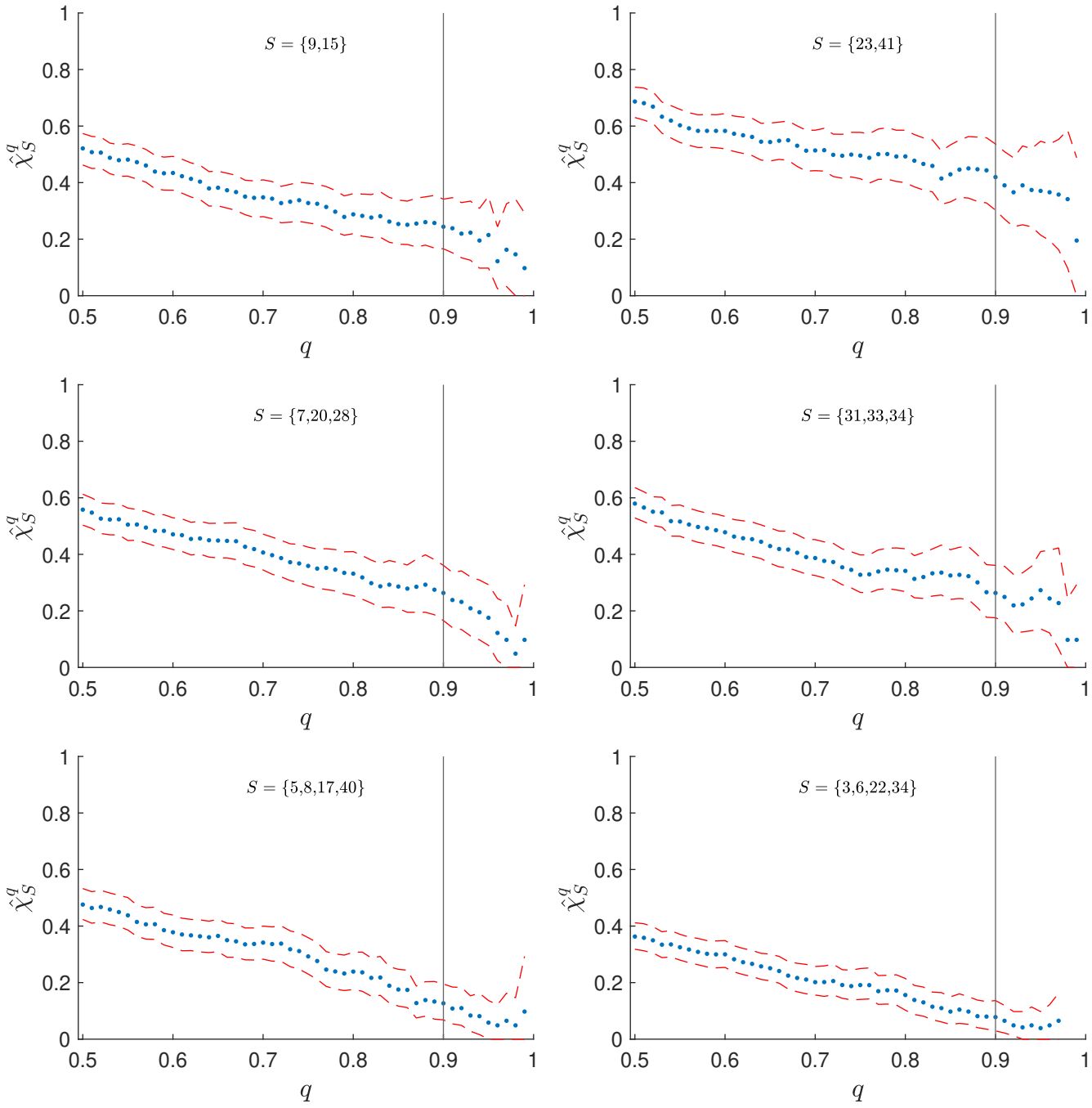

Figure 10: Estimated parameters $\hat{\chi}_S^q$ for randomly chosen subsets S of banks against quantile q, based on data from 2016-2019. The 95% confidence intervals are obtained from bootstrapping the original data, using 1000 resamples. The horizontal line corresponds to our chosen threshold quantile. The indices for the banks used can be found in Tables 7a and 7b.

A.4 Robustness study on threshold choice

In this section we perform a robustness study on the threshold parameter, to see how the threshold choice affects graphical estimations. To do this we estimate optimal graphs, using the methodology of Section 3.3, using several threshold parameters. We use the log-losses of 25 randomly chosen banks, such that there is no particular selection on average market capitalization. The resulting sample contains both small banks, for example Credito Valtellinese (index 22) and CaixiaBank (index 17), and large banks, for example BNP Paribas (index 15) and Lloyds Banking Group (index 36). We use data in the 4-year window 2016-2019 to obtain the estimated graphs. The threshold parameters u are based on the standard Pareto quantiles $q = 0.6, 0.7, 0.8, 0.85, 0.875, 0.9, 0.925, 0.95, 0.99$, through the equality $u = \frac{1}{1-q}$. The graphs obtained in the case of $q = 0.875, 0.9, 0.925$ are shown in Figure 11.

We notice that, even though the graphs differ, the general structures show quite some similarities. Similar edges are shown in red, and are especially apparent in the case of $q = 0.875$. For example we note that nodes 10, 41, 48 and 49 are grouped together similarly and joined to the other nodes at node 19, even though the precise connections are somewhat different. Also node 15, and to a lesser extend nodes 17, 19 and 53, occupy a central position in each of the three graphs. Other similarities are clear from the figure and the general structure is fairly stable under a small adjustment of the quantile.

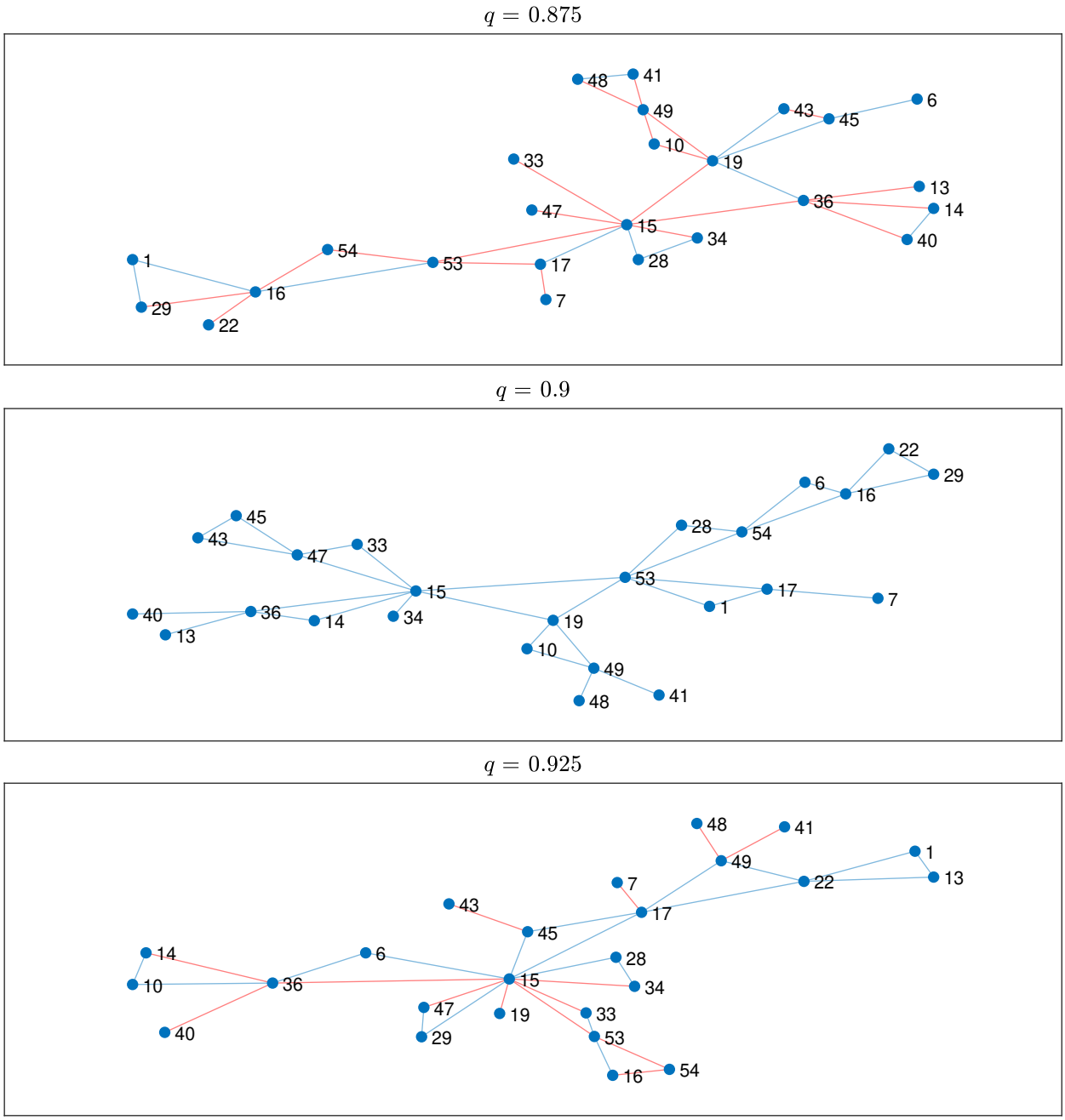

Figure 11: Estimated optimal graphs for quantiles $q = 0.875, 0.9, 0.925$. Red edges represent identical edges to edges in the graph corresponding to $q = 0.9$. The indices for the banks can be found in Tables 7a and 7b.

To further analyse the robustness we assess for all optimal graphs the number of identical edges, taking the graph obtained for threshold 0.9 as baseline. Figure 12 shows the number of identical edges to the optimal graph for $q = 0.9$, which has 33 edges. We note that there is a reasonable number of identical edges, even when comparing to

the lower quantile, which have more then 40% identical edges. We also note the large similarity of 21 edges for the graph corresponding to quantile $q = 0.875$..

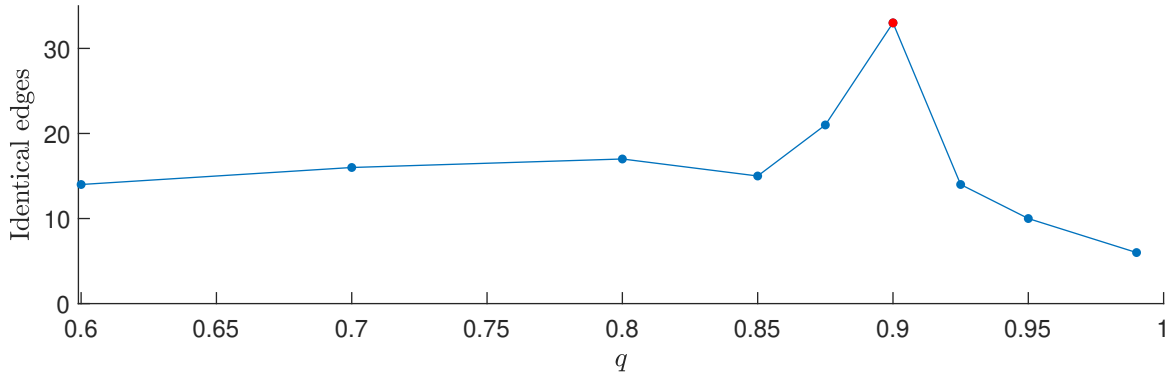

Figure 12: Number of identical edges for the estimated optimal graph for different quantiles q, when compared to the estimated graph for $q = 0.9$.

A.5 Parameter stability plots for empirical tail dependencies

In this section we determine the parameter m for the empirical tail dependencies given by

$$\chi_{ij}^{\text{em}} := \frac{1}{m} \sum_{n=1}^{N} \mathbb{1} \left(Y_i^{(n)} > \tilde{Y}_i^{(N-m)}, Y_j^{(n)} > \tilde{Y}_j^{(N-m)} \right),$$

where $\tilde{Y}_i$ and $\tilde{Y}_j$ denote the ordered versions of Y_i and Y_j, such that $\tilde{Y}_i^{(n)} < \tilde{Y}_i^{(n+1)}$ and $\tilde{Y}_j^{(n)} < \tilde{Y}_j^{(n+1)}$ for all $1 \leq n < N$. For 6 arbitrarily chosen pairs of indices i, j, and using data from time window 2016-2019, we plot the empirical tail dependencies for $1 \leq m \leq 300$. From the plots we choose a parameter of $m = 60$, due to the empirical tail dependency stabilizing around this value in all of the six cases.

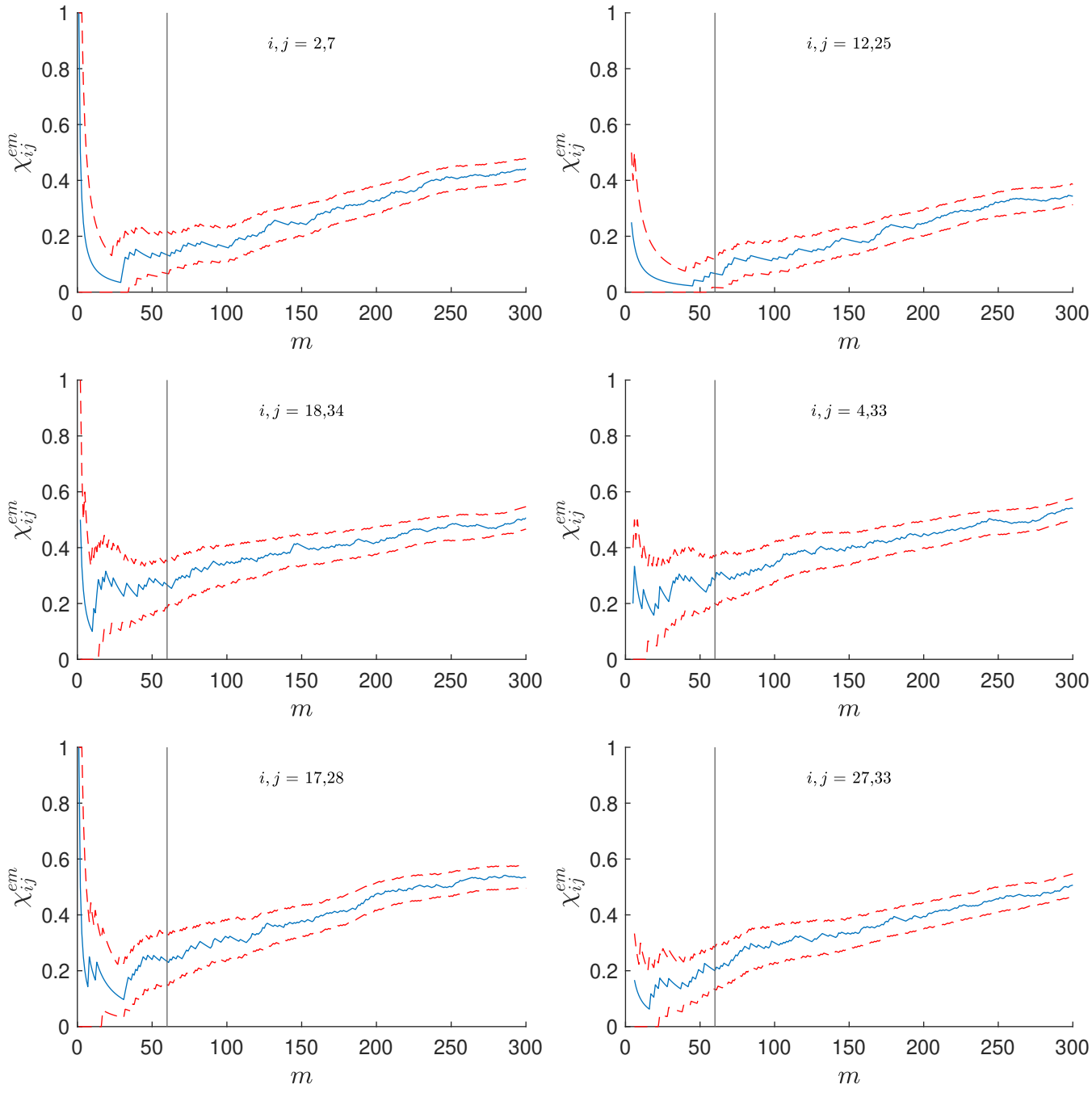

Figure 13: Empirical bivariate tail dependencies χ_{ij}^{em} for randomly chosen pairs i, j of banks against parameter m, based on data from 2016-2019. The 95% confidence intervals are obtained from bootstrapping the original data, using 1000 resamples. The horizontal line corresponds to our chosen parameter $m = 60$. The indices for the banks used can be found in Tables 7a and 7b.

A.6 Estimated graphical structure for subsample of banks

Figures 14, 15 and 16 show the estimated graphical structures for the subsample of 25 banks for the windows 2016-2019, 2012-2015 and 2008-2011 respectively. The variogram parameters, corresponding to the estimated graphs, are given in Appendix A.8.

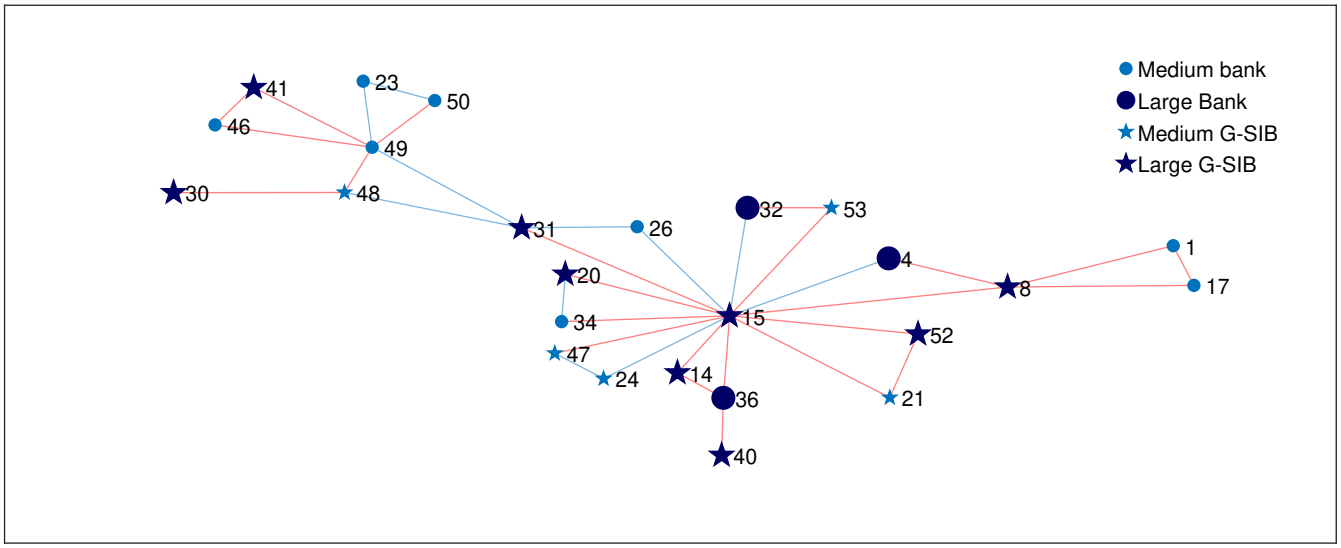

Figure 14: Estimated graphical structure for 2016-2019 for subsample of 25 banks in relation to size and a G-SIB indicator. Bank size is determined from average market capitalization in 2016-2019. A bank with an average market capitalization between 30 and 3 billion Euros is considered medium and a bank with an average market capitalization larger than 30 billion Euros is considered large. The G-SIB indicator indicates if the banks was considered a G-SIB at least once during 2016-2019. Red edges correspond to retained edges with respect to the graph of the full sample of 55 banks.

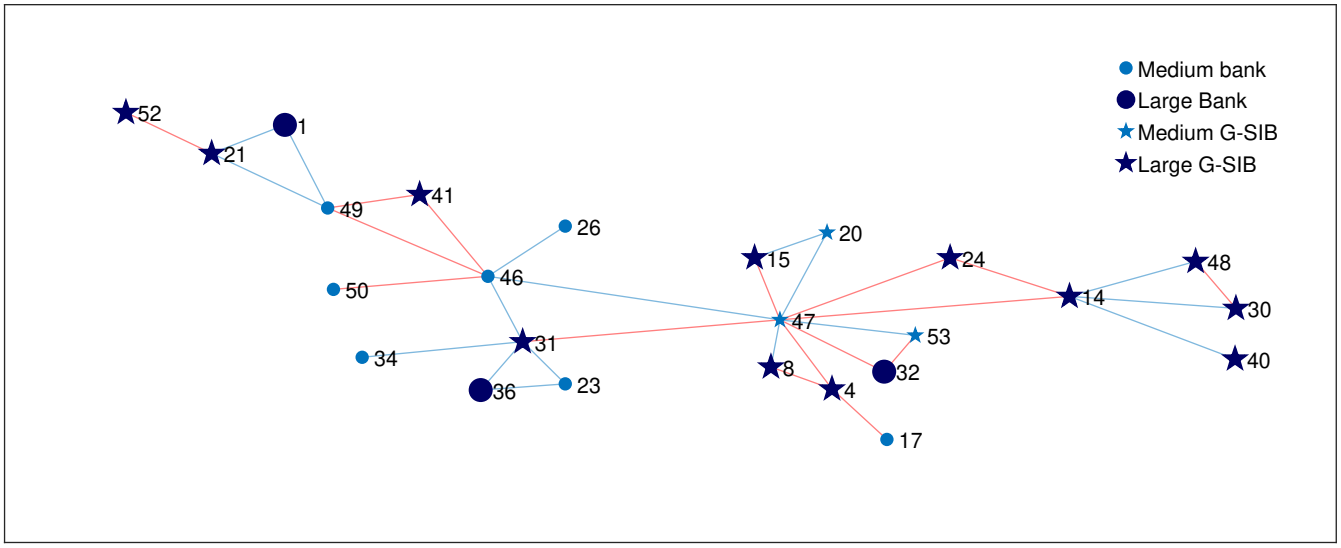

Figure 15: Estimated graphical structure for 2012-2015 for subsample of 25 banks in relation to size and a G-SIB indicator. Bank size is determined from average market capitalization in 2012-2015. A bank with an average market capitalization between 30 and 3 billion Euros is considered medium and a bank with an average market capitalization larger than 30 billion Euros is considered large. The G-SIB indicator indicates if the banks was considered a G-SIB at least once during 2012-2015. Red edges correspond to retained edges with respect to the graph of the full sample of 55 banks.

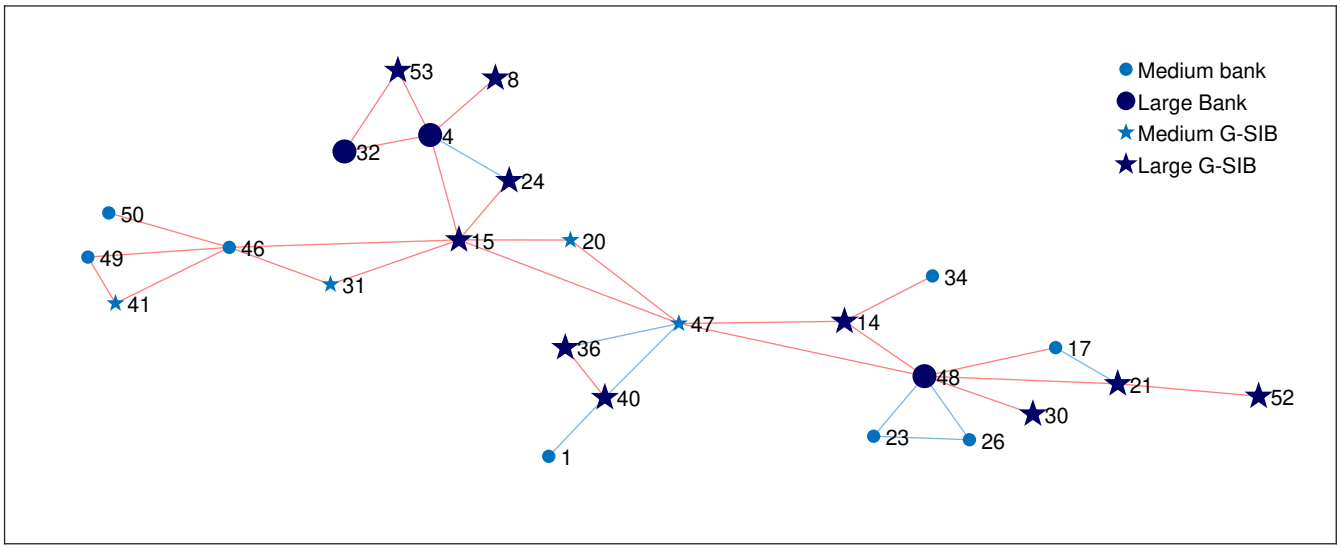

Figure 16: Estimated graphical structure for 2008-2011 for subsample of 25 banks in relation to size and a G-SIB indicator. Bank size is determined from average market capitalization in 2008-2011. A bank with an average market capitalization between 30 and 3 billion Euros is considered medium and a bank with an average market capitalization larger than 30 billion Euros is considered large. The G-SIB indicator indicates if the banks was considered a G-SIB in 2011. Red edges correspond to retained edges with respect to the graph of the full sample of 55 banks.

From the figures it is clear that the general structure is very similar compared to the estimated graphical structures of the full sample, as most edges are retained. The subsample 25 banks made up 26, 18 and 26 edges in the graphs of the full sample of 2016-2019, 2012-2015 and 2008-2011 respectively, and 24, 16 and 25 of these edges are retained in the graphs of the subsamples. The structure generally is unchanged. For example we observe the similar clusters of G-SIBs centered around BNP Paribas (index 15) in Figure 14 and around Societe Generale (index 47) in Figure 15 and around both in Figure 16. This shows the consistency of the estimated graph structure when using a smaller subsample of banks.

A.7 Univariate parameter estimates and Ljung-Box p-values

Tables 9 to 11 show the estimated parameters for the univariate models for the log-losses (see Section 3.1.1) for all 55 banks for time windows 2016-2019, 2012-2015 and 2008-2011 respectively. The tables also show the p-values for the Ljung-Box test on the filtered residuals Z_i. From these values we can assume most filtered residuals to be i.i.d. as necessary for the graphical extremal model. There are only a few exceptions for which we reject independence at 5% significance level, and only in the case of Dexia (index 25) and KBC Group (index 34) for 2016-2019 we reject independence at 1% significance level.

Table 9: Estimated parameters and Ljung-Box p-values for 2016-2019.

ID	$\hat{\mu}_i$ ($\times 10^3$)	$\hat{\phi}_i$	$\hat{\gamma}_i$ ($\times 10^4$)	$\hat{\alpha}_i$	$\hat{\beta}_i$	$\hat{\nu}_i$	p
1	0.600	-0.111	0.344	0.213	0.787	3.492	0.55
2	0.111	0.076	0.452	0.103	0.869	4.432	0.33
3	0.415	-0.035	0.208	0.112	0.844	4.728	0.96
4	0.125	0.037	0.063	0.047	0.931	6.359	0.99
5	0.133	0.051	0.164	0.092	0.893	7.031	0.23
6	0.024	0.037	0.219	0.154	0.829	5.024	0.55
7	0.125	0.063	0.243	0.067	0.885	4.190	0.56
8	0.048	0.035	0.068	0.051	0.926	6.559	0.73
9	-0.742	-0.116	0.164	0.090	0.824	5.355	0.45
10	0.331	0.003	0.063	0.077	0.916	6.575	0.14
11	0.111	0.032	0.033	0.025	0.961	6.508	0.88
12	-0.282	-0.005	0.042	0.049	0.931	5.887	0.89
13	-0.378	-0.141	0.049	0.070	0.867	7.574	0.53
14	0.262	0.066	0.433	0.165	0.716	5.508	0.74
15	-0.031	0.095	0.032	0.044	0.942	6.297	0.89
16	0.082	0.034	0.086	0.063	0.927	4.643	0.96
17	-0.199	0.044	0.654	0.155	0.686	6.095	0.94
18	-0.414	0.024	0.308	0.155	0.727	4.439	0.76
19	0.563	0.063	0.135	0.031	0.944	4.660	0.97
20	-0.280	0.077	0.083	0.073	0.898	5.021	0.49
21	-0.097	-0.012	0.049	0.044	0.940	6.438	0.67
22	2.069	0.068	0.800	0.171	0.778	4.057	0.04
23	-0.260	-0.042	0.084	0.104	0.874	3.772	0.92
24	0.805	0.052	0.094	0.037	0.946	5.535	0.65
25	1.730	-0.144	0.646	0.550	0.450	3.154	0.00
26	-0.645	0.010	0.050	0.041	0.937	4.862	0.99
27	-0.055	0.029	0.706	0.140	0.741	3.596	0.50
28	-0.381	-0.011	0.116	0.044	0.912	5.916	0.08
29	-0.129	0.099	0.636	0.113	0.853	4.652	0.70
30	-0.276	-0.038	0.304	0.177	0.665	4.495	0.59
31	0.081	0.052	0.025	0.053	0.941	4.171	0.97
32	-0.247	0.057	0.041	0.107	0.889	4.830	0.65
33	-0.016	-0.011	0.129	0.067	0.891	3.490	0.92
34	-0.343	0.016	0.053	0.086	0.894	5.514	0.01
35	-0.218	-0.005	0.073	0.129	0.834	4.065	0.14
36	0.404	0.060	0.093	0.101	0.874	4.121	0.48
37	-0.819	0.029	0.048	0.089	0.898	6.101	0.37
38	-0.415	0.088	0.972	0.114	0.823	4.355	0.52
39	-0.181	0.003	0.047	0.028	0.957	5.283	0.68
40	0.042	0.062	0.059	0.060	0.928	4.337	0.28
41	-0.416	0.038	0.174	0.098	0.817	5.205	0.19
42	0.734	0.119	1.932	0.198	0.758	3.626	0.78
43	-0.267	0.013	0.072	0.029	0.947	7.466	0.12
44	-1.289	0.005	0.995	0.147	0.634	4.817	0.72
45	0.224	-0.073	2.007	0.149	0.349	6.112	0.05
46	-0.312	0.017	0.083	0.047	0.910	4.131	0.55
47	0.113	0.099	0.044	0.050	0.937	4.691	0.94
48	-0.183	0.042	0.120	0.093	0.872	7.068	0.94
49	0.077	0.036	0.091	0.073	0.878	5.520	0.48
50	-0.526	0.061	0.390	0.137	0.681	3.875	0.76
51	-0.374	-0.022	0.700	0.191	0.559	3.670	0.54
52	-0.032	0.008	0.048	0.048	0.932	4.713	0.95
53	0.559	0.035	0.074	0.045	0.943	5.647	0.97
54	-0.080	0.033	0.183	0.081	0.895	7.651	0.49
55	-0.055	-0.087	0.018	0.032	0.956	4.237	0.95

Table 10: Estimated parameters and Ljung-Box p-values for 2012-2015.

ID	$\hat{\mu}_i$ ($\times 10^3$)	$\hat{\phi}_i$	$\hat{\gamma}_i$ ($\times 10^4$)	$\hat{\alpha}_i$	$\hat{\beta}_i$	$\hat{\nu}_i$	p
1	1.554	-0.188	3.065	0.199	0.654	4.502	0.09
2	-0.411	0.044	0.683	0.180	0.820	4.125	0.62
3	0.171	-0.062	0.629	0.135	0.742	7.07	0.63
4	-0.536	0.032	0.064	0.045	0.937	6.671	0.55
5	-0.257	0.043	0.071	0.021	0.971	5.863	0.89
6	0.522	0.027	1.565	0.188	0.704	4.373	0.69
7	0.736	0.089	0.536	0.063	0.854	3.565	0.75
8	-0.701	-0.010	0.077	0.058	0.922	6.079	0.46
9	1.244	0.013	1.011	0.342	0.583	3.306	0.99
10	-0.199	0.053	5.498	0.208	0.074	4.824	0.69
11	-0.233	0.032	0.102	0.056	0.908	15.463	0.12
12	-0.841	0.062	0.129	0.063	0.912	8.775	0.80
13	-0.561	-0.133	0.184	0.152	0.686	4.461	0.90
14	-0.416	0.024	0.026	0.015	0.979	4.847	0.54
15	-0.748	-0.032	0.052	0.052	0.934	9.517	0.11
16	-0.419	-0.024	0.169	0.048	0.934	7.425	0.95
17	-0.164	0.002	1.508	0.082	0.555	5.964	0.98
18	-1.320	0.047	0.962	0.126	0.323	5.857	0.59
19	0.153	0.012	0.015	0.017	0.979	5.891	0.91
20	-0.903	0.015	0.035	0.035	0.959	5.841	0.86
21	-0.233	-0.017	0.044	0.032	0.954	4.607	0.56
22	0.145	0.026	0.793	0.121	0.783	4.246	0.04
23	-0.966	-0.062	0.769	0.174	0.535	4.825	0.39
24	0.198	0.017	0.049	0.043	0.945	8.464	0.29
25	4.252	-0.368	0.896	0.235	0.765	4.518	0.56
26	-0.743	-0.006	0.031	0.030	0.961	4.752	0.36
27	-0.265	-0.053	0.432	0.092	0.835	3.499	0.67
28	-1.056	-0.016	0.312	0.061	0.882	5.350	0.63
29	2.535	0.035	1.576	0.233	0.767	3.736	0.71
30	-0.473	-0.059	0.032	0.045	0.938	5.844	0.06
31	-1.099	-0.019	0.074	0.054	0.928	9.563	0.39
32	-1.421	-0.084	0.100	0.042	0.940	8.688	0.10
33	-0.658	0.005	0.288	0.078	0.796	4.841	0.98
34	-1.505	-0.017	0.033	0.048	0.945	10.671	0.24
35	-0.367	0.053	0.121	0.041	0.905	7.429	0.12
36	-0.804	-0.024	0.008	0.020	0.977	7.314	0.60
37	-1.110	-0.022	0.098	0.045	0.937	11.364	0.60
38	1.977	0.065	2.567	0.311	0.689	3.838	0.88
39	-1.386	-0.022	0.084	0.038	0.943	5.611	0.52
40	-0.544	0.015	0.041	0.032	0.958	6.351	0.73
41	-0.776	-0.061	0.068	0.039	0.932	8.515	0.04
42	1.025	0.065	1.895	0.226	0.774	3.793	0.94
43	-0.009	0.076	0.110	0.049	0.904	10.844	0.48
44	0.660	0.013	0.082	0.058	0.936	4.177	0.66
45	-0.519	-0.048	0.015	0.093	0.907	6.573	0.88
46	-1.161	-0.038	0.193	0.093	0.821	7.184	0.02
47	-0.650	0.037	0.041	0.038	0.954	7.421	0.24
48	0.311	0.0260	0.086	0.087	0.894	4.955	0.71
49	-0.906	-0.030	0.510	0.131	0.603	5.088	0.07
50	-1.047	-0.022	0.401	0.130	0.679	6.297	0.02
51	-0.859	0.015	0.025	0.024	0.965	4.698	0.07
52	-0.603	-0.013	0.483	0.099	0.732	4.312	0.69
53	-0.966	-0.035	0.177	0.055	0.918	6.353	0.10
54	-0.842	-0.024	0.139	0.040	0.941	10.799	0.51
55	0.080	-0.080	0.240	0.110	0.797	3.662	0.54

Table 11: Estimated parameters and Ljung-Box p-values for 2008-2011.

ID	$\hat{\mu}_i$ ($\times 10^3$)	$\hat{\phi}_i$	$\hat{\gamma}_i$ ($\times 10^4$)	$\hat{\alpha}_i$	$\hat{\beta}_i$	$\hat{\nu}_i$	p
1	5.715	0.058	1.234	0.185	0.815	4.145	0.23
2	2.475	0.021	0.275	0.066	0.922	8.926	0.84
3	0.662	0.054	0.236	0.296	0.704	3.776	0.20
4	0.495	0.097	0.146	0.099	0.885	6.841	0.51
5	1.917	0.050	0.594	0.143	0.810	6.211	0.68
6	1.389	0.109	0.391	0.153	0.805	5.619	0.90
7	0.817	0.137	0.117	0.044	0.928	3.979	0.57
8	0.221	0.041	0.174	0.082	0.895	6.48	0.59
9	1.492	0.014	0.296	0.249	0.733	3.954	0.57
10	5.152	0.032	1.113	0.129	0.867	3.700	0.64
11	-0.008	0.019	0.046	0.069	0.927	9.805	0.35
12	1.265	0.016	0.181	0.088	0.889	8.705	0.56
13	-0.933	-0.047	0.097	0.089	0.892	4.771	0.86
14	1.078	0.052	0.173	0.098	0.896	6.458	0.21
15	0.070	0.028	0.125	0.093	0.898	7.664	0.48
16	1.578	0.012	0.323	0.163	0.817	3.636	0.43
17	-0.523	-0.036	0.061	0.096	0.894	6.376	0.54
18	-0.062	0.012	0.036	0.029	0.962	4.336	0.73
19	1.118	0.067	0.088	0.095	0.905	5.890	0.55
20	0.769	0.061	0.163	0.071	0.919	7.031	0.59
21	0.489	0.024	0.094	0.106	0.888	7.753	0.08
22	1.418	0.045	0.460	0.263	0.645	5.583	0.82
23	0.555	0.088	0.313	0.167	0.806	6.862	0.26
24	0.561	0.061	0.100	0.109	0.886	8.408	0.30
25	2.338	0.076	0.281	0.120	0.874	5.067	0.04
26	-0.305	-0.017	0.086	0.106	0.891	8.776	0.95
27	0.503	-0.001	0.082	0.050	0.946	4.465	0.74
28	-0.316	0.025	0.069	0.091	0.908	9.283	0.10
29	3.415	0.050	0.377	0.069	0.915	7.656	0.58
30	0.279	-0.048	0.066	0.076	0.913	5.435	0.48
31	-0.379	0.044	0.28	0.152	0.840	7.632	0.44
32	0.673	0.023	0.124	0.089	0.903	6.551	0.16
33	0.556	0.101	0.175	0.130	0.854	5.265	0.93
34	0.921	0.072	0.550	0.233	0.767	5.714	0.94
35	-0.195	0.026	0.119	0.142	0.858	4.521	0.07
36	1.401	0.066	0.142	0.077	0.918	6.845	0.04
37	0.758	0.041	0.227	0.108	0.851	6.178	0.22
38	2.978	0.006	0.997	0.102	0.845	6.363	0.08
39	0.850	0.037	0.456	0.168	0.832	3.820	0.19
40	1.343	0.076	0.322	0.118	0.873	5.420	0.33
41	0.150	-0.027	0.056	0.077	0.919	7.382	0.55
42	3.383	0.065	0.487	0.063	0.912	4.824	0.42
43	-0.057	0.064	0.061	0.075	0.920	7.329	0.30
44	0.729	0.044	0.115	0.091	0.906	6.543	0.95
45	-0.454	0.007	0.009	0.067	0.933	5.241	0.64
46	-0.216	0.006	0.090	0.106	0.892	7.426	0.51
47	0.503	0.103	0.232	0.105	0.882	7.611	0.41
48	-0.125	-0.038	0.102	0.097	0.895	6.736	0.20
49	-0.180	-0.018	0.040	0.088	0.909	8.068	0.62
50	-0.768	0.003	0.069	0.091	0.906	9.947	0.60
51	-0.037	0.091	0.205	0.166	0.809	6.015	0.32
52	0.161	0.030	0.064	0.070	0.925	7.729	0.53
53	1.045	0.008	0.214	0.111	0.875	10.211	0.61
54	0.909	-0.046	0.071	0.084	0.913	5.400	0.59
55	-0.390	-0.169	0.006	0.129	0.871	4.459	0.77

A.8 Estimated variogram parameters

Tables 12a to 14b show the variogram parameters that correspond to the estimated graphical structures for all 55 banks for time windows 2016-2019, 2012-2015 and 2008-2011 respectively. Tables 15 to 17 show the variogram parameters that correspond to the estimated graphical structures for the subsample of 25 banks (see Appendix A.6) for time windows 2016-2019, 2012-2015 and 2008-2011 respectively.

Table 12a: Variogram parameters of estimated graphical structure for 2016-2019 (1/2)

	1	2	3	4	5	6	7	8	9	10	11	12	13	14	15	16	17	18	19	20	21	22	23	24	25	26	27
1	0																										
2	18.65	0																									
3	15.13	9.82	0																								
4	7.77	13.92	10.41	0																							
5	14.01	8.69	5.18	9.29	0																						
6	16.97	11.66	8.15	12.25	7.02	0																					
7	9.05	15.96	12.45	5.08	11.33	14.29	0																				
8	6.25	12.4	8.89	1.52	7.77	10.73	3.56	0																			
9	16.96	20.11	16.6	12.23	15.48	18.44	14.27	10.71	0																		
10	13.1	14.99	11.48	8.37	10.36	13.32	10.42	6.85	14.56	0																	
11	25.74	8.31	16.91	21.02	15.79	18.75	23.06	19.5	27.2	22.09	0																
12	9.89	16.8	13.28	5.92	12.16	15.12	2.41	4.4	15.11	11.25	23.89	0															
13	15.37	18.52	15.01	10.64	13.89	16.85	12.68	9.12	9.11	12.98	25.62	13.52	0														
14	10.38	13.53	10.02	5.66	8.9	11.86	7.7	4.14	8.09	7.99	20.63	8.53	6.51	0													
15	7.75	10.9	7.39	3.02	6.27	9.23	5.06	1.5	9.21	5.35	18	5.9	7.62	2.63	0												
16	11.98	6.66	3.15	7.26	2.03	4.99	9.3	5.74	13.44	8.33	13.76	10.13	11.86	6.87	4.23	0											
17	7.47	14.38	10.87	3.5	9.75	12.71	1.58	1.98	12.69	8.84	21.48	2.41	11.11	6.12	3.48	7.72	0										
18	13.36	16.51	13	8.63	11.87	14.84	10.67	7.11	8.79	10.96	23.6	11.51	7.2	4.49	5.61	9.84	9.09	0									
19	9.68	11.57	8.06	4.96	6.94	9.9	7	3.44	11.15	3.42	18.67	7.83	9.56	4.57	1.94	4.91	5.42	7.54	0								
20	9	12.15	8.64	4.28	7.52	10.48	6.32	2.76	10.47	6.61	19.25	7.15	8.88	3.89	1.26	5.49	4.74	6.86	3.19	0							
21	10.03	13.18	9.67	5.3	8.55	11.51	7.35	3.78	11.49	7.64	20.28	8.18	9.91	4.92	2.28	6.52	5.77	7.89	4.22	3.54	0						
22	15.34	10.03	6.51	10.62	5.39	8.35	12.66	9.1	16.81	11.69	17.12	13.49	15.22	10.23	7.6	3.36	11.08	13.21	8.27	8.85	9.88	0					
23	18.06	12.74	9.23	13.34	8.11	7.09	15.38	11.81	19.52	14.41	19.84	16.21	17.94	12.95	10.31	6.08	13.8	15.92	10.99	11.57	12.6	9.44	0				
24	11.94	13.83	10.32	7.21	9.2	12.16	9.25	5.69	13.4	5.67	20.93	10.09	11.81	6.83	4.19	7.17	7.67	9.8	2.26	5.45	6.48	10.53	13.25	0			
25	18.98	20.87	17.36	14.25	16.24	19.2	16.29	12.73	20.44	12.71	27.97	17.13	18.85	13.87	11.23	14.21	14.71	16.84	9.3	12.49	13.51	17.57	20.29	11.55	0		
26	20.96	24.11	20.6	16.23	19.48	22.44	18.27	14.71	14.7	18.56	31.21	19.11	5.59	12.09	13.21	17.45	16.69	12.79	15.15	14.47	15.49	20.81	23.52	17.4	24.44	0	
27	15.87	14.28	10.77	11.15	9.65	12.61	13.19	9.63	17.34	12.22	21.38	14.02	15.75	10.76	8.13	7.62	11.61	13.74	8.8	9.38	10.41	10.98	13.7	11.06	18.1	21.34	0
28	13.93	12.34	8.83	9.2	7.7	10.67	11.24	7.68	15.39	10.28	19.43	12.08	13.8	8.82	6.18	5.67	9.67	11.79	6.86	7.44	8.47	9.04	11.75	9.11	16.15	19.39	9.57
29	17.53	2.86	8.7	12.8	7.58	10.54	14.84	11.28	18.99	13.87	9.96	15.68	17.4	12.42	9.78	5.55	13.26	15.39	10.46	11.04	12.06	8.91	11.63	12.71	19.75	22.99	13.16
30	19	20.9	17.38	14.28	16.26	19.22	16.32	12.76	20.47	11.12	27.99	17.15	18.88	13.89	11.26	14.23	14.74	16.87	9.32	12.51	13.54	17.59	20.31	11.58	18.62	24.47	18.12
31	9.02	12.18	8.66	4.3	7.54	10.5	6.34	2.78	10.49	6.63	19.27	7.17	8.9	3.91	1.28	5.51	4.76	6.89	3.21	2.53	3.56	8.87	11.59	5.47	12.51	14.49	9.4
32	11.45	9.85	6.34	6.72	5.22	8.18	8.76	5.2	12.91	7.79	16.95	9.6	11.32	6.33	3.7	3.19	7.18	9.31	4.37	4.95	5.98	6.55	9.27	6.63	13.67	16.91	7.08
33	11.64	14.79	11.28	6.91	10.16	13.12	8.95	5.39	13.1	9.24	21.89	9.79	11.51	6.53	3.89	8.13	7.37	9.5	5.83	5.15	6.17	11.49	14.21	8.08	15.12	17.1	12.02
34	9.78	12.93	9.42	5.06	8.3	11.26	7.1	3.53	11.24	7.39	20.03	7.93	9.66	4.67	2.03	6.27	5.52	7.64	3.97	3.29	4.32	9.63	12.35	6.23	13.27	15.24	10.16
35	13.28	18.72	15.21	8.56	14.09	17.05	10.6	7.03	17.03	13.17	25.82	11.43	15.44	10.46	7.82	12.06	9.02	13.43	9.76	9.08	10.1	15.42	18.13	12.01	19.05	21.03	15.95
36	10.76	13.91	10.4	6.04	9.28	12.24	8.08	4.52	6.19	8.37	21.01	8.91	4.61	1.9	3.02	7.25	6.5	2.59	4.95	4.27	5.3	10.61	13.33	7.21	14.25	10.19	11.14
37	11.95	10.36	6.85	7.23	5.73	8.69	9.27	5.7	13.41	8.3	17.45	10.1	11.83	6.84	4.2	3.69	7.69	9.81	4.88	5.46	6.49	7.06	9.77	7.14	14.17	17.41	7.59
38	17.12	1.53	8.29	12.39	7.17	10.13	14.43	10.87	18.58	13.46	8.62	15.27	16.99	12.01	9.37	5.14	12.85	14.98	10.05	10.63	11.65	8.5	11.22	12.3	19.34	22.58	12.76
39	10.19	13.34	9.83	5.46	8.71	11.67	7.5	3.94	11.65	7.79	20.44	8.34	10.06	5.08	2.44	6.68	5.92	8.05	4.38	2.16	4.72	10.04	12.76	6.63	13.67	15.65	10.57
40	12.52	15.67	12.16	7.8	11.04	14	9.84	6.27	7.95	10.13	22.77	10.67	6.36	3.66	4.77	9.01	8.26	4.35	6.71	6.03	7.06	12.37	15.09	8.97	16	11.95	12.9
41	17.8	19.69	16.18	13.08	15.06	18.02	15.12	11.56	19.27	9.92	26.79	15.95	17.68	12.69	10.06	13.03	13.54	15.66	8.12	11.31	12.34	16.39	19.11	10.38	17.42	23.27	16.92
42	18.86	4.19	10.03	14.13	8.91	11.87	16.17	12.61	20.32	15.2	11.29	17.01	18.73	13.75	11.11	6.88	14.59	16.72	11.79	12.37	13.39	10.24	12.96	14.04	21.08	24.32	14.49
43	15.32	21.47	17.96	9.81	16.84	19.8	12.63	9.07	19.78	15.92	28.57	13.47	18.19	13.21	10.57	14.81	11.05	16.18	12.51	11.83	12.85	18.17	20.89	14.76	21.8	23.78	18.7
44	16.71	11.39	7.88	11.99	6.76	9.72	14.03	10.46	18.17	13.06	18.49	14.86	16.59	11.6	8.96	4.73	12.45	14.57	9.64	10.22	11.25	5.71	10.81	11.9	18.94	22.17	12.35
45	12.63	18.78	15.27	7.12	14.15	17.11	9.94	6.38	17.09	13.23	25.87	10.78	15.5	10.51	7.88	12.11	8.36	13.49	9.82	9.14	10.16	15.48	18.19	12.07	19.11	21.09	16.01
46	17.35	19.24	15.73	12.62	14.6	17.57	14.66	11.1	18.81	9.46	26.33	15.5	17.22	12.23	9.6	12.57	13.08	15.21	7.66	10.85	11.88	15.94	18.65	9.92	16.96	22.81	16.47
47	9.14	12.29	8.78	4.41	7.66	10.62	6.45	2.89	10.6	6.74	19.39	7.29	9.01	4.03	1.39	5.63	4.87	7	3.33	2.65	3.67	8.99	11.71	5.58	12.62	14.6	9.52
48	19.84	21.74	18.22	15.12	17.1	20.06	17.16	13.6	21.31	11.96	28.83	17.99	19.72	14.73	12.1	15.07	15.58	17.71	10.16	13.35	14.38	18.43	21.15	12.42	19.46	25.31	18.96
49	14.76	16.65	13.14	10.03	12.02	14.98	12.08	8.51	16.22	6.88	23.75	12.91	14.64	9.65	7.01	9.99	10.5	12.62	5.08	8.27	9.3	13.35	16.07	7.33	14.37	20.22	13.88
50	17.5	19.39	15.88	12.77	14.76	17.72	14.81	11.25	18.96	9.62	26.49	15.65	17.37	12.39	9.75	12.73	13.24	15.36	7.82	11.01	12.04	16.09	18.81	10.07	17.11	22.96	16.62
51	14.26	16.16	12.64	9.54	11.52	14.48	11.58	8.02	15.73	8	23.25	12.41	14.14	9.15	6.52	9.49	10	12.13	4.58	7.77	8.8	12.85	15.57	6.84	8.64	19.73	13.38
52	10.25	13.4	9.89	5.53	8.77	11.73	7.57	4.01	11.72	7.86	20.5	8.4	10.13	5.14	2.51	6.74	5.99	8.12	4.44	3.76	1.81	10.1	12.82	6.7	13.74	15.72	10.63
53	10.12	8.53	5.02	5.39	3.89	6.86	7.43	3.87	11.58	6.46	15.62	8.27	9.99	5.01	2.37	1.86	5.85	7.98	3.05	3.63	4.65	5.22	7.94	5.3	12.34	15.58	5.76
54	11.36	8.13	4.61	6.63	3.49	6.45	8.67	5.11	12.82	7.7	15.22	9.51	11.23	6.24	3.61	1.46	7.09	9.22	4.29	4.87	5.89	4.82	7.54	6.54	13.58	16.82	6.99
55	15.1	16.99	13.48	10.37	12.36	15.32	12.41	8.85	16.56	8.83	24.09	13.25	14.97	9.99	7.35	10.33	10.83	12.96	5.42	8.61	9.63	13.69	16.41	7.67	14.71	20.56	14.22

Table 12b: Variogram parameters of estimated graphical structure for 2016-2019 (2/2)

	28	29	30	31	32	33	34	35	36	37	38	39	40	41	42	43	44	45	46	47	48	49	50	51	52	53	54	55
28	0																											
29	11.22	0																										
30	16.18	19.78	0																									
31	7.46	11.06	12.53	0																								
32	5.14	8.74	13.7	4.98	0																							
33	10.07	13.67	15.15	5.17	7.59	0																						
34	8.22	11.82	13.29	3.31	5.73	5.93	0																					
35	14	17.6	19.08	9.1	11.52	11.71	9.85	0																				
36	9.3	12.8	14.27	4.29	6.72	6.91	5.05	10.84	0																			
37	5.64	9.24	14.3	5.48	1.86	8.1	6.24	12.02	7.22	0																		
38	10.81	1.33	19.37	10.65	8.33	13.26	11.41	17.19	12.39	8.83	0																	
39	8.62	12.22	13.7	3.72	6.14	6.33	4.48	10.26	5.46	6.65	11.81	0																
40	10.96	14.55	16.03	6.05	8.47	8.67	6.81	12.59	1.76	8.98	14.14	7.22	0															
41	14.98	18.58	7.29	11.33	12.49	13.95	12.09	17.88	13.07	13	18.17	12.5	14.83	0														
42	12.55	1.33	21.11	12.39	10.07	15	13.15	18.93	14.13	10.57	2.66	13.55	15.88	19.91	0													
43	16.75	20.35	21.83	11.85	14.27	14.46	12.61	16.11	13.59	14.77	19.94	13.01	15.34	20.63	21.68	0												
44	10.4	10.28	18.96	10.24	7.92	12.86	11	16.78	11.98	8.42	9.87	11.41	13.74	17.76	11.61	19.54	0											
45	14.06	17.66	19.14	9.16	11.58	11.77	9.91	13.41	10.9	12.08	17.25	10.32	12.65	17.94	18.99	2.69	16.84	0										
46	14.52	18.12	6.83	10.88	12.04	13.49	11.63	17.42	12.61	12.54	17.71	12.04	14.37	2.53	19.45	20.17	17.3	17.48	0									
47	7.57	11.17	12.65	1.96	5.09	5.28	3.43	9.21	4.41	5.59	10.76	3.83	6.16	11.45	12.5	11.96	10.36	9.27	10.99	0								
48	17.02	20.62	2.71	13.37	14.54	15.99	14.13	19.92	15.11	15.04	20.21	14.54	16.87	8.13	21.95	22.67	19.8	19.98	7.67	13.49	0							
49	11.94	15.53	4.24	8.29	9.45	10.9	9.05	14.83	10.03	9.96	15.12	9.45	11.79	3.04	16.86	17.58	14.72	14.89	2.59	8.4	5.08	0						
50	14.67	18.27	6.98	11.03	12.19	13.64	11.79	17.57	12.77	12.7	17.86	12.19	14.53	5.78	19.6	20.32	17.46	17.63	5.33	11.14	7.82	2.74	0					
51	11.44	15.04	13.9	7.79	8.96	10.41	8.55	14.34	9.53	9.46	14.63	8.96	11.29	12.7	16.37	17.09	14.22	14.4	12.24	7.91	14.74	9.66	12.4	0				
52	8.69	12.29	13.76	3.78	6.21	6.4	4.54	10.33	5.52	6.71	11.88	4.95	7.28	12.56	13.62	13.08	11.47	10.39	12.1	3.9	14.6	9.52	12.26	9.02	0			
53	3.81	7.41	12.37	3.65	1.33	6.26	4.41	10.19	5.39	1.83	7	4.81	7.15	11.17	8.74	12.94	6.59	10.25	10.71	3.76	13.21	8.12	10.86	7.63	4.88	0		
54	5.05	7.01	13.61	4.89	2.57	7.5	5.64	11.43	6.63	3.07	6.6	6.05	8.38	12.41	8.34	14.18	6.19	11.49	11.95	5	14.45	9.36	12.1	8.87	6.12	1.24	0	
55	12.27	15.87	14.74	8.63	9.79	11.24	9.39	15.17	10.37	10.29	15.46	9.79	12.13	13.54	17.3	17.92	15.06	15.23	13.08	8.74	15.58	10.49	13.23	10	9.86	8.46	9.7	0

Table 13a: Variogram parameters of estimated graphical structure for 2012-2015 (1/2)

	1	2	3	4	5	6	7	8	9	10	11	12	13	14	15	16	17	18	19	20	21	22	23	24	25	26	27
1	0																										
2	20	0																									
3	17.43	21.98	0																								
4	14.91	19.46	4.36	0																							
5	16.41	20.96	4.09	3.34	0																						
6	13.46	18.02	15.44	12.92	14.42	0																					
7	16.99	21.55	6.45	2.08	5.43	15	0																				
8	15.83	20.39	5.29	0.92	4.27	13.85	3.01	0																			
9	16.79	3.22	18.77	16.25	17.75	14.8	18.33	17.17	0																		
10	7.72	12.28	9.7	7.18	8.68	5.74	9.27	8.11	9.06	0																	
11	17.73	22.29	11.64	9.12	10.62	15.74	11.2	10.05	19.07	10.01	0																
12	18.38	22.94	7.84	3.48	6.82	16.4	1.39	4.4	19.72	10.66	12.6	0															
13	18.4	22.96	17.31	14.79	16.29	16.42	16.88	15.72	19.74	10.68	17.62	18.27	0														
14	15.88	20.43	6.45	3.93	5.43	13.89	6.01	4.86	17.22	8.15	10.09	7.41	15.76	0													
15	14.19	18.74	4.76	2.24	3.74	12.2	4.33	3.17	15.53	6.46	8.4	5.72	14.07	3.21	0												
16	17.67	22.22	5.36	4.6	1.26	15.68	6.69	5.53	19.01	9.94	11.88	8.08	17.55	6.69	5	0											
17	16.96	21.52	6.42	2.06	5.4	14.98	1.73	2.98	18.3	9.24	11.18	3.12	16.85	5.99	4.3	6.66	0										
18	16.05	20.61	9.96	7.45	8.94	14.07	9.53	8.37	17.39	8.33	10.27	10.92	15.94	8.42	6.73	10.21	9.5	0									
19	14.65	19.2	8.56	6.04	7.54	12.66	8.12	6.96	15.99	6.92	8.86	9.51	14.53	7.01	5.32	8.8	8.09	7.19	0								
20	14.17	18.72	8.08	5.56	7.06	12.18	7.64	6.48	15.51	6.44	8.38	9.04	14.06	6.53	4.84	8.32	7.61	6.71	5.3	0							
21	15.58	20.14	9.49	6.97	8.47	13.6	9.06	7.9	16.92	7.86	9.8	10.45	15.47	7.94	6.26	9.73	9.03	8.12	6.71	6.24	0						
22	18.36	22.92	6.05	5.3	1.96	16.38	7.39	6.23	19.7	10.64	12.58	8.78	18.25	7.39	5.7	3.22	7.36	10.9	9.49	9.02	10.43	0					
23	11.86	16.41	13.84	11.32	12.82	9.87	13.4	12.24	13.2	4.13	14.14	14.79	14.81	12.29	10.6	14.08	13.37	12.46	11.06	10.58	11.99	14.77	0				
24	14.73	19.29	5.31	2.79	4.29	12.75	4.87	3.71	16.07	7.01	8.95	6.26	14.62	2.49	2.07	5.55	4.84	7.27	5.86	5.38	6.8	6.24	11.14	0			
25	22.41	26.97	14	11.48	12.98	20.43	13.57	12.41	23.75	14.69	16.63	14.96	22.3	12.45	10.76	14.24	13.54	14.95	13.54	13.06	14.48	14.94	18.82	11.31	0		
26	22.48	27.04	21.39	18.87	20.37	20.49	20.96	19.8	23.82	14.76	21.7	22.35	13.37	19.84	18.15	21.63	20.93	20.02	18.61	18.13	19.55	22.33	18.89	18.7	26.38	0	
27	14.37	13.05	16.35	13.83	15.33	12.38	15.91	14.75	9.83	6.65	16.65	17.31	17.32	14.8	13.11	16.59	15.88	14.98	13.57	13.09	14.51	17.29	10.78	13.65	21.33	21.4	0
28	15.01	19.57	8.92	6.4	7.9	13.02	8.48	7.33	16.35	7.29	9.22	9.88	14.9	7.37	5.68	9.16	8.46	7.55	3.94	5.66	7.08	9.86	11.42	6.23	13.91	18.98	13.93
29	21.84	1.84	23.82	21.3	22.8	19.86	23.39	22.23	5.06	14.12	24.13	24.78	24.8	22.27	20.58	24.06	23.36	22.45	21.04	20.57	21.98	24.76	18.25	21.13	28.81	28.88	14.89
30	20.67	25.22	19.58	17.06	18.56	18.68	19.14	17.98	22.01	12.94	19.88	20.54	11.56	18.03	16.34	19.82	19.11	18.21	16.8	16.32	17.74	20.52	17.08	16.88	24.56	15.64	19.59
31	13.76	18.32	5.36	2.84	4.34	11.78	4.92	3.76	15.1	6.04	7.98	6.31	13.65	3.81	2.12	5.6	4.89	6.3	4.89	4.42	5.83	6.29	10.17	2.66	8.65	17.73	12.69
32	14.87	19.42	2.56	1.81	1.54	12.88	3.89	2.73	16.21	7.14	9.08	5.28	14.76	3.89	2.2	2.8	3.86	7.41	6	5.52	6.94	3.5	11.28	2.75	11.45	18.83	13.79
33	12.09	16.65	14.07	11.55	13.05	10.1	13.63	12.47	13.43	4.37	14.37	15.03	15.04	12.52	10.83	14.31	13.6	12.7	11.29	10.81	12.23	15.01	3.51	11.37	19.05	19.12	11.01
34	13.84	18.39	7.75	5.23	6.73	11.85	7.31	6.15	15.18	6.11	8.05	8.7	13.72	6.2	4.51	7.99	7.28	6.37	4.97	2.41	5.9	8.68	10.25	5.05	12.73	17.8	12.76
35	10.57	19.44	16.86	14.34	15.84	12.9	16.43	15.27	16.22	7.16	17.17	17.82	17.84	15.31	13.62	17.1	16.4	15.49	14.08	13.61	15.02	17.8	11.29	14.17	21.85	21.92	13.81
36	15.09	19.64	9	6.48	7.98	13.1	8.56	7.4	16.43	7.36	9.3	9.96	14.98	7.45	5.76	9.24	8.53	3.62	6.22	5.74	7.16	9.94	11.5	6.3	13.98	19.05	14.01
37	16.54	21.1	4.23	3.48	3.21	14.56	5.56	4.41	17.88	8.82	10.76	6.96	16.43	5.57	3.88	4.47	5.54	9.08	7.67	7.2	8.61	5.17	12.95	4.42	13.12	20.51	15.47
38	21.94	3.51	23.91	21.4	22.9	19.95	23.48	22.32	5.15	14.21	24.22	24.87	24.89	22.37	20.68	24.16	23.45	22.54	21.14	20.66	22.07	24.85	18.35	21.22	28.9	28.97	14.98
39	11.76	16.31	5.67	3.15	4.65	9.77	5.23	4.07	13.1	4.03	5.97	6.63	11.64	4.12	2.43	5.91	5.2	4.3	2.89	2.41	3.83	6.61	8.17	2.97	10.65	15.72	10.68
40	12.28	16.83	14.26	11.74	13.24	10.29	13.82	12.66	13.62	4.56	14.56	15.22	15.23	12.71	11.02	14.5	13.79	12.89	11.48	11	12.42	15.2	8.69	11.56	19.24	19.31	11.2
41	24.67	29.23	23.58	21.06	22.56	22.69	23.15	21.99	26.01	16.95	23.89	24.54	6.98	22.03	20.35	23.82	23.12	22.21	20.8	20.33	21.74	24.52	21.08	20.89	28.57	19.64	23.59
42	19.97	1.55	21.95	19.43	20.93	17.99	21.51	20.35	3.18	12.25	22.25	22.91	22.92	20.4	18.71	22.19	21.49	20.58	19.17	18.69	20.11	22.89	16.38	19.26	26.94	27	13.02
43	18.38	22.94	12.29	9.77	11.27	16.39	11.85	10.7	19.72	10.66	3.9	13.25	18.27	10.74	9.05	12.53	11.83	10.92	9.51	9.03	10.45	13.23	14.79	9.6	17.28	22.35	17.3
44	17.93	22.49	9.52	7	8.5	15.95	9.09	7.93	19.27	10.21	12.15	10.48	17.82	7.97	6.29	9.76	9.06	10.47	9.06	8.58	10	10.46	14.34	6.83	11.95	21.9	16.85
45	17.07	21.63	19.05	16.53	18.03	15.09	18.61	17.46	18.41	9.35	19.35	20.01	20.03	17.5	15.81	19.29	18.59	17.68	16.27	15.79	17.21	19.99	13.48	16.36	24.04	24.1	15.99
46	24.45	29	23.36	20.84	22.34	22.46	22.92	21.76	25.79	16.72	23.66	24.32	6.75	21.81	20.12	23.6	22.89	21.99	20.58	20.1	21.52	24.3	20.86	20.66	28.34	19.42	23.37
47	13.43	17.98	4	1.48	2.98	11.44	3.56	2.41	14.77	5.7	7.64	4.96	13.31	2.45	0.76	4.24	3.54	5.97	4.56	4.08	5.49	4.94	9.84	1.31	10	17.39	12.35
48	21.44	26	20.35	17.83	19.33	19.46	19.92	18.76	22.78	13.72	20.66	21.31	12.33	18.81	17.12	20.6	19.89	18.98	17.57	17.1	18.51	21.29	17.85	17.66	25.34	16.41	20.37
49	22.97	27.52	21.88	19.36	20.86	20.98	21.44	20.28	24.31	15.24	22.18	22.84	5.27	20.33	18.64	22.12	21.41	20.51	19.1	18.62	20.04	22.82	19.38	19.18	26.86	17.94	21.89
50	25.77	30.33	24.68	22.16	23.66	23.79	24.25	23.09	27.11	18.05	24.99	25.64	8.08	23.13	21.44	24.92	24.22	23.31	21.9	21.43	22.84	25.62	22.18	21.99	29.67	20.74	24.69
51	16.77	21.33	10.68	8.17	9.66	14.79	10.25	9.09	18.11	9.05	10.99	11.64	16.66	9.14	7.45	10.93	10.22	9.31	7.9	7.43	8.84	11.62	13.18	7.99	15.67	20.74	15.7
52	14.78	19.33	8.69	6.17	7.67	12.79	8.25	7.09	16.12	7.05	8.99	9.64	14.66	7.14	5.45	8.93	8.22	7.32	5.91	5.43	2.14	9.63	11.19	5.99	13.67	18.74	13.7
53	15.93	20.49	3.62	2.87	2.6	13.95	4.95	3.79	17.27	8.21	10.15	6.35	15.82	4.96	3.27	3.86	4.92	8.47	7.06	6.58	8	4.56	12.34	3.81	12.51	19.9	14.85
54	15.9	20.46	3.59	2.84	1.04	13.92	4.92	3.77	17.24	8.18	10.12	6.32	15.79	4.93	3.24	2.3	4.9	8.44	7.03	6.56	7.97	3	12.31	3.78	12.48	19.87	14.82
55	13.75	18.31	12.67	10.15	11.65	11.77	12.23	11.07	15.09	6.03	12.97	13.62	4.65	11.12	9.43	12.91	12.2	11.3	9.89	9.41	10.82	13.6	10.17	9.97	17.65	8.73	12.68

Table 13b: Variogram parameters of estimated graphical structure for 2012-2015 (2/2)

	28	29	30	31	32	33	34	35	36	37	38	39	40	41	42	43	44	45	46	47	48	49	50	51	52	53	54	55
28	0																											
29	21.41	0																										
30	17.16	27.06	0																									
31	5.26	20.16	15.92	0																								
32	6.36	21.27	17.02	2.8	0																							
33	11.65	18.49	17.31	10.41	11.51	0																						
34	5.33	20.23	15.99	4.08	5.19	10.48	0																					
35	14.45	21.28	20.1	13.2	14.31	11.53	13.27	0																				
36	6.58	21.49	17.24	5.34	6.44	11.73	5.41	14.53	0																			
37	8.04	22.94	18.7	4.47	1.68	13.19	6.86	15.98	8.12	0																		
38	21.5	5.36	27.16	20.25	21.36	18.58	20.32	21.37	21.58	23.03	0																	
39	3.25	18.15	13.91	2.01	3.11	8.4	2.08	11.19	3.33	4.79	18.25	0																
40	11.84	18.68	17.5	10.6	11.7	8.92	10.67	11.72	11.92	13.38	18.77	8.59	0															
41	21.17	31.07	17.83	19.92	21.03	21.32	19.99	24.11	21.25	22.7	31.16	17.92	21.5	0														
42	19.53	3.39	25.19	18.29	19.39	16.61	18.36	19.41	19.61	21.07	1.97	16.28	16.8	29.2	0													
43	9.87	24.78	20.53	8.63	9.73	15.02	8.7	17.82	9.95	11.41	24.87	6.62	15.21	24.54	22.9	0												
44	9.43	24.33	20.08	4.17	6.97	14.58	8.25	17.37	9.5	8.64	24.42	6.17	14.76	24.09	22.46	12.8	0											
45	16.63	23.47	22.29	15.39	16.49	13.71	15.46	16.51	16.71	18.17	23.56	13.38	9.18	26.3	21.6	20	19.56	0										
46	20.94	30.84	17.6	19.7	20.8	21.09	19.77	23.88	21.02	22.48	30.94	17.69	21.28	1.21	28.97	24.31	23.86	26.07	0									
47	4.92	19.82	15.58	1.36	1.44	10.07	3.75	12.86	5	3.12	19.92	1.67	10.26	19.58	17.95	8.29	5.52	15.05	19.36	0								
48	17.94	27.84	3.19	16.69	17.8	18.09	16.76	20.88	18.02	19.47	27.93	14.69	18.27	18.61	25.97	21.31	20.86	23.07	18.38	16.35	0							
49	19.46	29.36	16.12	18.22	19.32	19.61	18.29	22.4	19.54	21	29.46	16.21	19.8	1.71	27.49	22.83	22.38	24.59	1.48	17.88	16.9	0						
50	22.27	32.17	18.93	21.02	22.13	22.41	21.09	25.21	22.35	23.8	32.26	19.02	22.6	2.54	30.3	25.64	25.19	27.4	1.33	20.68	19.7	2.81	0					
51	8.27	23.17	18.93	7.02	8.13	13.42	7.09	16.21	8.35	9.8	23.26	5.02	13.61	22.93	21.3	11.64	11.19	18.4	22.71	6.68	19.7	21.23	24.03	0				
52	6.27	21.17	16.93	5.03	6.13	11.42	5.1	14.21	6.35	7.8	21.27	3.02	11.61	20.93	19.3	9.64	9.19	16.4	20.71	4.69	17.71	19.23	22.03	8.04	0			
53	7.43	22.33	18.08	3.86	1.06	12.57	6.25	15.37	7.5	1.76	22.42	4.17	12.76	22.09	20.45	10.8	8.03	17.56	21.86	2.51	18.86	20.38	23.19	9.19	7.19	0		
54	7.4	22.3	18.06	3.83	1.03	12.55	6.22	15.34	7.48	2.71	22.39	4.15	12.73	22.06	20.43	10.77	8	17.53	21.83	2.48	18.83	20.36	23.16	9.16	7.16	2.1	0	
55	10.25	20.15	6.91	9	10.11	10.4	9.08	13.19	10.33	11.78	20.24	7	10.59	10.92	18.28	13.62	13.17	15.38	10.69	8.67	7.69	9.21	12.02	12.02	10.02	11.17	11.14	0

Table 14a: Variogram parameters of estimated graphical structure for 2008-2011 (1/2)

	1	2	3	4	5	6	7	8	9	10	11	12	13	14	15	16	17	18	19	20	21	22	23	24	25	26	27
1	0																										
2	12.64	0																									
3	14.95	7.7	0																								
4	22.05	14.81	17.11	0																							
5	25.83	18.58	20.89	3.78	0																						
6	15.3	8.05	10.35	17.46	21.24	0																					
7	23.47	16.22	18.53	1.41	5.19	18.87	0																				
8	22	14.75	17.06	0.35	4.13	17.4	1.76	0																			
9	12.63	5.38	7.68	14.79	18.57	8.03	16.2	14.73	0																		
10	3.08	9.56	11.87	18.97	22.75	12.21	20.39	18.92	9.54	0																	
11	17.42	10.18	12.48	19.59	23.36	12.83	21	19.53	10.16	14.34	0																
12	23.61	16.36	18.67	1.56	5.33	19.02	1.79	1.91	16.35	20.53	21.15	0															
13	22.37	15.12	17.43	13.48	17.25	17.78	14.89	13.42	15.11	19.29	19.9	15.03	0														
14	18.3	11.06	13.36	6.11	9.88	13.71	7.52	6.05	11.04	15.22	15.84	7.66	9.72	0													
15	20.61	13.36	15.67	1.45	5.22	16.01	2.86	1.39	13.34	17.53	18.14	3	12.03	4.66	0												
16	15.35	8.1	2.93	17.51	21.29	10.75	18.92	17.45	8.08	12.27	12.88	19.07	17.83	13.76	16.06	0											
17	19.58	12.33	14.64	10.68	14.46	14.98	12.1	10.62	12.31	16.5	17.11	12.24	4.96	6.93	9.24	15.03	0										
18	16.89	9.65	11.95	19.06	22.83	12.3	20.47	19	8.65	13.81	14.43	20.62	19.37	15.31	17.61	12.35	16.58	0									
19	15.25	8	10.31	17.42	21.19	10.66	18.83	17.36	7.99	12.17	12.79	18.98	17.73	13.67	15.97	10.71	14.94	12.26	0								
20	20.47	13.22	15.53	2.91	6.68	15.88	4.32	2.85	13.21	17.39	18.01	4.47	11.89	4.52	1.46	15.93	9.1	17.48	15.84	0							
21	15.3	8.06	10.36	10.56	14.33	10.71	11.97	10.5	8.04	12.22	12.84	12.11	10.87	6.81	9.11	10.76	8.08	12.31	10.67	8.98	0						
22	15.21	6.58	10.27	17.38	21.15	10.62	18.79	17.32	7.95	12.13	12.75	18.93	17.69	13.63	15.93	10.67	14.9	12.22	10.57	15.8	10.63	0					
23	15.73	8.48	10.79	17.9	21.67	11.14	19.31	17.84	8.47	12.65	13.27	19.45	18.21	14.15	16.45	11.19	15.42	12.74	11.1	16.32	11.15	11.05	0				
24	22.4	15.15	17.45	3.24	7.01	17.8	4.65	3.18	15.13	19.31	19.93	4.79	13.82	6.45	1.79	17.85	11.02	19.4	17.76	3.25	10.9	17.72	18.24	0			
25	25.38	18.13	20.44	6.22	9.99	20.78	7.63	6.16	18.11	22.3	22.91	7.77	16.8	9.43	4.77	20.83	14.01	22.38	20.74	6.23	13.88	20.7	21.22	6.56	0		
26	15.19	7.95	10.25	17.36	21.14	10.6	18.77	17.3	7.93	12.11	12.73	18.92	17.68	13.61	15.91	10.65	14.88	12.2	10.56	15.78	10.61	10.52	11.04	17.7	20.68	0	
27	16.52	9.27	11.58	18.69	22.46	11.93	20.1	18.63	9.26	13.44	14.05	20.24	19	14.93	17.24	11.98	16.21	13.52	11.88	17.1	11.94	11.84	12.36	19.03	22.01	4.44	0
28	17.42	10.17	12.47	19.58	23.36	12.82	20.99	19.52	10.15	14.34	14.95	21.14	19.9	15.83	18.13	12.87	17.1	14.42	5.74	18	12.83	12.74	13.26	19.92	22.9	12.72	14.05
29	11.34	1.31	6.4	13.5	17.28	6.74	14.92	13.44	4.07	8.26	8.87	15.06	13.82	9.75	12.05	6.79	11.02	8.34	6.7	11.92	6.75	5.27	7.18	13.84	16.82	6.64	7.97
30	17.47	10.22	12.52	8.57	12.35	12.87	9.99	8.51	10.2	14.39	15	10.13	8.89	4.82	7.12	12.92	6.09	14.47	12.83	6.99	5.97	12.79	13.31	8.91	11.89	12.77	14.1
31	22.75	15.51	17.81	3.59	7.37	18.16	5.01	3.54	15.49	19.67	20.29	5.15	14.18	6.8	2.15	18.21	11.38	19.76	18.12	3.61	11.26	18.08	18.6	3.93	2.62	18.06	19.38
32	23.75	16.5	18.81	1.7	2.08	19.16	3.11	2.05	16.49	20.67	21.29	3.25	15.17	7.8	3.14	19.21	12.38	20.76	19.12	4.61	12.25	19.07	19.6	4.93	7.91	19.06	20.38
33	15.97	8.72	11.02	18.13	21.91	11.37	19.55	18.07	8.7	12.89	13.5	19.69	18.45	14.38	16.68	11.42	15.65	12.97	11.33	16.55	11.38	11.29	3.14	18.47	21.45	11.27	12.6
34	21.46	14.21	16.51	9.26	13.03	16.86	10.67	9.2	14.19	18.37	18.99	10.81	12.88	3.15	7.81	16.91	10.08	18.46	16.82	7.68	9.96	16.78	17.3	9.6	12.58	16.76	18.09
35	15.95	8.7	11.01	18.11	21.89	11.35	19.53	18.06	8.68	12.87	5.99	19.67	18.43	14.36	16.67	11.41	15.64	12.95	11.31	16.53	11.36	11.27	11.79	18.45	21.44	11.25	12.58
36	10.15	10.27	12.58	19.69	23.46	12.93	21.1	19.63	10.26	7.07	15.06	21.24	20	15.94	18.24	12.98	17.21	14.53	12.89	18.11	12.94	12.84	13.36	20.03	23.01	12.83	14.15
37	25.96	18.72	21.02	3.91	4.29	21.37	5.32	4.26	18.7	22.88	23.5	5.47	17.39	10.02	5.36	21.42	14.59	22.97	21.33	6.82	14.47	21.29	21.81	7.14	10.13	21.27	22.6
38	9.94	2.7	5	12.11	15.89	5.35	13.52	12.05	2.68	6.86	7.48	13.67	12.43	8.36	10.66	5.4	9.63	6.95	5.31	10.53	5.36	5.27	5.79	12.45	15.43	5.25	6.58
39	22.76	15.52	17.82	5.2	8.98	18.17	6.61	5.14	15.5	19.68	20.3	6.76	14.19	6.81	3.75	18.22	11.39	19.77	18.13	2.29	11.27	18.09	18.61	5.54	8.52	18.07	19.4
40	7.98	8.1	10.41	17.51	21.29	10.75	18.93	17.46	8.09	4.89	12.88	19.07	17.83	13.76	16.07	10.81	15.04	12.35	10.71	15.93	10.76	10.67	11.19	17.86	20.84	10.65	11.98
41	25.5	18.25	20.56	6.34	10.11	20.9	7.75	6.28	18.23	22.42	23.03	7.9	16.92	9.55	4.89	20.95	14.13	22.5	20.86	6.35	14	20.82	21.34	6.68	7.35	20.8	22.13
42	11.66	4.41	6.72	13.83	17.6	7.07	15.24	13.77	4.4	8.58	9.2	15.39	14.14	10.08	12.38	7.12	11.35	8.67	7.03	12.25	7.08	6.98	7.51	14.17	17.15	6.97	8.29
43	15.56	8.31	10.62	17.72	21.5	10.96	19.14	17.66	8.29	12.48	1.87	19.28	18.04	13.97	16.28	11.01	15.25	12.56	10.92	16.14	10.97	10.88	11.4	18.06	21.05	10.86	12.19
44	15.32	8.07	10.38	17.49	21.26	10.73	18.9	17.43	8.06	12.24	12.86	19.04	17.8	13.74	16.04	10.78	15.01	12.33	3.64	15.91	10.74	10.64	11.16	17.83	20.81	10.63	11.95
45	18.73	11.49	13.79	20.9	24.68	14.14	22.31	20.84	11.47	15.65	3.45	22.46	21.22	17.15	19.45	14.19	18.42	15.74	14.1	19.32	14.15	14.06	14.58	21.24	24.22	14.04	15.37
46	23.8	16.55	18.86	4.64	8.41	19.2	6.05	4.58	16.53	20.72	21.33	6.19	15.22	7.85	3.19	19.25	12.43	20.8	19.16	4.65	12.3	19.12	19.64	4.98	5.65	19.1	20.43
47	18.84	11.59	13.9	3.22	6.99	14.25	4.63	3.16	11.58	15.76	16.37	4.77	10.26	2.89	1.77	14.3	7.47	15.84	14.2	1.63	7.34	14.16	14.68	3.56	6.54	14.14	15.47
48	15.47	8.23	10.53	6.58	10.36	10.88	7.99	6.52	8.21	12.39	13.01	8.14	6.9	2.83	5.13	10.93	4.1	12.48	10.84	5	3.98	10.8	11.32	6.92	9.9	10.78	12.11
49	25.71	18.46	20.77	6.55	10.33	21.12	7.96	6.49	18.45	22.63	23.24	8.11	17.13	9.76	5.1	21.17	14.34	22.71	21.07	6.56	14.21	21.03	21.55	6.89	7.56	21.02	22.34
50	24.98	17.73	20.04	5.82	9.6	20.39	7.23	5.76	17.72	21.9	22.51	7.38	16.4	9.03	4.37	20.44	13.61	21.98	20.34	5.83	13.48	20.3	20.82	6.16	6.83	20.29	21.61
51	18.07	10.82	13.13	20.23	24.01	13.47	21.65	20.18	10.8	14.99	15.6	21.79	20.55	16.48	18.79	13.52	17.76	15.07	13.43	18.65	13.48	13.39	2.34	20.57	23.56	13.37	14.7
52	17.65	10.4	12.71	12.9	16.68	13.05	14.31	12.84	10.38	14.57	15.18	14.46	13.22	9.15	11.45	13.1	10.42	14.65	13.01	11.32	2.34	12.97	13.49	13.24	16.22	12.95	14.28
53	23.73	16.48	18.79	1.68	3.72	19.14	3.09	2.03	16.47	20.65	21.27	3.23	15.15	7.78	3.13	19.19	12.36	20.74	19.1	4.59	12.24	19.06	19.58	4.91	7.9	19.04	20.36
54	26.1	18.85	21.16	4.04	2.62	21.51	5.46	4.39	18.84	23.02	23.63	5.6	17.52	10.15	5.49	21.56	14.73	23.1	21.46	6.95	14.6	21.42	21.94	7.28	10.26	21.4	22.73
55	19.85	12.61	14.91	22.02	25.8	15.26	23.43	21.96	12.59	16.77	17.39	23.58	22.34	18.27	20.57	15.31	19.54	16.86	15.22	20.44	15.27	15.18	15.7	22.36	25.34	15.16	16.49

Table 14b: Variogram parameters of estimated graphical structure for 2008-2011 (2/2)

	28	29	30	31	32	33	34	35	36	37	38	39	40	41	42	43	44	45	46	47	48	49	50	51	52	53	54	55
28	0																											
29	8.86	0																										
30	14.99	8.91	0																									
31	20.28	14.2	9.27	0																								
32	21.28	15.2	10.27	5.29	0																							
33	13.49	7.41	13.54	18.83	19.83	0																						
34	18.98	12.9	7.97	9.96	10.95	17.53	0																					
35	13.48	7.4	13.52	18.81	19.81	12.03	17.51	0																				
36	15.05	8.97	15.1	20.39	21.39	13.6	19.09	13.58	0																			
37	23.49	17.41	12.48	7.5	2.21	22.04	13.17	22.02	23.6	0																		
38	7.47	1.39	7.52	12.81	13.81	6.02	11.51	6	7.58	16.02	0																	
39	20.29	14.21	9.28	5.9	6.9	18.84	9.97	18.82	20.4	9.11	12.82	0																
40	12.88	6.8	12.93	18.21	19.21	11.43	16.92	11.41	2.17	21.42	5.4	18.22	0															
41	23.02	16.95	12.01	4.73	8.04	21.57	12.7	21.56	23.13	10.25	15.55	8.64	20.96	0														
42	9.19	3.11	9.24	14.53	15.53	7.74	13.23	7.72	9.3	17.74	1.72	14.54	7.12	17.27	0													
43	13.08	7	13.13	18.42	19.42	11.63	17.12	4.12	13.19	21.63	5.61	18.43	11.02	21.17	7.33	0												
44	2.09	6.77	12.9	18.19	19.18	11.4	16.89	11.38	12.95	21.4	5.38	18.2	10.78	20.93	7.09	10.99	0											
45	16.26	10.18	16.31	21.6	22.6	14.81	20.3	7.3	16.37	24.81	8.79	21.61	14.19	24.34	10.51	3.18	14.17	0										
46	21.32	15.24	10.31	3.03	6.33	19.87	11	19.86	21.43	8.55	13.85	6.94	19.26	1.7	15.57	19.47	19.23	22.64	0									
47	16.37	10.29	5.36	3.91	4.91	14.92	6.04	14.9	16.47	7.13	8.89	3.92	14.3	6.66	10.61	14.51	14.27	17.68	4.96	0								
48	13	6.92	1.99	7.28	8.28	11.55	5.98	11.53	13.11	10.49	5.53	7.29	10.93	10.02	7.25	11.14	10.91	14.32	8.32	3.36	0							
49	23.24	17.16	12.23	4.94	8.25	21.79	12.91	21.77	23.34	10.46	15.77	8.86	21.17	1.44	17.48	21.38	21.14	24.56	1.91	6.87	10.24	0						
50	22.51	16.43	11.5	4.21	7.52	21.06	12.18	21.04	22.61	9.73	15.04	8.13	20.44	2.88	16.75	20.65	20.41	23.83	1.18	6.14	9.51	3.1	0					
51	15.59	9.51	15.64	20.93	21.93	5.47	19.63	14.13	15.7	24.14	8.12	20.94	13.53	23.68	9.84	13.74	13.5	16.91	21.98	17.02	13.65	23.89	23.16	0				
52	15.17	9.09	8.31	13.6	14.6	13.72	12.3	13.71	15.28	16.81	7.7	13.61	13.11	16.34	9.42	13.31	13.08	16.49	14.64	9.68	6.32	16.56	15.83	15.83	0			
53	21.26	15.18	10.25	5.27	1.64	19.81	10.94	19.79	21.37	3.85	13.79	6.88	19.19	8.02	15.51	19.4	19.17	22.58	6.31	4.89	8.26	8.23	7.5	21.91	14.58	0		
54	23.63	17.55	12.62	7.64	2.35	22.18	13.3	22.16	23.73	4.56	16.15	9.24	21.56	10.38	17.87	21.77	21.53	24.94	8.68	7.26	10.62	10.59	9.86	24.28	16.94	3.99	0	
55	17.38	11.3	17.43	22.72	23.72	15.93	21.42	15.91	17.49	25.93	9.91	22.73	15.31	25.46	9.88	15.52	15.29	18.7	23.76	18.8	15.44	25.68	24.95	18.03	17.61	23.7	26.06	0

Table 15: Variogram parameters of estimated graphical structure for subsample of 25 banks for 2016-2019

ID	1	4	8	14	15	17	20	21	23	24	26	30	31	32	34	36	40	41	46	47	48	49	50	52	53
1	0																								
4	7.83	0																							
8	6.25	1.59	0																						
14	10.43	4.57	4.18	0																					
15	7.79	1.94	1.55	2.63	0																				
17	7.47	3.57	1.98	6.16	3.53	0																			
20	8.99	3.14	2.75	3.83	1.2	4.73	0																		
21	10.08	4.22	3.83	4.92	2.28	5.81	3.48	0																	
23	18.37	12.52	12.13	13.21	10.58	14.11	11.78	12.86	0																
24	10.41	4.55	4.16	5.25	2.62	6.15	3.82	4.9	13.2	0															
26	12.25	6.39	6	7.09	4.45	7.98	5.65	6.74	13.4	7.07	0														
30	15.62	9.76	9.37	10.46	7.83	11.36	9.03	10.11	12.79	10.44	10.65	0													
31	9.04	3.18	2.8	3.88	1.25	4.78	2.45	3.53	9.33	3.87	4.07	6.58	0												
32	9.85	3.99	3.6	4.69	2.05	5.58	3.25	4.34	12.63	4.67	6.51	9.88	3.3	0											
34	9.79	3.94	3.55	4.63	2	5.53	2.28	4.28	12.58	4.62	6.45	9.83	3.25	4.05	0										
36	10.81	4.95	4.56	1.9	3.02	6.55	4.22	5.3	13.6	5.63	7.47	10.84	4.26	5.07	5.02	0									
40	12.57	6.71	6.32	3.66	4.77	8.3	5.97	7.06	15.35	7.39	9.23	12.6	6.02	6.83	6.77	1.76	0								
41	16.48	10.62	10.23	11.32	8.68	12.21	9.88	10.96	7.98	11.3	11.5	10.89	7.43	10.74	10.68	11.7	13.45	0							
46	16.02	10.16	9.77	10.86	8.22	11.75	9.42	10.51	7.53	10.84	11.05	10.43	6.98	10.28	10.22	11.24	13	2.53	0						
47	9.24	3.38	2.99	4.08	1.45	4.98	2.65	3.73	12.03	2.64	5.9	9.27	2.7	3.5	3.45	4.46	6.22	10.13	9.67	0					
48	12.94	7.08	6.7	7.78	5.15	8.68	6.35	7.43	10.11	7.77	7.97	2.68	3.9	7.2	7.15	8.16	9.92	8.21	7.75	6.59	0				
49	13.43	7.57	7.19	8.27	5.64	9.17	6.84	7.92	4.94	8.26	8.46	7.85	4.39	7.69	7.64	8.65	10.41	3.04	2.59	7.08	5.17	0			
50	16.12	10.26	9.87	10.96	8.32	11.85	9.52	10.61	4.85	10.94	11.14	10.53	7.07	10.38	10.32	11.34	13.1	5.73	5.27	9.77	7.85	2.69	0		
52	10.3	4.44	4.05	5.14	2.51	6.04	3.71	1.81	13.09	5.12	6.96	10.33	3.75	4.56	4.51	5.52	7.28	11.19	10.73	3.95	7.65	8.14	10.83	0	
53	10.06	4.2	3.81	4.9	2.26	5.79	3.46	4.55	12.84	4.88	6.72	10.09	3.51	1.34	4.26	5.28	7.04	10.94	10.49	3.71	7.41	7.9	10.59	4.77	0

Table 16: Variogram parameters of estimated graphical structure for subsample of 25 banks for 2012-2015

ID	1	4	8	14	15	17	20	21	23	24	26	30	31	32	34	36	40	41	46	47	48	49	50	52	53
1	0																								
4	16.83	0																							
8	17.21	0.9	0																						
14	17.83	3.91	4.28	0																					
15	16.17	2.25	2.63	3.25	0																				
17	18.95	2.11	3.02	6.02	4.37	0																			
20	17.04	3.12	3.5	4.12	1.97	5.24	0																		
21	10.27	10.92	11.3	11.92	10.26	13.04	11.13	0																	
23	19.26	6.05	6.42	7.04	5.39	8.16	6.26	13.35	0																
24	16.68	2.76	3.14	2.49	2.1	4.88	2.97	10.77	5.9	0															
26	17.06	9.4	9.77	10.39	8.74	11.51	9.61	11.15	11.82	9.25	0														
30	21.11	7.19	7.56	3.28	6.53	9.3	7.4	15.2	10.32	5.77	13.67	0													
31	15.96	2.75	3.13	3.75	2.09	4.86	2.96	10.05	3.3	2.6	8.52	7.03	0												
32	16.78	2.86	3.24	3.86	2.21	4.98	3.08	10.87	6	2.71	9.35	7.14	2.7	0											
34	17.95	4.73	5.11	5.73	4.08	6.85	4.95	12.04	5.28	4.59	10.51	9.01	1.99	4.69	0										
36	19.27	6.06	6.43	7.05	5.4	8.17	6.27	13.36	4.73	5.91	11.83	10.33	3.31	6.01	5.29	0									
40	20.54	6.62	6.99	2.71	5.96	8.73	6.83	14.63	9.76	5.2	13.1	5.99	6.46	6.57	8.44	9.76	0								
41	12.48	5.79	6.17	6.79	5.14	7.91	6.01	6.57	8.22	5.64	6.03	10.07	4.92	5.75	6.91	8.23	9.5	0							
46	12.25	4.58	4.96	5.58	3.92	6.7	4.79	6.34	7.01	4.43	4.81	8.86	3.71	4.53	5.7	7.02	8.29	1.21	0						
47	15.38	1.45	1.83	2.45	0.8	3.57	1.67	9.47	4.59	1.31	7.94	5.73	1.29	1.41	3.28	4.6	5.16	4.34	3.13	0					
48	22.1	8.18	8.56	4.28	7.52	10.3	8.39	16.19	11.32	6.76	14.67	3.45	8.02	8.13	10.01	11.33	6.99	11.07	9.85	6.73	0				
49	10.77	6.06	6.44	7.06	5.4	8.18	6.27	4.86	8.49	5.91	6.29	10.34	5.19	6.01	7.18	8.5	9.77	1.71	1.48	4.61	11.33	0			
50	13.58	5.91	6.28	6.9	5.25	8.02	6.12	7.67	8.33	5.76	6.14	10.18	5.04	5.86	7.02	8.34	9.61	2.54	1.33	4.45	11.18	2.81	0		
52	12.33	12.98	13.36	13.98	12.32	15.09	13.19	2.06	15.41	12.83	13.21	17.26	12.11	12.93	14.09	15.42	16.69	8.62	8.4	11.52	18.25	6.92	9.72	0	
53	16.95	3.03	3.4	4.02	2.37	5.14	3.24	11.04	6.16	2.88	9.51	7.3	2.87	0.99	4.85	6.17	6.73	5.91	4.7	1.57	8.3	6.18	6.02	13.1	0

Table 17: Variogram parameters of estimated graphical structure for subsample of 25 banks for 2008-2011

ID	1	4	8	14	15	17	20	21	23	24	26	30	31	32	34	36	40	41	46	47	48	49	50	52	53
1	0																								
4	11.52	0																							
8	11.87	0.35	0																						
14	11.14	6.16	6.51	0																					
15	10.02	1.5	1.85	4.66	0																				
17	15.78	10.8	11.15	6.99	9.29	0																			
20	9.88	2.97	3.31	4.52	1.46	9.16	0																		
21	15.5	10.52	10.87	6.71	9.02	3.81	8.88	0																	
23	16.31	11.34	11.68	7.53	9.83	8.86	9.7	8.58	0																
24	11.74	2.07	2.42	6.38	1.72	11.02	3.19	10.74	11.56	0															
26	15.72	10.74	11.09	6.93	9.24	8.26	9.1	7.99	4.1	10.96	0														
30	13.61	8.63	8.98	4.82	7.12	6.15	6.99	5.88	6.69	8.85	6.09	0													
31	12.17	3.65	4	6.8	2.15	11.44	3.61	11.16	11.98	3.87	11.38	9.27	0												
32	13.22	1.7	2.05	7.86	3.2	12.5	4.66	12.22	13.03	3.77	12.44	10.33	5.35	0											
34	14.29	9.31	9.66	3.15	7.81	10.14	7.68	9.86	10.68	9.53	10.08	7.97	9.96	11.01	0										
36	6.27	7.17	7.51	6.78	5.66	11.42	5.53	11.14	11.96	7.39	11.36	9.25	7.81	8.86	9.94	0									
40	4.09	7.43	7.78	7.05	5.92	11.68	5.79	11.41	12.22	7.65	11.62	9.51	8.07	9.13	10.2	2.18	0								
41	14.91	6.4	6.74	9.55	4.89	14.19	6.35	13.91	14.72	6.61	14.13	12.01	4.73	8.09	12.7	10.55	10.82	0							
46	13.21	4.69	5.04	7.85	3.19	12.48	4.65	12.21	13.02	4.91	12.43	10.31	3.03	6.39	11	8.85	9.11	1.7	0						
47	8.25	3.27	3.62	2.89	1.77	7.53	1.63	7.25	8.06	3.49	7.47	5.36	3.91	4.97	6.04	3.89	4.16	6.66	4.96	0					
48	11.62	6.64	6.99	2.83	5.13	4.16	5	3.88	4.7	6.86	4.1	1.99	7.28	8.34	5.98	7.26	7.52	10.02	8.32	3.36	0				
49	15.12	6.61	6.96	9.76	5.1	14.4	6.56	14.12	14.93	6.83	14.34	12.23	4.94	8.3	12.91	10.76	11.03	1.44	1.91	6.87	10.24	0			
50	14.39	5.88	6.23	9.03	4.37	13.67	5.83	13.39	14.2	6.1	13.61	11.5	4.21	7.58	12.18	10.03	10.3	2.88	1.18	6.14	9.51	3.1	0		
52	17.84	12.86	13.21	9.06	11.36	6.15	11.23	2.34	10.92	13.08	10.33	8.22	13.51	14.56	12.21	13.48	13.75	16.25	14.55	9.59	6.23	16.46	15.73	0	
53	13.2	1.68	2.03	7.84	3.18	12.48	4.64	12.2	13.01	3.75	12.42	10.31	5.33	1.64	10.99	8.84	9.11	8.07	6.37	4.95	8.32	8.29	7.56	14.54	0

A.9 Model-implied systemic importance measures

Tables 18, 19 and 20 show the graph-induced centrality measures and simulated systemic impact measures, and their (averaged) rank, for all 55 banks for respectively 2016-2019, 2012-2015 and 2008-2011. The first three measures are the closeness, betweenness and degree centrality, described in Section 3.4.1 and obtained from the corresponding estimated graphical structures. The other two measures are the average affected number of banks and average affected proportion capital, described in Section 3.4.2, and obtained from 1,000,000 simulations using the estimated variogram parameters (Appendix A.8). The ranks are averaged ranks, meaning that we average the range of ranks in case multiple banks have the same measure value.

Table 18: Model-implied systemic importance measures and averaged rank for 2016-2019.

ID	$C_c(i)$		$C_b(i)$		$C_d(i)$		$\overline{A}_b(i)$		$\overline{A}_c(i)$ (%)	
1	0.263	31½	0	34	0.037	27	5.97	42	12.45	37
2	0.213	49½	0	34	0.037	27	5.99	41	7.19	53
3	0.261	38½	0	34	0.019	48½	7.39	28	11.32	41
4	0.262	35	0	34	0.037	27	9.68	16	23.31	12
5	0.261	38½	0	34	0.019	48½	8.40	21	13.28	34
6	0.262	35	0	34	0.037	27	6.26	39	9.48	47
7	0.212	52	0	34	0.037	27	7.97	24	16.27	25
8	0.348	5	0.238	5	0.111	6½	12.24	4	30.07	2
9	0.257	41	0	34	0.037	27	5.37	49	9.90	45
10	0.305	22	0	34	0.037	27	7.84	26	15.61	26
11	0.213	49½	0	34	0.037	27	3.40	55	4.08	55
12	0.212	52	0	34	0.037	27	7.17	31	14.31	30
13	0.258	40	0.037	11	0.056	11	6.33	37	12.62	36
14	0.329	8	0	34	0.037	27	10.15	13	23.93	9
15	0.462	1	0.654	1	0.259	1	14.33	1	34.38	1
16	0.351	4	0.361	3	0.185	2	11.35	7	18.62	21
17	0.266	30	0.073	8½	0.074	8½	9.64	19	21.08	17
18	0.255	42½	0	34	0.019	48½	7.33	29	15.13	27
19	0.415	3	0.354	4	0.148	3½	12.40	3	26.20	6
20	0.320	12½	0	34	0.037	27	11.62	5	27.04	4
21	0.320	12½	0	34	0.037	27	9.98	14	23.52	11
22	0.262	35	0	34	0.037	27	7.25	30	10.90	42
23	0.262	35	0	34	0.037	27	5.67	48	9.94	44
24	0.295	26½	0	34	0.019	48½	8.77	20	18.44	22
25	0.297	24½	0	34	0.037	27	4.65	53	7.57	52
26	0.206	55	0	34	0.019	48½	4.05	54	8.51	50
27	0.305	22	0	34	0.019	48½	6.40	35	10.87	43
28	0.305	22	0	34	0.019	48½	7.57	27	14.16	32
29	0.267	29	0.037	11	0.056	11	6.79	34	8.21	51
30	0.241	45½	0	34	0.037	27	5.25	50	21.96	14
31	0.320	12½	0	34	0.037	27	11.50	6	27.65	3
32	0.307	19½	0	34	0.037	27	10.42	10	21.25	16
33	0.318	16½	0	34	0.019	48½	8.03	23	16.45	24
34	0.318	16½	0	34	0.019	48½	10.19	12	23.27	13
35	0.333	7	0	34	0.037	27	5.86	44	11.61	39
36	0.340	6	0.176	7	0.111	6½	10.29	11	24.53	8
37	0.307	19½	0	34	0.037	27	9.64	18	18.16	23
38	0.269	28	0.073	8½	0.074	8½	7.08	32	8.78	49
39	0.320	12½	0	34	0.037	27	9.66	17	21.46	15
40	0.255	42½	0	34	0.019	48½	8.07	22	18.91	20
41	0.241	45½	0	34	0.037	27	5.71	47	14.42	29
42	0.212	52	0	34	0.019	48½	5.79	45	6.74	54
43	0.209	54	0	34	0.019	48½	4.85	52	9.06	48
44	0.262	35	0	34	0.037	27	6.38	36	9.82	46
45	0.263	31½	0.037	11	0.056	11	6.10	40	11.93	38
46	0.241	45½	0	34	0.037	27	5.94	43	14.21	31
47	0.320	12½	0	34	0.037	27	11.29	8	26.32	5
48	0.241	45½	0	34	0.037	27	4.85	51	14.75	28
49	0.314	18	0.177	6	0.130	5	7.86	25	19.17	19
50	0.240	48	0	34	0.019	48½	5.77	46	13.72	33
51	0.297	24½	0	34	0.037	27	6.98	33	12.89	35
52	0.320	12½	0	34	0.037	27	9.69	15	23.86	10
53	0.435	2	0.479	2	0.148	3½	12.83	2	25.30	7
54	0.327	9	0	34	0.037	27	11.25	9	19.99	18
55	0.295	26½	0	34	0.019	48½	6.33	38	11.56	40

Table 19: Model-implied systemic importance measures and averaged rank for 2012-2015.

ID	$C_c(i)$		$C_b(i)$		$C_d(i)$		$\overline{A}_b(i)$		$\overline{A}_c(i)$ (%)	
1	0.289	25½	0	35	0.037	29	4.37	43	9.85	38
2	0.237	46½	0.037	12½	0.056	12½	4.20	45	3.46	53
3	0.243	42½	0	35	0.019	49½	8.12	22	14.64	25
4	0.314	18	0.142	6	0.093	6	11.56	4	25.62	4
5	0.249	38	0.073	9	0.074	8½	10.01	10	17.56	18
6	0.287	30½	0	35	0.019	49½	5.08	37	7.83	44
7	0.243	42½	0.037	12½	0.056	12½	8.92	17	17.35	19
8	0.240	45	0	35	0.019	49½	9.88	11	23.41	7
9	0.302	19	0.140	7	0.074	8½	4.59	42	4.75	51
10	0.400	2½	0.414	3	0.204	2	9.54	12	16.93	21
11	0.320	11	0	35	0.037	29	6.31	32	11.34	35
12	0.196	52	0	35	0.019	49½	7.43	27	13.78	27
13	0.286	32	0	35	0.037	29	4.80	39	8.19	42
14	0.289	25½	0	35	0.037	29	8.93	15	20.30	9
15	0.287	30½	0	35	0.019	49½	11.46	5	25.80	2
16	0.200	50½	0	35	0.019	49½	8.33	21	14.11	26
17	0.242	44	0	35	0.037	29	8.72	18	17.69	17
18	0.320	11	0	35	0.037	29	7.26	28	13.49	28
19	0.320	11	0	35	0.037	29	8.39	20	15.85	23
20	0.320	11	0	35	0.037	29	8.92	16	17.77	16
21	0.320	11	0	35	0.037	29	7.66	25	16.78	22
22	0.200	50½	0	35	0.019	49½	7.65	26	12.69	30
23	0.289	25½	0	35	0.037	29	5.98	33	10.39	37
24	0.289	25½	0	35	0.037	29	10.55	7	23.01	8
25	0.269	36½	0	35	0.037	29	4.74	40	7.69	45
26	0.280	35	0	35	0.019	49½	3.31	55	6.34	49
27	0.295	20	0	35	0.037	29	4.94	38	7.11	47
28	0.320	11	0	35	0.037	29	8.04	24	15.00	24
29	0.192	53½	0	35	0.019	49½	3.50	53	2.64	55
30	0.281	33½	0	35	0.037	29	3.96	48	18.42	13
31	0.362	5	0.073	10	0.074	8½	11.41	6	24.23	5
32	0.320	11	0.240	5	0.130	4	12.00	3	24.02	6
33	0.289	25½	0	35	0.037	29	5.89	35	9.32	39
34	0.320	11	0	35	0.037	29	9.34	13	18.26	15
35	0.289	25½	0	35	0.037	29	4.62	41	7.35	46
36	0.320	11	0	35	0.037	29	8.09	23	18.37	14
37	0.244	40½	0	35	0.037	29	9.22	14	17.32	20
38	0.192	53½	0	35	0.019	49½	3.50	54	2.83	54
39	0.462	1	0.687	1	0.278	1	12.86	2	25.76	3
40	0.289	25½	0	35	0.037	29	5.79	36	12.37	32
41	0.228	49	0	35	0.037	29	3.80	50	8.33	40
42	0.237	46½	0.037	12½	0.056	12½	4.20	44	3.50	52
43	0.320	11	0	35	0.037	29	5.94	34	10.61	36
44	0.269	36½	0	35	0.037	29	6.79	30	12.59	31
45	0.289	25½	0	35	0.037	29	3.95	49	6.23	50
46	0.229	48	0.037	12½	0.056	12½	4.02	47	8.03	43
47	0.400	2½	0.454	2	0.130	4	13.10	1	28.19	1
48	0.281	33½	0	35	0.037	29	3.71	51	12.20	33
49	0.290	21	0.107	8	0.074	8½	4.12	46	8.22	41
50	0.187	55	0	35	0.019	49½	3.52	52	6.97	48
51	0.318	17	0	35	0.019	49½	6.70	31	11.72	34
52	0.320	11	0	35	0.037	29	8.44	19	19.27	11
53	0.244	40½	0	35	0.037	29	10.07	9	20.06	10
54	0.247	39	0	35	0.037	29	10.50	8	19.24	12
55	0.386	4	0.269	4	0.130	4	6.83	29	12.82	29

Table 20: Model-implied systemic importance measures and averaged rank for 2008-2011.

ID	$C_c(i)$		$C_b(i)$		$C_d(i)$		$\overline{A}_b(i)$		$\overline{A}_c(i)$ (%)	
1	0.225	40½	0	36½	0.019	48½	3.97	54	5.49	52
2	0.224	43	0	36½	0.019	48½	7.16	20	10.04	33
3	0.284	21½	0	36½	0.037	29½	5.73	36	7.55	42
4	0.258	30	0.237	5	0.111	4	9.99	3	28.74	3
5	0.176	53½	0	36½	0.037	29½	6.67	24	15.81	19
6	0.283	27	0	36½	0.019	48½	5.32	42	7.44	43
7	0.207	47½	0	36½	0.037	29½	8.06	13	20.75	13
8	0.250	32	0	36½	0.037	29½	9.78	4	29.20	2
9	0.284	21½	0	36½	0.037	29½	7.01	21	9.95	35
10	0.289	9½	0.037	13	0.056	13	5.15	45	7.55	41
11	0.227	37½	0	36½	0.037	29½	4.92	46	6.72	48
12	0.207	47½	0	36½	0.037	29½	7.91	16	20.14	14
13	0.283	27	0	36½	0.037	29½	4.75	48	9.99	34
14	0.318	5	0.037	13	0.056	13	8.11	11	22.43	10
15	0.316	6	0.473	3	0.130	2½	10.49	1	30.26	1
16	0.284	21½	0	36½	0.037	29½	5.45	40	7.10	46
17	0.283	27	0	36½	0.037	29½	6.00	30	14.45	28
18	0.284	21½	0	36½	0.037	29½	4.65	51	6.08	51
19	0.286	16	0	36½	0.037	29½	5.57	38	7.99	39
20	0.290	7½	0.037	13	0.056	13	9.26	7	25.34	7
21	0.331	4	0.037	13	0.056	13	7.34	18	18.52	16
22	0.286	16	0	36½	0.037	29½	5.44	41	7.24	45
23	0.287	12½	0.037	13	0.056	13	5.60	37	7.66	40
24	0.241	36	0	36½	0.019	48½	7.92	15	22.21	11
25	0.199	52	0	36½	0.019	48½	6.16	29	14.82	26
26	0.284	21½	0	36½	0.037	29½	5.52	39	8.22	36
27	0.284	21½	0	36½	0.037	29½	4.91	47	6.51	50
28	0.224	43	0	36½	0.019	48½	4.74	49	6.67	49
29	0.287	12½	0.037	13	0.056	13	8.55	9	12.26	29
30	0.281	29	0	36½	0.019	48½	7.18	19	26.41	5
31	0.248	34	0.037	13	0.056	13	8.30	10	22.06	12
32	0.212	45	0.108	6½	0.093	5½	8.57	8	23.07	8
33	0.286	16	0	36½	0.037	29½	5.32	43	6.80	47
34	0.242	35	0	36½	0.019	48½	5.85	32	14.60	27
35	0.287	12½	0	36½	0.037	29½	5.31	44	7.26	44
36	0.225	40½	0	36½	0.019	48½	4.71	50	10.18	32
37	0.175	55	0	36½	0.019	48½	6.44	27	15.63	22
38	0.391	1	0.718	1	0.389	1	10.24	2	15.63	21
39	0.226	39	0	36½	0.019	48½	6.86	22	17.31	17
40	0.289	9½	0.037	13	0.056	13	5.80	34	12.03	30
41	0.201	49½	0	36½	0.037	29½	6.57	25	16.05	18
42	0.284	21½	0	36½	0.037	29½	7.91	17	11.49	31
43	0.290	7½	0.073	8	0.074	7½	5.88	31	8.19	37
44	0.287	12½	0.037	13	0.056	13	5.81	33	8.18	38
45	0.227	37½	0	36½	0.037	29½	4.37	53	5.37	53
46	0.250	32	0.108	6½	0.093	5½	7.96	14	19.06	15
47	0.355	3	0.465	4	0.074	7½	9.64	5	26.74	4
48	0.388	2	0.554	2	0.130	2½	9.28	6	26.00	6
49	0.201	49½	0	36½	0.037	29½	6.45	26	15.06	25
50	0.201	51	0	36½	0.019	48½	6.79	23	15.73	20
51	0.224	43	0	36½	0.019	48½	4.49	52	5.37	54
52	0.250	32	0	36½	0.019	48½	5.73	35	15.27	23
53	0.209	46	0	36½	0.037	29½	8.09	12	22.68	9
54	0.176	53½	0	36½	0.037	29½	6.44	28	15.23	24
55	0.284	21½	0	36½	0.037	29½	3.72	55	4.64	55

A.10 Additional binary logistic regression results

Tables 21 to 24 contain results for the binary logistic regressions for the periods 2012-2015 and 2008-2011, discussed in Section 3.4.3. The results are comparable to the results for the period 2016-2019, which are discussed in Section 4.2.2.

Table 21: Parameters estimates (with standard errors), McFadden R^2 and Hit Rates (both for all banks and G-SIBs only) for logistic regression of the G-SIB indicator against, log-capitalization, closeness centrality, all centrality measures (closeness, betweenness and degree respectively), average affected number of banks and average affected proportion of capital. A single asterisk denotes significance of the predictor at 5% significance level, while a double asterisk denotes significance of the predictor at 1% significance level. Data and graphical estimates are from the time window 2012-2015.

Predictor(s)	None	$log\,(c_i)$	$C_c(i)$	$C_c(i); C_b(i); C_d(i)$	$\overline{A}_b(i)$	$\overline{A}_c(i)$
$\hat{a}_0$	-0.98	-38.97	-2.70	-4.41	-3.06	-4.72
	(0.30)	(12.83)	(1.65)	(2.41)	(1.02)	(1.25)
$\hat{a}_1$		3.80**	5.98	15.95	0.27*	23.69**
		(1.25)	(5.56)	(8.77)	(0.12)	(7.04)
$\hat{a}_2$				4.41		
				(8.48)		
$\hat{a}_3$				-28.14		
				(25.97)		
McFadden R^2	0	0.62	0.02	0.06	0.09	0.27
Hit Rate (All)	0.73	0.91	0.71	0.73	0.76	0.84
Hit Rate (G-SIBs)	0	0.93	0	0.07	0.29	0.57

Table 22: Parameters estimates (with standard errors), McFadden R^2 and Hit Rates (both for all banks and G-SIBs only) for logistic regression of the G-SIB indicator against jointly log-average market capitalization (predictor 1) and respectively closeness centrality, average affected number of banks and average affected proportion of capital (predictor 2). A single asterisk denotes significance of the predictor at 5% significance level, while a double asterisk denotes significance of the predictor at 1% significance level. Data and graphical estimates are from the time window 2012-2015.

Predictor 2	$C_c(i)$	$\overline{A}_b(i)$	$\overline{A}_c(i)$
$\hat{a}_0$	-40.74	-40.28	-38.12
	(13.33)	(13.23)	(13.05)
$\hat{a}_1$	3.82^{**}	3.76^{**}	3.51^{**}
	(1.24)	(1.26)	(1.26)
$\hat{a}_2$	5.31	0.22	12.56
	(9.61)	(0.17)	(8.61)
McFadden R^2	0.62	0.65	0.66
Hit Rate (All)	0.91	0.93	0.91
Hit Rate (G-SIBs)	0.93	1	0.93

Table 23: Parameters estimates (with standard errors), McFadden R^2 and Hit Rates (both for all banks and G-SIBs only) for logistic regression of the G-SIB indicator against, log-capitalization, closeness centrality, all centrality measures (closeness, betweenness and degree respectively), average affected number of banks and average affected proportion of capital. A single asterisk denotes significance of the predictor at 5% significance level, while a double asterisk denotes significance of the predictor at 1% significance level. Data and graphical estimates are from the time window 2008-2011.

Predictor(s)	None	$log\,(c_i)$	$C_c(i)$	$C_c(i); C_b(i); C_d(i)$	$\overline{A}_b(i)$	$\overline{A}_c(i)$
$\hat{a}_0$	-0.89	-25.41	-1.98	-1.52	-3.91	-3.67
	(0.30)	(6.67)	(1.67)	(2.12)	(1.36)	(0.95)
$\hat{a}_1$		2.56^{**}	4.14	5.45	0.44^{*}	17.63^{**}
		(0.68)	(6.19)	(8.39)	(0.19)	(5.23)
$\hat{a}_2$				5.63		
				(4.59)		
$\hat{a}_3$				-23.77		
				(19.74)		
McFadden R^2	0	0.53	0.01	0.05	0.09	0.23
Hit Rate (All)	0.71	0.91	0.71	0.71	0.73	0.82
Hit Rate (G-SIBs)	0	1	0	0.07	0.29	0.64

Table 24: Parameters estimates (with standard errors), McFadden R^2 and Hit Rates (both for all banks and G-SIBs only) for logistic regression of the G-SIB indicator against jointly log-average market capitalization (predictor 1) and respectively closeness centrality, average affected number of banks and average affected proportion of capital (predictor 2). A single asterisk denotes significance of the predictor at 5% significance level, while a double asterisk denotes significance of the predictor at 1% significance level. Data and graphical estimates are from the time window 2008-2011.

Predictor 2	$C_c(i)$	$\overline{A}_b(i)$	$\overline{A}_c(i)$
$\hat{a}_0$	-25.17	-29.27	-30.45
	(6.72)	(8.76)	(9.78)
$\hat{a}_1$	2.66**	3.27**	3.22**
	(0.72)	(1.09)	(1.12)
$\hat{a}_2$	-4.63	-0.44	-8.65
	(9.03)	(0.40)	(9.77)
McFadden R^2	0.54	0.56	0.55
Hit Rate (All)	0.91	0.89	0.91
Hit Rate (G-SIBs)	1	0.93	1

B Matlab Code

all_cliques.m

```
function clique_list = all_cliques(G)
% Obtains list of all cliques of a block graph G

d=numnodes(G);
clique_list = {};
for i=1:d-1
    nb_i = neighbors(G,i)';
    for j=intersect(i+1:d,nb_i)
        nb_j = neighbors(G,j)';
        nb_ij = intersect(nb_i,nb_j);
        if isempty(nb_ij) | min(nb_ij) > j
            clique_ij = [i,j,intersect(nb_i,nb_j)];
            clique_list{end+1} = clique_ij;
        end
    end
end
```

Gamma_to_par.m

```
function Gamma_par = Gamma_to_par(Gamma)
% Transforms variogram Gamma to vector of variogram parameters

d=size(Gamma,1);
Gamma_par = zeros(1,(d*(d-1))/2);
n=0;
for i=1:d
    for j=i+1:d
        n=n+1;
        Gamma_par(n) = Gamma(i,j);
    end
end
end
```

Gamma_to_Sigma.m

```
function [Sigma_k,Gamma_vec] = Gamma_to_Sigma(Gamma,k)
% Transforms variogram Gamma to Sigma^\k matrix, based on index k

d = size(Gamma,1);
Gamma_vec = Gamma(k,:);
Sigma_k = (repmat(Gamma_vec',1,d) + repmat(Gamma_vec,d,1) - Gamma)./2;
Sigma_k(:,k) = [];
Sigma_k(k,:) = [];
Gamma_vec(k) = [];
end
```

graph_to_Gamma.m

```
function [Gamma,Gamma_par,clique_list] = graph_to_Gamma(G)
% Obtains variogram Gamma (parameters) from block graph with weights
    Gamma_ij

Gamma = full(adjacency(G,'weighted'));
```

```
cliques_left = all_cliques(G);
clique_list = cliques_left;

nodes_in = cliques_left{1};
cliques_left(1) = [];
% Recursively choose new cliques and change Gamma
while ~isempty(cliques_left)
    clique_new = [];
    n=0;
    while isempty(clique_new)
        n=n+1;
        clique_maybe = cliques_left{n};
        if ~isempty(intersect(clique_maybe,nodes_in))
           clique_new = clique_maybe;
        end
    end
    k=intersect(nodes_in,clique_new);
    for i=nodes_in
        for j=clique_new
            Gamma(i,j) = Gamma(i,k) + Gamma(j,k);
            Gamma(j,i) = Gamma(i,j);
        end
    end
    nodes_in = [nodes_in,clique_new];
    cliques_left(n) = [];
end
Gamma_par = Gamma_to_par(Gamma);
end
```

greedy_graph_3clique.m

```
function [graph_list,llh_list,AIC_list] = greedy_graph_3clique(Y,G_init)
% Obtains list of underlying graphs, log-likelihoods and AICs (using
% Husler-Reiss distribution) by adding edges forming block graphs with
% clique size of at most 3, and initial graph must be too.

disp("graph 0: initial graph")
d = size(Y,2);
N_edges = numedges(G_init);
[~,Gamma_par_init] = graph_to_Gamma(G_init);
graph_list = {G_init};
llh_list = HR_llh_cens(Y,Gamma_par_init);
AIC_list = 2*N_edges - 2*llh_list;

% Start of greedy algorithm
last_edge = false;
Gamma3_mat = NaN(d-2,d-1,d,3); % Stores ML-Gamma parameters
while ~last_edge
disp("graph "+(size(graph_list,2)+1))
G_prev = graph_list{end};
G_prev_adj = full(adjacency(G_prev));
N_edges = N_edges + 1;
llh_to_beat = -Inf;
last_edge = true;
    % Loop through triplets of connected edges
    for i=1:d-1
        for j=neighbors(G_prev,i)'
            nb_j = intersect(i+1:d,neighbors(G_prev,j)');
            for k=nb_j
```

```
                % potential edge: new edge & not part of other 3clique
                if G_prev_adj(i,k)==0 && ...
                   max(sum(G_prev_adj([i,j],:)))<2 && ...
                   max(sum(G_prev_adj([j,k],:)))<2
                    disp("trying edge: ("+i+","+k+")")
                    G_temp = addedge(G_prev,i,k,NaN);
                    ijk = sort([i,j,k]);
                    % Obtain Gamma parameters on 3clique
                    Gamma_par= NaN(1,3);
                    Gamma_par(1) = Gamma3_mat(ijk(1),ijk(2),ijk(3),1);
                    Gamma_par(2) = Gamma3_mat(ijk(1),ijk(2),ijk(3),2);
                    Gamma_par(3) = Gamma3_mat(ijk(1),ijk(2),ijk(3),3);
                    if isnan(Gamma_par(1))
                        [~,Gamma_par,~] = HR_est_cens(Y(:,ijk));
                        Gamma3_mat(ijk(1),ijk(2),ijk(3),1) = Gamma_par(1);
                        Gamma3_mat(ijk(1),ijk(2),ijk(3),2) = Gamma_par(2);
                        Gamma3_mat(ijk(1),ijk(2),ijk(3),3) = Gamma_par(3);
                    end
                    G_temp.Edges.Weight(findedge(G_temp,ijk(1),ijk(2))) =
                        Gamma_par(1);
                    G_temp.Edges.Weight(findedge(G_temp,ijk(1),ijk(3))) =
                        Gamma_par(2);
                    G_temp.Edges.Weight(findedge(G_temp,ijk(2),ijk(3))) =
                        Gamma_par(3);
                    % Check if llh is better
                    [~,Gamma_par_temp,~] = graph_to_Gamma(G_temp);
                    llh_temp = HR_llh_cens(Y,Gamma_par_temp);
                    if llh_temp > llh_to_beat
                        G_to_beat = G_temp;
                        llh_to_beat = llh_temp;
                        AIC_to_beat = 2*N_edges - 2*llh_to_beat;
                        last_edge = false;
                    end
                end
            end
        end
    end
    % Update lists if an edge is added
    if ~last_edge
        graph_list{end+1} = G_to_beat;
        llh_list = [llh_list,llh_to_beat];
        AIC_list = [AIC_list,AIC_to_beat];
    end
end
end
```

HR_est_cens.m

```
function [Gamma_ML,Gamma_par_ML,llh,H] = HR_est_cens(y)
% ML estimation of Husler-Reiss distribution assuming fully connected
% underlying graph (used for parameter estimation on cliques). Based on
% censored likelihood.
% Largely based on R-code from:
% https://github.com/sebastian-engelke/graphicalExtremes/tree/master/R

% Determine initial variogram parameters
d = size(y,2);
Gamma_init = zeros(d,d);
for k=1:d
```

```
        Sigma_k = cov(log(y(y(:,k)>1,:)));
        Gamma_init = Gamma_init + ones(d,1)*diag(Sigma_k)' + ...
                     diag(Sigma_k)*ones(1,d) - 2*Sigma_k;
    end
    Gamma_init = Gamma_init/d;
    Gamma_par_init = Gamma_to_par(Gamma_init);

    % Minimize negative censored likelihood
    neg_llh = @(Gamma_par)-HR_llh_cens(y,Gamma_par);
    options = optimoptions('fmincon','display','none');
    [Gamma_par_ML,llh,~,~,~,H] = fmincon(neg_llh,Gamma_par_init,[],...
        [],[],[],zeros(1,(d*(d-1))./2),[],[],options);

    % Return estimated Gamma matrix/parameters, log-likelihood and Hessian
    Gamma_ML = par_to_Gamma(Gamma_par_ML);
    llh = -llh;
    H=-H;
    end
```

HR_llh_cens.m

```
    function llh = HR_llh_cens(Y,Gamma_par)
    % Obtains censored log likelihood given data Y and variogram parameters
    % Gamma_par.

    Y = Y(max(Y,[],2)>1,:);
    Y(Y<=1) = 1;
    N = size(Y,1);
    Gamma = par_to_Gamma(Gamma_par);
    [Sigma_1,~] = Gamma_to_Sigma(Gamma,1);
    if min(eig(Sigma_1))>0
        llh = HR_logemd_cens(Y,Gamma_par) - N*HR_logLambda(Gamma_par);
    else % In case Sigma_1 matrix is not strictly conditionally negative
        definite
        llh = -Inf;
    end
```

HR_logemd_cens.m

```
    function loglambda = HR_logemd_cens(Y,Gamma_par)
    % Obtains censored log exponent measure density given data Y and variogram
    % parameters Gamma_par.
    % Largely based on R-code from:
    % https://github.com/sebastian-engelke/graphicalExtremes/tree/master/R

    d = size(Y,2);
    th_sum = sum(Y>1,2);
    Gamma = par_to_Gamma(Gamma_par);
    Sigma_list = zeros(d-1,d-1,d);
    for k=1:d
        [Sigma_list(:,:,k),~] = Gamma_to_Sigma(Gamma,k);
    end
    loglambda = 0;

    % Calculate loglambda for realizations entirely not needing censoring.
    y_nc = Y(th_sum==d,:);
    N_nc = size(y_nc,1);
    Sigma_1 = Sigma_list(:,:,1);
    for n=1:N_nc
```

```
    y_1 = log(y_nc(n,2:d)) + Gamma(1,2:d)/2 - log(y_nc(n,1));
    loglambda = loglambda - (d-1)*log(2*pi)/2 - log(det(Sigma_1))/2 ...
                - ((y_1/Sigma_1)*y_1')/2 - sum(log(y_nc(n,:))) - log(y_nc(n
                    ,1));
end

% Calculate loglambda for realizations with exactly d-1 needing censoring.
y_c1 = Y(th_sum==1,:);
N_c1 = size(y_c1,1);
for n=1:N_c1
    k = find(y_c1(n,:)>1);
    id_nok = 1:d;
    id_nok(k)=[];
    y_nok = log(y_c1(n,id_nok)/y_c1(n,k)) + Gamma(k,id_nok)/2;
    Sigma_k = Sigma_list(:,:,k);
    loglambda = loglambda + log(mvncdf_60(y_nok',0,Sigma_k,...
                statset('TolFun',0.001,'MaxFunEvals',25000)));
    loglambda = loglambda - 2*log(y_c1(n,k));
end

% Calculate loglambda for realizations with 1<i<d-1 needing censoring.
y_c2 = Y(th_sum>1 & th_sum<d,:);
N_c2 = size(y_c2,1);
for n=1:N_c2
    K = find(y_c2(n,:)>1);
    m = numel(K);
    k = min(K);
    id_noK = 1:d;
    id_noK(K)=[];
    K_nok = K-1;
    K_nok(1) = [];
    Sigma_k = Sigma_list(:,:,k);
    Sigma_K = Sigma_k(K_nok,K_nok);
    Sigma_noK = Sigma_k;
    Sigma_noK(K_nok,:) = [];
    Sigma_noK_K = Sigma_noK;
    Sigma_noK(:,K_nok) = [];
    Sigma_noK_K = Sigma_noK_K(:,K_nok);
    y_noK = log(y_c2(n,id_noK)/y_c2(n,k)) + Gamma(k,id_noK)/2;
    y_K = log(y_c2(n,K)/y_c2(n,k)) + Gamma(k,K)/2;
    y_K(1) = [];
    Sigma_C = Sigma_noK - (Sigma_noK_K/Sigma_K)*Sigma_noK_K';
    Sigma_C = (Sigma_C + Sigma_C')/2;
    loglambda = loglambda + log(mvncdf_60(y_noK' - (Sigma_noK_K/Sigma_K)*
        y_K',0,...
                Sigma_C,statset('TolFun',0.001,'MaxFunEvals',25000)));
    loglambda = loglambda - (m-1)*log(2*pi)/2 - log(det(Sigma_K))/2 ...
                - ((y_K/Sigma_K)*y_K')/2 - sum(log(y_c2(n,K))) - log(y_c2(n,k
                    ));
end
end
```

HR_logLambda.m

```
function logLambda = HR_logLambda(Gamma_par)
% Obtains log normalization constant given variogram parameters Gamma_par.

d=round((1+sqrt(1+8*numel(Gamma_par)))/2,0);
Gamma = par_to_Gamma(Gamma_par);
```

```
Lambda = 0;
for k=1:d
    [Sigma_tilde_k,Gamma_k] = Gamma_to_Sigma(Gamma,k);
    Lambda = Lambda + mvncdf_60(Gamma_k/2,0,Sigma_tilde_k,...
             statset('TolFun',0.001,'MaxFunEvals',25000));
end
logLambda = log(Lambda);
end
```

HR_simulation.m

```
function Y_sim = HR_simulation(Gamma,N)
% Simulates N HR realizations based on variogram Gamma.
% Largely based on R-code from:
% https://github.com/sebastian-engelke/graphicalExtremes/tree/master/R

d = size(Gamma,1);
Y_sim = zeros(N,d);
n=1;
rand_k = randi(d,1,N);
for k=1:d
    n_k = sum(rand_k==k);
    while n_k>0
        Sigma_k = Gamma_to_Sigma(Gamma,k);
        chol_k = chol(Sigma_k);
        chol_k0 = [zeros(1,d);zeros(d-1,1),chol_k];
        if k>1
            chol_k0([k,1:k-1],:) = chol_k0(1:k,:);
            chol_k0(:,[k,1:k-1]) = chol_k0(:,1:k);
        end
        W_k = randn(n_k,d)*chol_k0 - Gamma(k,:)/2;
        U_k = exp(W_k);
        P_k = 1./( 1 - rand(n_k,1) );
        Y_k = (P_k.*U_k)./sum(U_k,2);
        Y_k = Y_k(max(Y_k,[],2)>1,:);
        n_size = size(Y_k,1);
        Y_sim(n:n+n_size-1,:) = Y_k;
        n = n+n_size;
        n_k = n_k - n_size;
    end
end
end
```

L_to_X.m

```
function [X_mat,model_est,resid,sigma_sq,tdis] = L_to_X(L_mat)
% Obtains standard Pareto transformed residuals, AR/GARCH-model estimates,
% GARCH residuals and t-distributions from matrix of log-losses L_mat.

T=size(L_mat,1);
d=size(L_mat,2);
Z_mat = zeros(T,d);
X_mat = zeros(T,d);
model_est = cell(1,d);
resid = zeros(T,d);
sigma_sq = zeros(T,d);
tdis = cell(1,d);
for i=1:d
    disp("Bank ID: "+i)
```

```
15      % AR(1)/GARCH(1,1) fitting
16      model_var_t = garch('GARCHLags',1,'ARCHLags',1,'Distribution','t');
17      model_t = arima('ARLags',1,'Variance',model_var_t);
18      Est_t = estimate(model_t,L_mat(:,i),'Display','off');
19      model_est{i} = Est_t;
20
21      % Obtain GARCH-residuals and estimated parameters
22      [resid(:,i),sigma_sq(:,i),~] = infer(Est_t,L_mat(:,i));
23      Z_mat(:,i) = resid(:,i)./sqrt(sigma_sq(:,i));
24
25      % Obtain transformed residuals
26      DoF = Est_t.Variance.Distribution.DoF;
27      tdis{i} = makedist('tLocationScale','mu',0,'sigma',sqrt((DoF-2)/DoF),'
            nu',DoF);
28      X_mat(:,i) = 1./(1-cdf(tdis{i},Z_mat(:,i)));
29  end
30  end
```

min_span_tree.m

```
1   function [T_min,T_min_weights] = min_span_tree(y)
2   % Obtain the spanning tree that maximizes the censored log likelihood based
3   % on data Y.
4
5   % Create fully connected graph with negative log-likelihood-terms as
        weights.
6   y = y(max(y,[],2)>1,:);
7   d = size(y,2);
8   G_full = graph(ones(d)-eye(d));
9   Gamma_par = zeros(1,(d*(d-1))/2);
10  weights = Gamma_par;
11  m=0;
12  for i=1:d-1
13      for j=i+1:d
14          disp("(i,j)=("+i+","+j+")")
15          m=m+1;
16          [~,Gamma_par_ML,llh] = HR_est_cens(y(:,[i,j]));
17          Gamma_par(m) = Gamma_par_ML;
18          weights(m) = -llh - 2*sum(log(y(y(:,i)>1,i))) - 2*sum(log(y(y(:,j)
                >1,j)));
19      end
20  end
21
22  % Obtain minimal spanning tree
23  G_full.Edges.Weight = weights';
24  T_min_weights = minspantree(G_full,'Method','sparse');
25  T_min_weights.Edges.Weight = - T_min_weights.Edges.Weight;
26
27  % Create tree with with variogram parameters as weights
28  T_min = T_min_weights;
29  Gamma = par_to_Gamma(Gamma_par);
30  for m=1:numedges(T_min)
31      i = T_min.Edges.EndNodes(m,1);
32      j = T_min.Edges.EndNodes(m,2);
33      T_min.Edges.Weight(m) = Gamma(i,j);
34  end
35  end
```

mvncdf_60.m
This is a small tweak of the code **mvncdf.m** from the Matlab Statistics and Machine Learning Toolbox, such that it can take 60-dimensional data. Its only change is the replacement of line 263 **elseif d <= 25** by **elseif d <= 60**.

References

Basel Committee on Banking Supervision. (2010). *Guidance to assess the systemic importance of financial institutions, markets and instruments: Initial considerations* (Tech. Rep.). Bank for International Settlements.

Basel Committee on Banking Supervision. (2011). *Global systemically important banks: assessment methodology and the additional loss absorbency requirement* (Tech. Rep.). Bank for International Settlements.

Bedford, T., & Cooke, R. M. (2002). A new graphical model for dependent random variables. *The Annals of Statistics*, *30*(4), 1031-1068.

Beirlant, J., Goegebeur, Y., Teugels, J., Segers, J., de Waal, D., & Ferro, C. (2004). *Statistics of extremes: Theory and applications*. John Wiley & Sons, Ltd.

Engelke, S., & Hitz, A. S. (2020). Graphical model for extremes. *Journal of the Royal Statistical Society: Series B (Statistical Methodology)*, *84*(4), 871-932.

Engelke, S., Malinowski, A., Kabluchko, Z., & Schlather, M. (2015). Estimation of Hüsler-Reiss distributions and Brown-Resnick processes. *Journal of the Royal Statistical Society: Series B (Statistical Methodology)*, *77*(1), 239-265.

Freeman, L. C. (1978). Centrality in social networks: Conceptual clarification. *Social Networks*, *1*, 215-239.

Gissibl, N., & Klüppelberg, C. (2018). Max-linear models on directed acyclic graphs. *Bernoulli*, *24*(4A), 2693-2720.

Hüsler, J., & Reiss, R.-D. (1989). Maxima of normal random vectors: between independence and complete dependence. *Statistics and Probability Letters*, *7*(4), 283-286.

Kiriliouk, A., Rootzén, H., Segers, J., & Wadsworth, J. (2018). Peaks over thresholds

modeling with multivariate generalized pareto distributions. *Technometrics*, *61*(1), 123-135.

Krause, A., & Giasante, S. (2012). Interbank lending and the spread of bank failures: A network model of systemic risk. *Journal of Economic Behavior & Organization*, *83*, 583-608.

Krupskii, P., & Joe, H. (2013). Factor copula models for multivariate data. *Journal of Multivariate Analysis*, *120*, 85-101.

Kruskal, J. B. (1956). On the shortest spanning subtree of a graph and the traveling salesman problem. *Proceedings of the American Mathematical Society*, *7*(1), 48-50.

Lauritzen, S. L. (1996). *Graphical models*. Clarendon Press, Oxford.

Low, R. K. Y. (2018). Vine copulas: modelling systemic risk and enhancing higher-moment portfolio optimisation. *Accounting & Finance*, *58*, 423-463.

Low, R. K. Y., Alcock, J., Faff, R., & Brailsford, T. (2013). Canonical vine copulas in the context of modern portfolio management: Are they worth it? *Journal of Banking & Finance*, *37*, 3085-3099.

McNeil, A. J., Frey, R., & Embrechts, P. (2015). *Quantitative risk management: Concepts, techniques and tools*. Princeton University Press, Princeton, New Jersey.

Oh, D. H., & Patton, A. J. (2017). Modeling dependence in high dimensions with factor copulas. *Journal of Business & Economic Statistics*, *35*(1), 139-154.

Rootzén, H., & Tajvidi, N. (2006). Multivariate generalized pareto distributions. *Bernoulli*, *12*(5), 917-930.